LA-4465-MS

C: 1

LOS ALAMOS SCIENTIFIC LABORATORY
of the
University of California

LOS ALAMOS • NEW MEXICO

LASL Contributions to the 3rd International Symposium on Polarization Phenomena in Nuclear Reactions

UNITED STATES
ATOMIC ENERGY COMMISSION
CONTRACT W-7405-ENG. 36

Printed in the United States of America. Available from
Clearinghouse for Federal Scientific and Technical Information
National Bureau of Standards, U. S. Department of Commerce
Springfield, Virginia 22151
Price: Printed Copy $3.00; Microfiche $0.65

Distributed: July 1970

LA-4465-MS
UC-34, PHYSICS
TID-4500

LOS ALAMOS SCIENTIFIC LABORATORY
of the
University of California
LOS ALAMOS • NEW MEXICO

LASL Contributions to the 3rd International Symposium on Polarization Phenomena in Nuclear Reactions

Madison, Wisconsin, August 31-September 4, 1970

FOREWORD

This report includes all Los Alamos Scientific Laboratory (LASL) contributions to the Third International Symposium on Polarization Phenomena in Nuclear Reactions, held in Madison, Wisconsin, August 31-September 4, 1970. In a number of cases, the authors of individual papers have included appendices containing supplemental or explanatory materials, as indicated in the Table of Contents.

It is a pleasure to acknowledge the skill and enthusiasm of Mrs. Judy Elder, who did the majority of the secretarial work involved in the typing and assembly of this document.

Gerald G. Ohlsen
Compiler

TABLE OF CONTENTS

Phase Shifts from n-^{4}He Elastic Scattering Experiments Near 20 MeV*

A. Niiler, M. Drosg, J. C. Hopkins, and J. D. Seagrave

Los Alamos Scientific Laboratory, University of California
Los Alamos, New Mexico 87544

Optical model calculations[1] and a recent energy-dependent phase-shift analysis[2] of n-^{4}He elastic scattering in the energy range of 15-25 MeV have arrived at sets of phase shifts which at some energies are in significant disagreement with the set put forward by Hoop and Barschall[3]. Since the n-^{4}He system is widely used as a neutron polarization analyzer, a reliable set of phase shifts is essential.

None of the above authors had available the complete set of recent n-^{4}He polarization data of Broste and Simmons[4] in the energy range 11-30 MeV. Furthermore, all n-^{4}He cross section measurements used in these analyses were made by the ^{4}He recoil method. By this method, angular distributions cannot be extended reliably into the forward angles in this energy region. Thus, rather large uncertainties may enter in the normalization of the integral of the angular distributions to total cross sections.

We have measured the n-^{4}He differential cross sections at 17.6, 20.9, and 23.7 MeV with a neutron time-of-flight technique using a 1-mole sample of liquid ^{4}He as a scatterer. The energies of 17.6 and 23.7 MeV were chosen to match Broste and Simmons' polarization measurements, and 20.9 MeV was chosen to give an intermediate point. Neutron-proton scattering was also measured to give an absolute normalization of the n-^{4}He points to the well-known n-p cross sections[5]. Multiple scattering effects were corrected for by the Aldermaston code MAGGIE[6].

At all three energies, single-energy phase-shift searches were carried out using the general reaction matrix code EIA2. At 23.7 MeV, Hoop and Barschall's inelastic parameters were used and kept fixed in all searches. Starting the phase shifts at several different values, a unique set was always reached. Maximum L values of 2, 3, 4, and 5 were searched on and at all energies the minimum weighted variance was obtained with $L_{max} = 4$. Thus, subsequent searches were made with $L_{max} = 4$ only. These single-energy sets are shown as the last entries of table 1. The next step was to obtain a smooth phase-shift set which would extrapolate smoothly to the optical model and the two-level resonance model[7] values near 10 MeV. This smoothed set is also shown in table 1 along with that of Hoop and Barschall and the optical model set of Satchler et al.[1]. Since both $\sigma(\theta)$ and $P(\theta)$ were available at 17.6 and 23.7 MeV, the phase shifts at these two energies were given more weight than the 20.9-MeV values in obtaining the smoothed set.

Table 1: n-^{4}He Phase Shifts in Degrees

	E_n (MeV)	$S_{1/2}$	$P_{3/2}$	$P_{1/2}$	$D_{5/2}$	$D_{3/2}$	$F_{7/2}$	$F_{5/2}$	$G_{9/2}$	$G_{7/2}$
Ref. 3	17.6	93	95	56	6	3	1	1		
	20.9	90	92	53	9	6	3	3		
	23.7	86	89	52	12	6	4	4		
Ref. 1	17.6	89	93	52	7.2	3.2	0.4	0.2		
	20.9	84	88	47	9.4	4.0				
Present Values Smooth Set	17.6	87	95	53.5	8	7.2	2.1	1.5	1.5	0.2
	20.9	79	92.5	48.5	11	10	3	3	3	0.8
	23.7	73	89	45.5	18.5	10.8	6.5	5.2	3.8	2.0
Present Values Single Energy	17.6	84	95	52.5	9.1	7.9	2.1	1.8	2.2	0.6
	20.9	83.7	97.7	45.7	8.5	15.7	1.2	4.6	6.5	-0.3
	23.7	71.2	88.3	45.6	19.7	10.8	6.8	5.7	3.3	1.9

*Work performed under the auspices of the U. S. Atomic Energy Commission.

The most significant differences between our set and that of ref. 3 are smaller values of the $S_{1/2}$ and $P_{1/2}$ phases, the somewhat larger values for the D and F waves and the need for small amounts of G waves.

Our single-energy set gives excellent fits to the angular distributions at all three energies. Our smoothed set fits equally well at 17.6 and 23.7 but not quite so well at 20.9 MeV. See fig. 1 for these fits. A derivation of the phase shifts from the cross section data alone (without the constraints of the polarization data) did not give acceptable results for $L_{max} \geq 3$ (at 17.6 MeV) and $L_{max} \geq 4$ (at 23.7 MeV). The usefulness of having both differential cross section and polarization data available at the same energy cannot be overstated.

The authors are indebted to D. Dodder for use of the code EIA2.

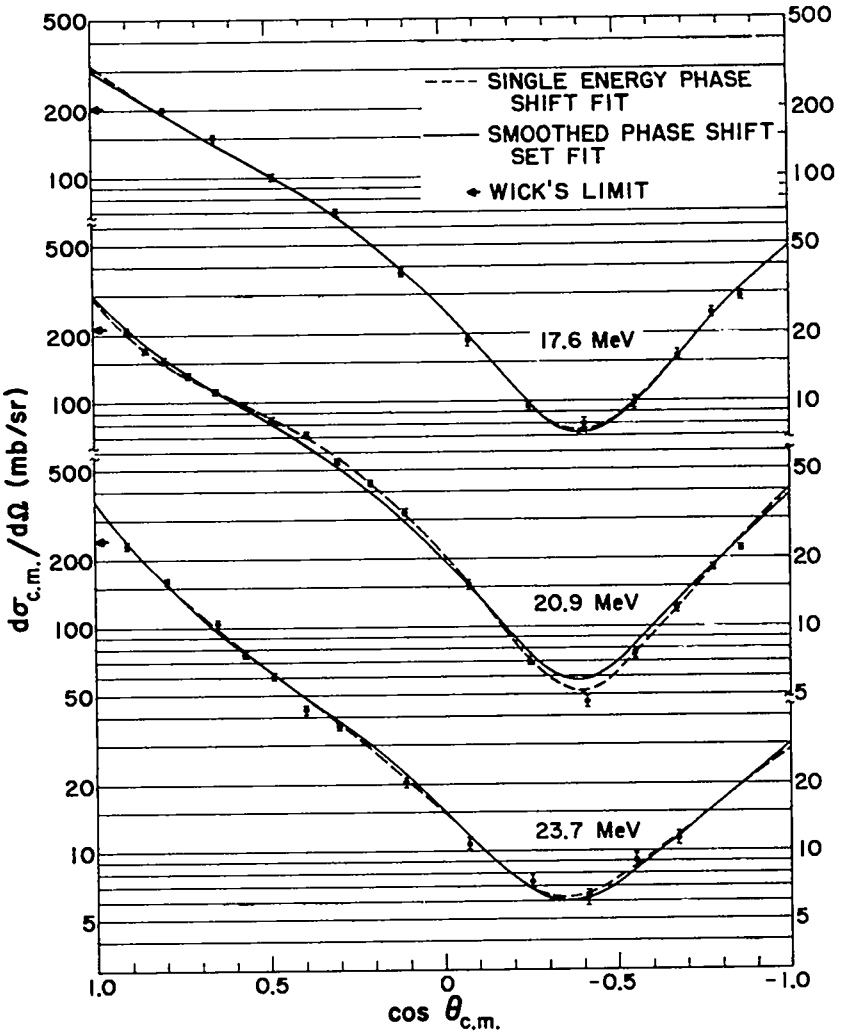

Fig. 1. Present data compared with cross sections from the smooth and single-energy phase-shifts sets.

References

1. G. R. Satchler, L. W. Owen, A. J. Elwyn, G. L. Morgan, and R. L. Walter, Nucl. Phys. A112 (1968) 1

2. R. A. Arndt and L. D. Roper, Phys. Rev. 1C (1970) 903

3. B. Hoop, Jr., and H. H. Barschall, Nucl. Phys. 83 (1966) 65

4. W. B. Broste, J. E. Simmons, and G. S. Mutchler, Bull. Am. Phys. Soc. 14 (1969) 1230; and private communication

5. J. C. Hopkins and G. Breit (to be published)

6. J. B. Parker, J. H. Towle, D. Sams, W. B. Gilboy, A. D. Purnell, and H. J. Stevens, Nucl. Inst. Meth. 30 (1964) 77

7. G. L. Morgan and R. L. Walter, Phys. Rev. 168 (1968) 1114

A Reactance Matrix Analysis of the d-^{3}He, p-^{4}He System at 10 MeV Deuteron Laboratory Energy

G. M. Hale, D. C. Dodder, and K. Witte

Los Alamos Scientific Laboratory, University of California
Los Alamos, New Mexico 87544

We are in the process of finding a set of reactance-matrix elements (presently at a single energy) to represent the scattering data for two-body reactions in the five-nucleon system. The hope that such an analysis will produce a single solution is prompted by having such detailed measurements as the polarization transfer coefficients and vector and tensor analyzing powers for $^3\mathrm{He}(\vec{d},d)^3\mathrm{He}$ [1] and $^3\mathrm{He}(\vec{d},p)^4\mathrm{He}$ [2], reported elsewhere in this symposium.

The analysis is done assuming that all states from (p,^{4}He) and (d,^{3}He) having the same total angular momentum and parity (J^P) are coupled. In the region where all nuclear potentials vanish, one expects the radial wave function for n states coupled at fixed J^P to be

$$\sim F+GQ_N^{J^P} ,$$

where F and G are diagonal matrices of the regular and irregular Coulomb functions for the n states. Q_N is a real, symmetric matrix, so that the collision matrix,

$$U = e^{i\Omega}(1+iQ_N)(1-iQ_N)^{-1}e^{i\Omega} ,$$

is unitary. Ω is the diagonal matrix of relative Coulomb "phase shifts," $\omega_\ell = \sigma_\ell - \sigma_0$. An equivalent description uses the matrices

$$Q = (\sin\Omega+\cos\Omega Q_N)(\cos\Omega-\sin\Omega Q_N)^{-1} \quad \text{and} \quad U = (1+iQ)(1-iQ)^{-1} .$$

The search has been carried out with the Los Alamos Energy Independent Reactance Matrix Code (EIA2)[3], using Q-matrix elements as parameters to fit simultaneously data from the $^3\mathrm{He}(d,d)^3\mathrm{He}$, $^3\mathrm{He}(d,p)^4\mathrm{He}$, and $^4\mathrm{He}(p,p)^4\mathrm{He}$ reactions. Allowing $\ell_{max} = 4$ in the (p,^{4}He) channel and $\ell_{max} = 3$ in the (d,^{3}He) channel gives 59 parameters to fit 237 data points from the three reactions. The best fit to date gives a weighted variance (χ^2 per degree of freedom) of 20, so that a solution has not yet been found. Searches have also been made with smaller values for ℓ_{max} in the (p,^{4}He) and (d,^{3}He) channels which give weighted variances in the range 30-70, indicating that the partial waves we have included are important at this energy.

One such possible use of such a reactance-matrix analysis would be to guide a coupled-channel calculation that uses effective phenomenological potentials to describe the two-body reactions among five nucleons. Effective potentials for $^4\mathrm{He}(p,p)^4\mathrm{He}$ are easy to classify because of the simple structure in spin space. A classification scheme for the reaction potentials has been suggested by

*Work performed under the auspices of the U. S. Atomic Energy Commission.

J. L. Gammel, based on Moravcsik's expansion for the reaction M-matrix[4]. The idea is to consider the terms of the expansion as momentum-space transforms of all the allowed potential operators. When these terms are transformed to coordinate space, one obtains in general nonlocal potentials which act, however, like local potentials with the identification of

$$\underline{k}+\underline{k}' \text{ with } \underline{p} = -i\nabla_{\underline{r}} \ , \quad \underline{k}-\underline{k}' \text{ with } \underline{r} \ , \quad \text{and} \quad \underline{k}\times\underline{k}' \text{ with } \underline{r}\times\underline{p} = \underline{L} \ .$$

The coordinate-space operators contain analogs of the familiar spin-orbit, tensor, and spin-spin terms. The matrix elements, which differ somewhat from the familiar case, are cited in table 1. There are obvious generalizations of the scheme that classify the ^{3}He(d,d)^{3}He potentials as well, allowing the five-nucleon reactions to be described by as few as ten effective potentials.

Table 1. Potential matrix elements $(J\ell'S'=\frac{1}{2}|V|J\ell S)$ for analogs of the spin-orbit, tensor, and spin-spin operators. $\underline{\chi}^\dagger$ represents the three deuteron (adjoint) spinors, and $\underline{\sigma}$ the three Pauli spin matrices.

		$\underline{\chi}^\dagger \cdot \underline{L}$		$3\underline{\chi}^\dagger\cdot\hat{r}\underline{\sigma}\cdot\hat{r}-\underline{\chi}^\dagger\cdot\underline{\sigma}$		$\underline{\chi}^\dagger \cdot \underline{\sigma}$	
J	ℓ'	$S=\frac{1}{2}$	$S=\frac{3}{2}$	$S=\frac{1}{2}$	$S=\frac{3}{2}$	$S=\frac{1}{2}$	$S=\frac{3}{2}$
$\ell+\frac{3}{2}$	$\ell+2$				$\sqrt{\frac{\ell+1}{2\ell+3}}$		
$\ell+\frac{1}{2}$	ℓ	$-\frac{1}{\sqrt{3}}\ell$	$\frac{1}{\sqrt{3}}\sqrt{\ell(2\ell+3)}$	0	$-\frac{1}{\sqrt{3}}\sqrt{\frac{\ell}{2\ell+3}}$	$-\sqrt{3}$	0
$\ell-\frac{1}{2}$	ℓ	$\frac{1}{\sqrt{3}}(\ell+1)$	$\frac{1}{\sqrt{3}}\sqrt{(\ell+1)(2\ell-1)}$	0	$\frac{1}{\sqrt{3}}\sqrt{\frac{\ell+1}{2\ell-1}}$	$-\sqrt{3}$	0
$\ell-\frac{3}{2}$	$\ell-2$				$-\sqrt{\frac{\ell}{2\ell-1}}$		

References

1. D.C. Dodder, D.D. Armstrong, P.W. Keaton, Jr., G.P. Lawrence, J.L. McKibben, and G.G. Ohlsen, "A Study of ^{3}He($\vec{d}$,d)^{3}He Scattering at 10 and 12 MeV," Proc. 3rd Internatl. Symp. on Polarization Phenomena (to be published)
2. P.W. Keaton, Jr., D.D. Armstrong, D.C. Dodder, G.P. Lawrence, J.L. McKibben, and G.G. Ohlsen, "A Study of the ^{3}He(d,p)^{4}He Reaction," same as above
3. D. C. Dodder and K. Witte (to be published)
4. P.L. Csonka, M.J. Moravcsik, and M.D. Scadron, Phys. Rev. 143 (1966) 775

Comparison of Double Scattering and Polarized Ion Source Measurements of $^4He(d,d)^4He$ Polarization at 11.5 MeV*

V. S. Starkovich and G. G. Ohlsen

Los Alamos Scientific Laboratory, University of New Mexico
Los Alamos, New Mexico 87544

A comparison is made between previously reported d-α double scattering measurements at 11.5 MeV[1] and recent d-α data taken with the Los Alamos Scientific Laboratory (LASL) polarized ion source. The latter measurements were taken at three deuteron energies near 11.5 MeV, and for c.m. angles 108°-126°, in order to permit the calculation of suitable averages for comparison to the low-resolution double scattering measurements. Since the double scattering measurements were regarded as primarily useful in the determination of the vector polarization of a deuteron beam[2], our primary objective was to provide an independent check of the absolute vector polarization of the beam produced by the LASL polarized ion source.

The differential cross section can be written as

$$I(\theta,\phi) = I_o(\theta)[1+\tfrac{3}{2}\langle P_y\rangle P^o_y(\theta)+\tfrac{2}{3}\langle P_{xz}\rangle P^o_{xz}(\theta)+\tfrac{1}{6}\langle P_{xx}-P_{yy}\rangle (P^o_{xx}(\theta)-P^o_{yy}(\theta))+\tfrac{1}{2}\langle P_{zz}\rangle P^o_{zz}(\theta)], \quad (1$$

where $I_o(\theta)$ is the cross section for an unpolarized beam. The quantities in brackets represent the beam polarization values and the remaining parameters represent the analyzing tensors for the reaction. A right-handed coordinate system with the z axis along $\vec{k}_{in}$ and the y axis along $\vec{k}_{in} \times \vec{k}_{out}$ is assumed for both the beam and the analyzing tensor quantities.

The analyzing tensors in Eq. (1) can be written in terms of the beam polarization which would be produced in the inverse reaction as follows:

$$P^o_{xz}(\theta_{cm}) = -\langle P_{xz}(\theta_{cm})\rangle \ , \quad P^o_{xx}(\theta_{cm})-P^o_{yy}(\theta_{cm}) = \langle P_{xx}(\theta_{cm})-P_{yy}(\theta_{cm})\rangle \ ,$$
$$P^o_{zz}(\theta_{cm}) = \langle P_{zz}(\theta_{cm})\rangle \ , \quad P^o_y(\theta_{cm}) = \langle P_y(\theta_{cm})\rangle \ , \qquad (2)$$

where the right-hand quantities in Eq. (2) represent the beam polarization produced in the inverse reaction referred to a coordinate system with the outgoing center-of-mass direction, $\vec{k}_{out}$ (c.m.) as the z axis, and $\vec{k}_{in} \times \vec{k}_{out}$ as the y axis.

Expressing both types of quantities in Eq. (1) in terms of the "inverse polarizations," we obtain

$$I(\theta,\phi) = I_o(\theta)[1+\tfrac{3}{2}\langle P_y\rangle^{lab}\langle P_y(\theta_{cm})\rangle-\tfrac{2}{3}\langle P_{xz}\rangle^{lab}\langle P_{xz}(\theta_{cm})\rangle+\tfrac{1}{6}\langle P^{lab}_{xx}-P^{lab}_{yy}\rangle\langle P_{xx}(\theta_{cm})$$
$$-P_{yy}(\theta_{cm})\rangle+\tfrac{1}{2}\langle P_{zz}\rangle^{lab}\langle P_{zz}(\theta_{cm})\rangle] \ . \qquad (3)$$

For the first scattering of the double scattering experiment, we used α particles and observed recoil deuterons at 31° (118° c.m.). Thus the "lab" quantities in Eq. (3) are related to the "c.m." quantities for $\theta_{cm} = 118°$ by a rotation about the y axis through $\beta = (118°-31°) \approx 87°$:

$$\langle P_y\rangle^{lab} = \langle P_y(118°)\rangle$$
$$\langle P_{xx}\rangle^{lab} = \langle P_{xx}(118°)\rangle\cos^2\beta+\langle P_{zz}(118°)\rangle\sin^2\beta-2\langle P_{xz}(118°)\rangle\sin\beta\cos\beta$$
$$\langle P_{yy}\rangle^{lab} = \langle P_{yy}(118°)\rangle \qquad (4)$$

*Work performed under the auspices of the U. S. Atomic Energy Commission.

$$\langle P_{zz}\rangle^{lab} = \langle P_{xx}(118°)\rangle \sin^2\beta + \langle P_{zz}(118°)\rangle \cos^2\beta + 2\langle P_{xz}(118°)\rangle \sin\beta\cos\beta$$

$$\langle P_{xz}\rangle^{lab} = \langle P_{xx}(118°)\rangle \sin\beta\cos\beta - \langle P_{zz}(118°)\rangle \sin\beta\cos\beta + \langle P_{xz}(118°)\rangle (\cos^2\beta - \sin^2\beta) \ .$$

Values of the ratio

$$\frac{2(L-R)}{L+R+U+D} = \frac{\frac{3}{2}\langle P_y\rangle^{lab}\langle P_y(\theta_{cm})\rangle - \frac{2}{3}\langle P_{xz}\rangle^{lab}\langle P_{xz}(\theta_{cm})\rangle}{1+\frac{1}{2}\langle P_{zz}\rangle^{lab}\langle P_{zz}(\theta_{cm})\rangle} \qquad (5)$$

obtained in the double scattering experiment at 11.5 MeV and for c.m. angles θ = 108°-126° are illustrated in Fig. 1 (triangles). In this expression L, R, U, and D represent the mean values of the number of counts recorded in the left, right, up, and down positions by the four telescopes. The angular resolution of these measurements was ±4° (c.m.) and the energy resolution was ±0.5 MeV. The circles represent values of the ratio (Eq. (5)) computed from averages of the analyzing tensors measured at 11.13, 11.50, and 12.00 MeV with the LASL polarized ion source. The beam polarization was assumed to be correctly given by the quench ratio measurements[3]. The errors in the values of the ratio (Eq. (5)) derived from the ion-source measurements were based on an assumed maximum systematic error of ±0.015 for P_y^o. (The systematic uncertainty arises chiefly from imperfect alignment of the scattering chamber and instability in the beam polarization.) For the ion-source data, the statistical error is in all cases much smaller than ±0.015. The errors presented in Fig. 1 for the double scattering measurements are statistical errors only.

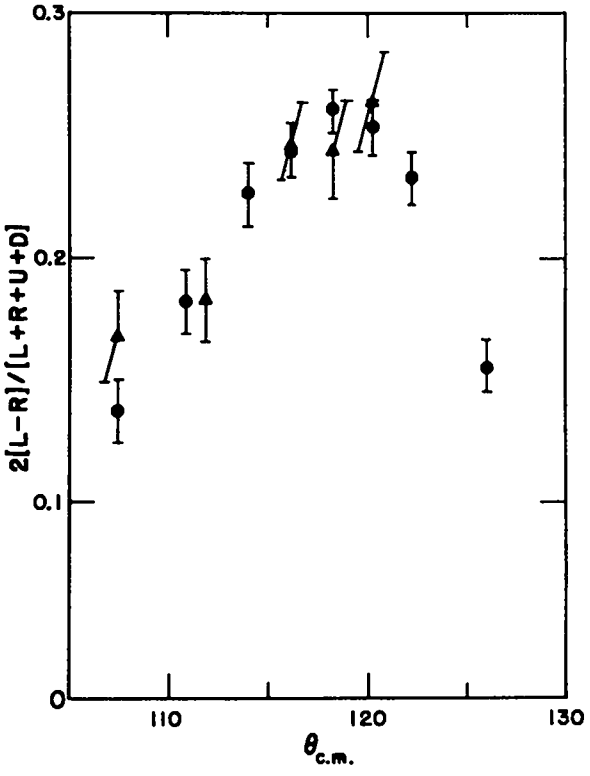

Fig. 1. Comparison of double scattering (triangles) and ion-source (circles) measurements.

If the actual vector and tensor polarization of the ion source beam is assumed to differ from the value given by the quench ratio determination by the factor K, a comparison of the value of the ratio (Eq. (5)) obtained from the two methods gives a value K = 0.984±0.028, where only the statistical error is taken into account for the double scattering. Thus, this experiment confirms within the error of the measurement that the ion source beam polarization is as given by the quench ratio method.

For additional detail see Los Alamos Scientific Laboratory Report LA-4465-MS.

References

1. V. S. Starkovich, Ph.D. Thesis, University of Wyoming, 1969; Los Alamos Scientific Report LA-4191 (1969)
2. G. G. Ohlsen, V. S. Starkovich, W. G. Simon, and E. M. Bernstein, Phys. Letters 28B (1969) 404
3. G.G.Ohlsen, G.P.Lawrence, P.W.Keaton, J.L.McKibben, and D.D.Armstrong, "Absolute Beam Polarization Determination for the LASL Lamb-Shift Source by the Quench Ratio Method," Proc. 3rd Internatl. Symp. Polarization Phenomena in Nuclear Reactions (to be published)

APPENDIX: Tables of the $^4He(\vec{d},d)$ Observables

The d-^{4}He tensors as measured with the polarized ion source, the 2(L-R)/(L+R+U+D) ratio which these tensors predict would be measured in the double scattering experiment, and the values of the ratio measured in the double scattering experiment are given in table 1.

For mostly historical reasons, we compare the predicted double scattering beam polarization with the best values previously obtained by a phase shift fit of the available double scattering data. See table 2.

Table 1

θ_L	θ_{cm}	P^o_{xz}	$\frac{1}{2}(P^o_{xx}-P^o_{yy})$	P^o_{zz}	P^o_y	$\frac{2(L-R)}{L+R+U+D}$ (Ion Source)	$\frac{2(L-R)}{L+R+U+D}$ (Double Scattering)
78°	107.50°	0.181	0.544	0.2537	-0.285	0.137±0.013	0.168±0.019
81°	110.82°	0.171	0.523		-0.332	0.182±0.013	
84°	114.04°	0.163	0.493		-0.380	0.226±0.013	
86°	116.15°	0.152	0.464		-0.398	0.262±0.011	0.262±0.018
88°	118.21°	0.137	0.430	0.2132	-0.411	0.260±0.009	0.244±0.020
90°	120.23°	0.126	0.382		-0.408	0.274±0.011	0.274±0.020
92°	122.21	0.111	0.325		-0.392	0.233±0.011	
96°	126.04	0.080	0.182	0.1563	-0.312	0.156±0.011	

Table 2: Spin tensors for $D(\alpha,\vec{d})\alpha$ scattering at $\theta_{lab} = 31°$

Tensors	Predicted from Phase Shift Fit of Double Scattering Data	Predicted from Polarized Ion Source Measurements
$\langle P_y \rangle$	-0.432	-0.408
$\langle P_{xz} \rangle$	-0.127	+0.142
$\frac{1}{2}\langle P_{xx}-P_{yy} \rangle$	0.285	+0.379
$\langle P_{zz} \rangle$	0.067	+0.308

Characteristics of AlK and $Al(NH_4)$ Alum as New Materials for Polarized Proton Targets

Philip J. Bendt, Los Alamos Scientific Laboratory, University of California, Los Alamos, New Mexico 87544

Dynamic proton polarization by the "solid effect" has been studied in $AlK(SO_4)_2 \cdot 12H_2O$ and $Al(NH_4)(SO_4)_2 \cdot 12H_2O$, in which a small fraction (< 0.5%) of the diamagnetic Al was replaced with paramagnetic Cr^{3+} ions. Over 50% proton polarization was attained in three alum crystals weighing 300 to 500 mg with 190 to 290 mW microwave power, at 1 K and $\sim$ 19.5 kG. With (111) planes oriented perpendicular to the magnetic field, the electron paramagnetic resonance (EPR) spectra was dominated by a single narrow line (10 to 22 G wide) corresponding to the (-1/2, 1/2) transition of the Cr^{3+} ions. The proton line widths varied from 7 to 15 G, and the proton line shape did not change as the polarization was increased. A 357 mG crystal of lanthanum magnesium nitrate (LMN) was polarized in the same apparatus, for comparison with the alum crystals.

Since the allowed and "forbidden" EPR transitions are well separated in alums, the theory of dynamic polarization by Jeffries[1] and Borghini[2] applies. The steady state polarization is given by

$$P_s = \frac{P_o}{(1 + f)} \frac{S}{(S + S_{\frac{1}{2}})} ,$$

where P_o is the thermal equilibrium polarization of the Cr^{3+} ions[3], f is the leakage factor[4], S is the EPR saturation factor, and $S_{\frac{1}{2}}$ is a constant which depends on the crystal properties and the magnetic field. The polarization grows with a time constant τ,

$$p(t) = p_s(1 - e^{-t/\tau}) ,$$

where τ is given by

$$\tau = T_{1p}\left[1 + \frac{S}{S_{\frac{1}{2}}(1 + f)}\right]^{-1} .$$

T_{1p} is the proton spin-lattice relaxation time. S depends on the ion relaxation times T_{1e} and T_{2e} as follows,

$$S = T_{1e}T_{2e}(\gamma_e H_{1e})^2 ,$$

where γ_e is the ion gyromagnetic ratio, and H_{1e} is the microwave field in the cavity.

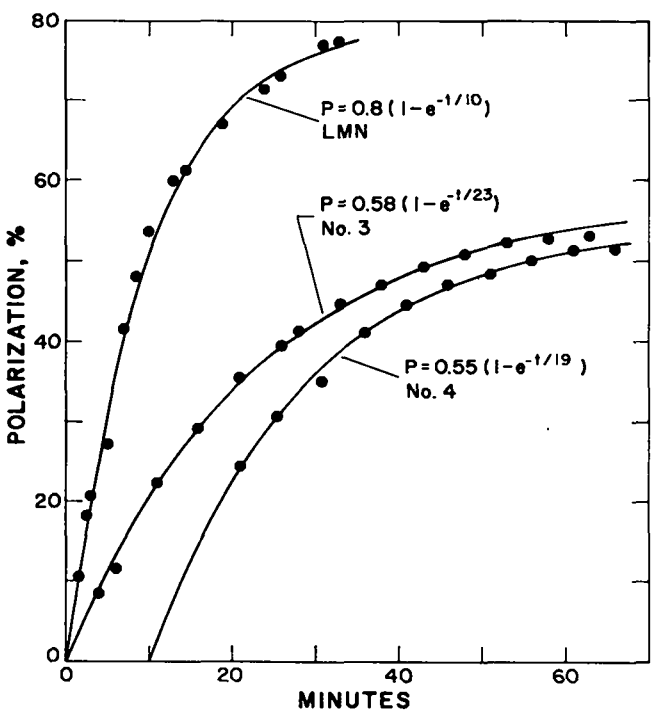

Fig. 1. Polarization growth rate curves for $Al(NH_4)$ alums and LMN. The polarizations are negative, and the solid lines fit the equations given.

Table I. Properties of the crystals, and polarization measurements.

Crystal:	AlK No.1	AlK No.2	Al(NH_4) No.3	Al(NH_4) No.4	LMN
Al:Cr ratio	435	215	380	590	100[a]
T_{1p} at 0.93 K (s)	13,000	3,950	3,350	1,350	1,320
T_{1e} at 0.96 K (ms)	2.5	2.0	3.0	2.8	11.5
EPR line width (G)	20	15	22	10	6
p_{max} (- %)	54	43	53	51	77
p_s (- %)	64	50	58	55	80
τ (minutes)	90	53	23	19	10
Microwave power (mW)	190	190	290	260	200
Saturation S	31	32	50	92	480
$S/(S + S_{\frac{1}{2}})$	0.74	0.58	0.68	0.66	0.86

[a] The nominal La:Nd ratio.

Both p_s and τ were obtained from polarization growth rate curves, three of which are shown in Fig. 1. T_{1e} was measured, and T_{2e} was calculated using $T_{2e} = (\gamma_e \delta H)^{-1}$, where δH is the half-width of the EPR line. The values p_{max} in Table I are the maximum (negative) polarizations we measured. From measurements of T_{1p} on AlK alum No. 1 at three temperatures, we estimate T_{1p} in this crystal will be about three days at 0.5 K. Such a long relaxation time would make pure AlK alum very useful for "storing" proton polarization.

The large value of S for LMN is due partly to the narrow EPR line, and partly to the long (phonon-bottlenecked) relaxation time T_{1e}. The measured values of $T_{1e}T_{2e}$ were 7 to 15 times smaller in alums than in LMN, which makes S smaller for the same microwave power. The experiments show it takes 3 times as much microwave power in alums as in LMN to obtain the same value of $S/(S + S_{\frac{1}{2}})$. Our polarization measurements were power-limited; both p_s and $1/\tau$ would have been larger with more microwave power.

The alum crystals have the advantage over LMN of higher hydrogen density by weight, by factors of 1.6 for AlK alum and 1.97 for Al(NH_4) alum. LMN has a larger P_o in a given magnetic field, and requires less microwave power. At 26 kG, and using a high-power microwave oscillator, these advantages will provide only 5% additional polarization in LMN, while using Al(NH_4) alum will expose approximately twice the number of polarized protons to the beam for the same charged particle energy loss. If alums have any advantage over the recently developed hydrocarbon targets, it results from the convenience of handling a solid crystal at room temperature, the reliability of using a crystal whose performance has been measured before it is put in the beam, and the simplicity of a target system that does not require cooling with liquid ^3He.

(1) T. J. Schmugge and C. D. Jeffries, Phys. Rev. 138, A1785 (1965); T. E. Gunter and C. D. Jeffries, Phys. Rev. 159, 290 (1967).
(2) M. Borghini, Phys. Rev. Letters 16, 318 (1966).
(3) At 1 K and 19.5 kG, P_o equals 0.86 for Cr^{3+} in alum, and equals 0.94 for Nd^{3+} in LMN.
(4) Values of the leakage factor varied from 0.002 to 0.034.

Elastic Scattering of Polarized Tritons*

D. D. Armstrong, P. W. Keaton, Jr., and L. R. Veeser

Los Alamos Scientific Laboratory, University of California
Los Alamos, New Mexico 87544

1. $^4He(t,\vec{t})^4He$ Reaction. The measurement at Los Alamos of the polarization of tritons[1] elastically scattered from ^4He has established this reaction as a good polarizer (or analyzer) for tritons[2]. Recently we have extended the polarization measurements over a sufficient angular and energy range (see Fig. 1) to allow a phase shift analysis (based on the work of Spiger and Tombrello[3]) and including their cross section data) which more accurately describes both the cross section and polarization data. Some information about mass-7 nuclei will result from this analysis. However, the physical interpretation of the analysis is complicated because the decay of the $t+^4He$ compound system can occur through many channels.

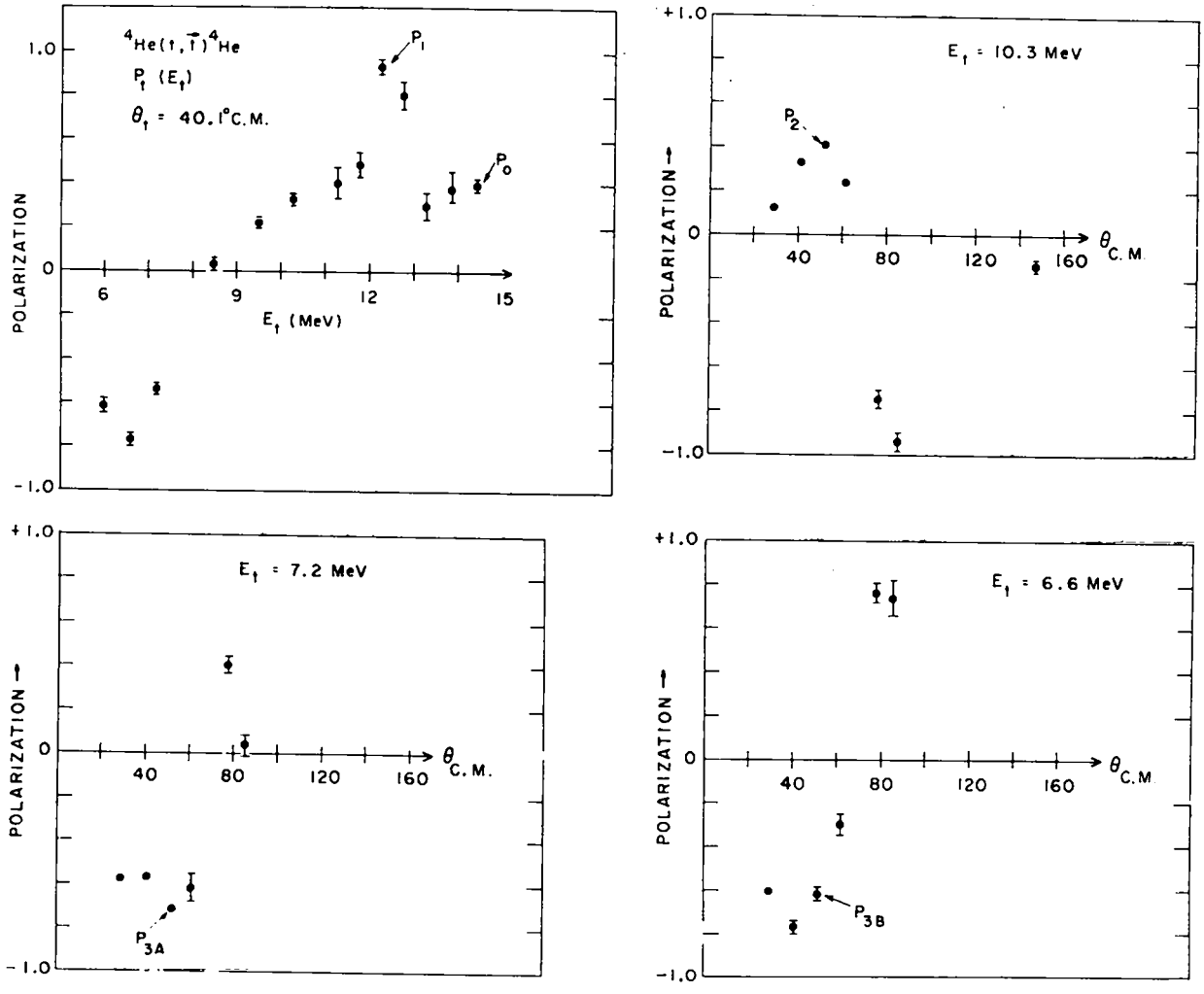

Fig. 1: Polarization of tritons elastically scattered from ^4He.

*Work performed under the auspices of the U. S. Atomic Energy Commission.

2. $H(\vec{t},\hat{t})H$ Reaction. A study of the elastic scattering of polarized tritons from protons gives information about the excited states of ^{4}He. We obtained data for 6.4-9.5 MeV (lab) tritons corresponding to an excitation of the order of 20 MeV in ^{4}He. For this region of excitation only the p+t and n+^{3}He channels need be considered. A two-channel analysis of our data and other relevant data from the literature was done using a computer program which calculates the cross sections and polarizations from the formulas of R-matrix theory[4].

3. $D(\vec{t},n)^4\hat{H}e$ Reaction. Using a polarized ^{3}He target, Baker et al.[5] measured the left-right asymmetry, A, of protons in the $^3\vec{H}e(d,\hat{p})^4$He reaction. Theoretical interest was aroused[6] when they pointed out that $A \approx -P$, where P is the proton polarization in ^{3}He$(d,\vec{p})^4$He. We have taken equivalent data with a polarized ^{3}He beam[7] $(D(^3\vec{H}e,\hat{\alpha})H)$ and also with a polarized triton beam $(D(\vec{t},\hat{\alpha})n)$. Although we have not made any theoretical deductions of our own at this time, it is clear that a theory which assumes or predicts $P \equiv -A$ is in serious error.

4. Optical Model for Tritons. Based on the assumption that the optical model potential for a triton is just the sum of the optical model potentials of its constituent nucleons suitably averaged over their internal motion in the triton[8], the polarization of tritons elastically scattered from nuclei is expected to be small. Our measurements (at angles $\lesssim 60°$) give small polarizations for tritons elastically scattered from Ni and ^{54}Fe. However, the measurement of the polarization at back angles is the most definitive test of this model. Such measurements are best done with a beam from a polarized ion source which we expect to be available soon at the Los Alamos Van de Graaff facility.

References

1. P. W. Keaton, Jr., D. D. Armstrong, and L. R. Veeser, Phys. Rev. Letters 20 (1968) 1392

2. P. W. Keaton, Jr., D. D. Armstrong, and L. R. Veeser, "The Absolute Polarization Determination of Mass-3 Nuclei," Proc. 3rd Internatl. Symp. on Polarization Phenomena in Nuclear Reactions (to be published)

3. R. J. Spiger and T. A. Tombrello, Phys. Rev. 163 (1967) 964

4. L. R. Veeser, D. D. Armstrong, and P. W. Keaton, Jr., Nucl. Phys. A140 (1970) 177

5. S. D. Baker, G. Roy, G. C. Phillips, and G. K. Walters, Phys. Rev. Letters 15 (1965) 115

6. P. L. Csonka, M. J. Moravcsik, and M. D. Scadron, Phys. Rev. 143 (1966) 775

7. D. D. Armstrong, L. L. Catline, P. W. Keaton, Jr., and L. R. Veeser, Phys. Rev. Letters 23 (1969) 135

8. P. W. Keaton, E. Aufdembrink, and L. R. Veeser, Los Alamos Scientific Laboratory Report LA-4379-MS (1969) (unpublished)

A Study of the $^3He(d,p)^4He$ Reaction*

P. W. Keaton, Jr., D. D. Armstrong, D. C. Dodder
G. P. Lawrence, J. L. McKibben, and Gerald G. Ohlsen

Los Alamos Scientific Laboratory, University of California
Los Alamos, New Mexico 87544

Vector and tensor analyzing powers for the $^3He(\vec{d},p)^4He$ reaction have been measured at a deuteron bombarding energy of 10.0 MeV. For the data obtained at laboratory angles greater than 20°, the apparatus and methods of refs. 1 and 2 were used. The slit system for the E-ΔE detector pairs were arranged for two-degree angular resolutions (FWHM). The scattering chamber was filled with ^3He to a pressure of 200 Torr. The ^3He was periodically recycled through a liquid-nitrogen-cooled charcoal trap by means of a mechanical pump so that no impurity problems were experienced.

The small angle P^o_{zz} measurements are of particular interest with respect to the interpretations of 0° polarization transfer coefficients. Therefore, measurements of P^o_{zz} at 5°, 10°, and 15° (laboratory angle) were made by setting the deuteron spin axis, β, to 0° and determining $m_I = 1$ to $m_I = 0$ ratios. However, since the detector assembly intercepted the beam at angles less than about 10°, it was necessary to determine the total charge delivered by means of monitor detectors rather than with a faraday cup. This is only possible if the value of P^o_{zz} at the monitor angle has been previously determined. We used a monitor laboratory angle of 45° (53.3° center-of-mass) where P^o_{zz} is -0.378±0.015.

The present data, together with previously determined values[3,4] of the vector analyzing power, P^o_y, are presented in fig. 1. The functions P^o_y, P^o_{xz}, and $(P^o_{xx}-P^o_{yy})/2$ are odd functions of the scattering angle, θ, and therefore must vanish for θ = 0. The even function, $P^o_{zz}(\theta)$, approaches a large value (-1.4) at θ = 0°.

The scattering matrix, M, for this reaction can be written[5,6] in terms of spin-one base vectors, $\chi_1^\dagger = (1,0,0)$, $\chi_o^\dagger = (0,1,0)$, $\chi_{-1}^\dagger = (0,0,1)$, and the Pauli spin matrices, $\vec{\sigma}$. The M matrix becomes

$$M = A(\vec{\chi}^\dagger\cdot\hat{n})+B(\vec{\chi}^\dagger\cdot\hat{n})(\vec{\sigma}\cdot\hat{n})+C(\vec{\chi}^\dagger\cdot\hat{n})(\vec{\sigma}\cdot\hat{p}')+D(\vec{\chi}^\dagger\cdot\hat{p})(\vec{\sigma}\cdot\hat{k}')+E(\vec{\chi}^\dagger\cdot\hat{k})(\vec{\sigma}\cdot\hat{p}')+F(\vec{\chi}^\dagger\cdot\hat{k})(\vec{\sigma}\cdot\hat{k}') ,$$

where $\hat{k}$ ($\hat{k}'$) is along $\vec{k}_{in}$ ($\vec{k}_{out}$), $\hat{n}$ is along $\vec{k}_{in}\times\vec{k}_{out}$, and $\hat{p}$ ($\hat{p}'$) is along $\hat{n}\times\hat{k}$ ($\hat{n}\times\hat{k}'$). The spatial components of $\vec{\chi}$ are $\vec{\chi}\cdot\hat{n} = i(\chi_1+\chi_{-1})/\sqrt{2}$, $\vec{\chi}\cdot\hat{p} = (-\chi_1+\chi_{-1})/\sqrt{2}$, and $\vec{\chi}\cdot\hat{k} = \chi_o$.

It has been previously noticed[3] that P^o_y in the present reaction has an angular dependence similar to the analyzing power observed in $^3\vec{He}(d,p)^4He$ (polarized target) experiments. This condition requires the following relation among the elements of M:

$$4ReAB^*-4ImCD^*-4ImEF^* = -4ImCE^*-4ImDF^*.$$

This relation is satisfied nondynamically by insisting that the entrance channel spin, S, differ from the exit channel spin by one. This imposes the restrictions F = -(B+C) and E = -iA+D, since only ΔS = -1 is allowed. This hypothesis predicts, however, that the polarization transfer coefficient, P^y_y, at zero degrees is -2/3. As a test we measured, in a preliminary experiment, the vector polarization transfer coefficient at 0° and found that $P^y_y(0°) = +0.57\pm0.10$. This is very close to the assumption ΔS = 0 which requires B = C = F and iA = -D = -E, and predicts $P^y_y(0°) = +2/3$. Therefore, it appears that ΔS = -1 dominates over most of the angular range, but that ΔS = 0 competes strongly at zero degrees.

*Work performed under the auspices of the U. S. Atomic Energy Commission.

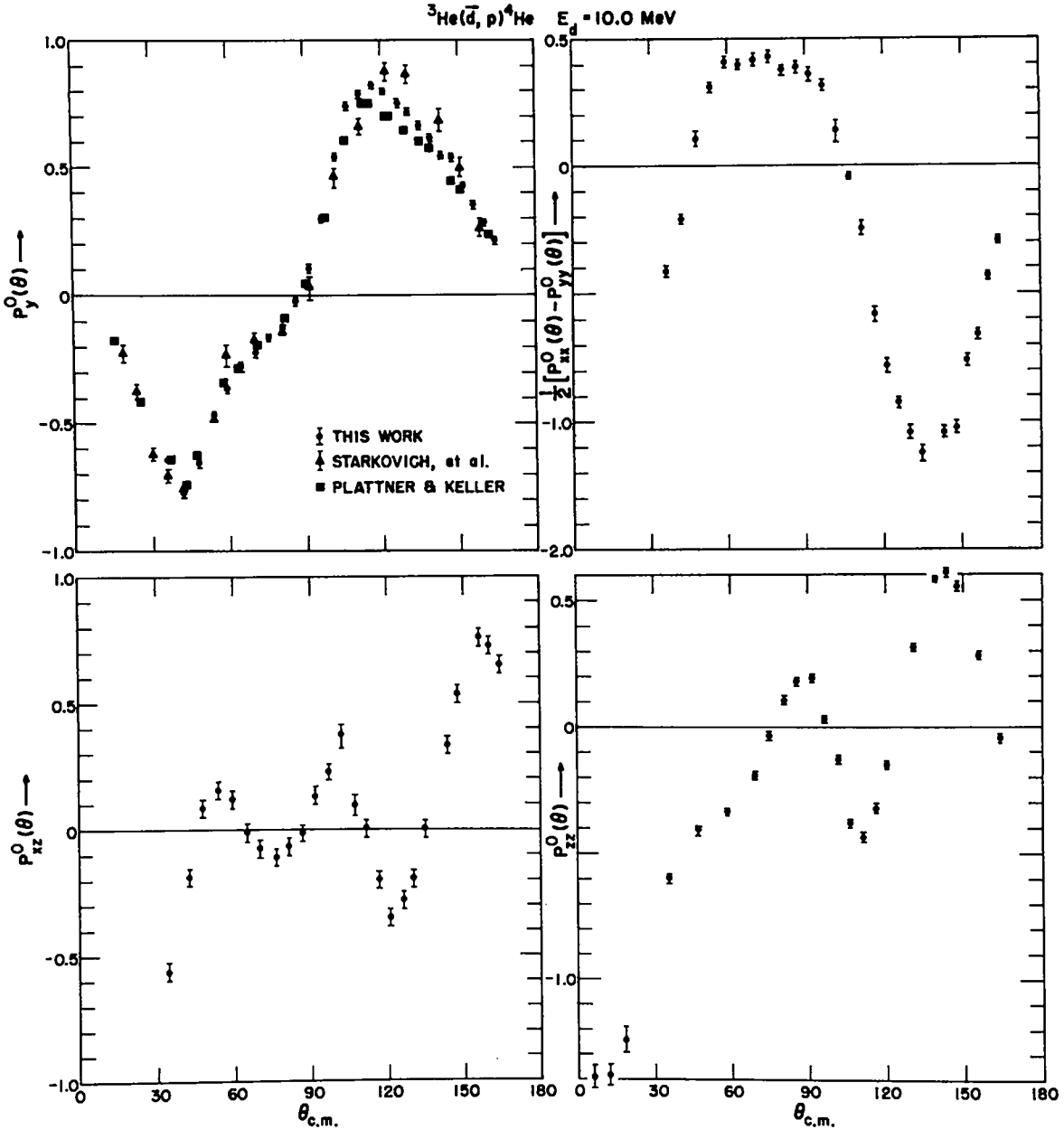

Fig. 1. Measured vector and tensor analyzing power for the $^3He(\vec{d},p)^4He$ reaction at 10 MeV.

References

1. G. P. Lawrence, G.G.Ohlsen, J.L.McKibben, P.W.Keaton, and D.D.Armstrong, "A Rapid Method for the Measurement of Analyzing Tensors in Reactions Induced by Polarized Deuterons," Proc. 3rd Internatl. Symp. on Polarization Phenomena in Nuclear Reactions (to be published)
2. D.C.Dodder, D.D. Armstrong, P.W.Keaton, G.P.Lawrence, J.L.McKibben, and G.G. Ohlsen, "A Study of $^3He(\vec{d},d)^3He$ Scattering at 10 and 12 MeV" same as above
3. G.R. Plattner and L.G. Keller, Phys. Letters 29B (1969) 301
4. V.Starkovich, Ph.D. Thesis, University of Wyoming, 1969; and LA-4191
5. P. L. Csonka, M. J. Moravcsik, and M. D. Scadron, Phys. Rev. 143 (1966) 775
6. J. L. Gammel, P. W. Keaton, Jr., and G. G. Ohlsen, to be published

An Underground Nuclear Explosion as a Polarized Neutron Source*

G. A. Keyworth and J. R. Lemley

Los Alamos Scientific Laboratory, University of California
Los Alamos, New Mexico 87544

Whereas an underground nuclear explosion is not the most conventional neutron source, it offers definite advantages, primarily connected with beam intensity. Each burst contains approximately one mole (10^{24}) of neutrons which are emitted in less than 0.1 μsec. A moderator is used to increase the neutron flux down to ∿20 eV, at which point the velocities of the moderator and of the neutrons are equal. Thus, neutrons from 20 eV to several MeV are available and are resolved by time-of-flight techniques. The experimental techniques for using nuclear explosions as neutron sources have been amply treated[1] in the literature and will not be discussed here.

The primary purpose of this particular experimental program is to determine spins of neutron resonances by the straightforward method of measurements with a polarized target and a polarized neutron beam. Until fairly recently, however, there was no satisfactory method of producing a polarized neutron beam from ∿50 eV to 100 keV. Shapiro[2] proposed utilizing the strong spin dependence of the (n,p) interaction to produce such a polarized neutron beam. In this energy range, the cross section for (n,p) scattering through the singlet state of the system is about 20 times larger than through the triplet state. Thus, an unpolarized neutron beam is polarized by passage through a suitably thick target of polarized protons. Shapiro has demonstrated this technique using neutrons up to 150 eV from a pulsed fast reactor.

The polarized proton target which we have used is a relatively common tool in high energy physics laboratories. It involves dynamic polarization of the protons in the waters of hydration of crystals of $La_2Mg_3(NO_3)_{12}\cdot 24H_2O$, i.e., LMN[3]. The crystal stack (2-cm diameter by 1.8 cm thick) was mounted in a copper microwave cavity which was located in the center of a superconducting split-pair coil operating at 20.3 kG. The coil was immersed in a liquid helium bath at 4°K in a cryostat which permitted room temperature access to the coil bore. The microwave cavity was contained in a separate cryostat whose tail was inserted into the bore of the superconducting coil. This latter cryostat contained liquid helium maintained at ∿1°K by a 1400 liter/sec mechanical pump. The cryostats contain thin windows to allow transit of the vertical neutron beam. The coil is located with its bore in the horizontal plane and the neutron beam passes through apertures in the gap.

The axis of the crystals was located perpendicular to the magnetic field direction. Under these conditions, microwaves of frequency 76.6 GHz are required to polarized the free protons. The microwave power was generated by a reflex klystron and transmitted by oversize (8-mm) waveguide to the cavity.

In the summer of 1969, an experiment was performed on the Physics 8 event at the Atomic Energy Commission's Nevada Test Site to determine the feasibility of polarizing such an intense beam in this manner. Of some concern was the extent of depolarization in the target due to heating from the neutron beam. Comparatively little energy deposit occurs as a result of the initial burst of gamma radiation. Calculations of neutron heating indicated a total temperature rise in the target of 3°K.

One of the features of LMN which makes it an excellent source of polarized protons is its long proton relaxation time (∿1 hr at 1°K). This same feature allows us to maintain constant polarization during the 3-4 msec duration between

*Work performed under the auspices of the U. S. Atomic Energy Commission.

arrival of the highest and lowest energy neutrons. At 4°K, the calculated final temperature, the proton relaxation time is still >100 sec. This estimate was confirmed on the Physics 8 event.

Measurement of the target polarization is normally made by use of the "Q-meter" nuclear magnetic resonance technique. In this method a small fraction of the protons in the target are caused to flip by an electromagnetic field from a coil near the sample. The coil is part of a tuned circuit whose electrical characteristics are altered by the proton transitions. The most common technique employed involves sweeping the NMR oscillator through the proton line in several minutes. In our case, we wished to monitor the polarization during the ∿4 msec duration of the neutron burst. We thus swept the frequency at a rate of 1 kHz and displayed the results of the sweep on an oscilloscope. The oscilloscope was then photographed by a high speed moving-film camera. Subsequent examination of the film showed no change in polarization in the target during the entire film exposure, which ended 1 sec after detonation. Thus we feel confident that this is a practical method of producing polarized neutrons over the energy range 20 eV to 100 keV.

Because this fast sweep NMR system was designed primarily to determine the change in polarization, it was not suited for accurate absolute polarization determination. The thermal equilibrium (TE) signal, i.e., the signal due to brute force polarization before microwave pumping, is compared to the enhanced signal to determine absolute polarization. With the system used in the Physics 8 experiment, the TE signal was nearly unobservable. However, since that experiment, we have acquired a PDP-15 computer with which we average the signal from the fast sweep to accurately determine the TE signal.

As discussed above, the proton polarization was perpendicular to the beam direction in the Physics 8 experiment. This offers the disadvantage that the beam must pass through the coil gap, thereby making it difficult to avoid Majorana depolarization. This problem is serious with the LMN system but far more serious with the actual target system, discussed in another contribution to this conference. For the case of s-wave neutrons, how the polarization vectors are oriented with respect to the beam direction is of no consequence as there is no transfer of angular momentum. Although in our energy range penetration considerations suggest that s-wave resonances predominate, it is still desirable to preserve the capability of spin determination of p-wave resonances. However, although not tacitly obvious, calculations of resonance formation probabilities reveal that, for targets of reasonably high spin, e.g., 5/2, approximately equal amounts of information regarding the spin configurations of p-wave resonances are determined for the polarization perpendicular or parallel to the beam direction.

We now have under construction a new LMN beam polarization system consisting of a high homogeneity coil (field uniformity ∿1 G over a 2.5-cm sphere), 10-watt extended interaction oscillator for a microwave power source, and a single cryostat whose 1°K bath is capable of being continuously filled from a 4°K bath. We expect this system to produce neutron beam polarizations of 60-70% with transmissions of 18%. This equipment, with a polarized subthreshold fissionable target, will be used in an experiment on the Physics 9 event in 1971 to measure spins of intermediate structure resonances.

References

1. B.C.Diven, Proceedings of the International Conference on the Study of Nuclear Structure with Neutrons, Antwerp, 1965 (North Holland, Amsterdam, 1966) p. 441.
2. F. L. Shapiro, ibid., p. 223
3. A. Abragham, M. Borghini, Progress in Low Temperature Physics (North Holland, Amsterdam, 1964) Vol. 4, p. 385; C. D. Jeffries, Dynamic Nuclear Orientation (Interscience Publishers, New York, 1963)

A Proposed Ultra-Low Temperature Polarized Target for Use with Single-Burst Neutron Sources*

J. R. Lemley and G. A. Keyworth

Los Alamos Scientific Laboratory, University of California
Los Alamos, New Mexico 87544

An underground nuclear explosion of the type used in physics experiments by the Los Alamos Scientific Laboratory (LASL)[1] produces approximately 1 mole (10^{24}) of neutrons with a generally continuous energy spectrum from about 40 eV to several MeV. These neutrons reach a target at the end of a 250-m flight path over a period of 3 msec; the neutron energy is determined by a time-of-flight technique. Beam area at the target is about 3 cm^2. After collimation and transmission through an LMN spin filter to polarize the beam, about 10^{15} neutrons reach the target. For a variety of nuclear reactions this high neutron flux produces events with good statistical frequency over a wide energy range in a very short time. The long flight path increases energy resolution.

An experiment currently being prepared for the next physics shot requires both a polarized neutron beam and a polarized target. Polarization of the neutron beam has been discussed in another paper at this conference[2]. The neutron-induced fission cross sections of certain nuclei such as ^{237}Np exhibit large subthreshold fission resonances due to coupling of the compound nuclear wave functions with states in the second potential minimum in the fission barrier. Presumably the coupling is between only states of the same J value. When a polarized neutron beam impinges upon a polarized ^{237}Np target, the probability of finding certain spin combinations is increased or decreased depending upon the relative polarizations of beam and target. Amplitudes of fission resonances with a specific J value will be increased or decreased relative to their areas when polarization is zero.

The nature of the neutron beam places several requirements upon the design of a polarized ^{237}Np target. Beam direction is necessarily vertical, and the cryostat must be designed to accommodate this. Since both the LMN target used to polarize the beam and the ^{237}Np target involve high magnetic fields, Majorana depolarization must be avoided in the field gradients along the beam path. Relative orientation of target spin, beam spin, and beam momentum must maximize the effect of the reaction to be studied in the angular distribution of the radiation to be detected. This is not necessarily consistent with minimizing Majorana depolarization when p-wave resonances are to be studied. In order for fission fragments from the $^{237}Np(n,f)$ reaction to escape from the target and reach counters, the ^{237}Np nuclei must lie within about 5 μm of the target surface but remain within a matrix which will permit polarization of the ^{237}Np nuclei. Target nuclei not close to the surface would be useless for counting purposes, and in addition their fissioning would cause excessive heating resulting in depolarization of the entire target. It is therefore necessary to use a minimum amount of ^{237}Np and to confine it to the surface of the target. Since the beam contains neutrons in the MeV energy range, no fissionable nuclei other than the ^{237}Np may be present. Many compounds of actinide elements, such as $UO_2Rb(NO_3)_3$, which might be suitable host matrices for dilution and polarization of ^{237}Np are eliminated.

Probably the greatest problem concerned with the ^{237}Np target is dissipation of heat produced by interaction of the beam and target. The major source of heating is the $^{237}Np(n,f)$ reaction with total fission fragment energy of 170 MeV. Using the neutron flux from a previous experiment and assuming that half

*Work performed under the auspices of the U. S. Atomic Energy Commission.

of the fission fragment energy is deposited in the target, 10 mg of ^{237}Np will deposit energy at the rate of approximately 10^4 erg/sec.

To prevent immediate warming and depolarization of the ^{237}Np nuclei, we propose to use as a heat sink the heat capacity of a system of nuclear spins in a high magnetic field at ultra-low temperatures. Using a ^3He-^4He dilution refrigerator, target temperatures of less than 20 mK can be maintained indefinitely before application of the neutron beam. At these temperatures it is possible to polarize the nuclear spins of (nonfissionable) metals such as thallium so that there is a relatively large heat capacity associated with alignment of the spins.

The effectiveness of a large nuclear heat capacity as a heat sink depends on the thermal resistance R_{SL} between the lattice and the nuclear spins. At very low temperatures for a metal in the nonsuperconducting state, the "lattice" is the thermal bath of the conduction electrons since lattice vibrations are in their ground states. R_{SL} is related to the nuclear spin-lattice relaxation time T_1 according to $R_{SL}C_S = T_1$ which is the time constant with which the spin temperature approaches that of a lattice maintained at constant temperature. C_S is the nuclear spin heat capacity. R_{SL} may be estimated from Korringa's relation, $T_1T_S = K$ where K is Korringa's constant and T_S is the spin temperature. The Korringa constant is commonly derived from measurements of the Knight shift when T_1 is not measured directly. $R_{SL}C_S = K/T$. If the nuclear heat capacity is given by $C_S = bH^2/T_S^2$ where b is a constant, the heat flow to the nuclei is $\dot{Q} = (T_S-T_L)/R_{SL} = (bH^2/K)(T_L-T_S)/T_S$ where T_L is the lattice (or electron) temperature. For thallium K is small (0.006 sec °K) and the nuclear moment is relatively large (1.6 nm)[3]. For the easily attainable field of 50 kG and 10 cm^3 of Tl, $|(T_S-T_L)/T_S| = 0.1$ when $\dot{Q} = 0.7\times10^4$ erg/sec. This ratio is temperature independent as long as the expressions for C_S and T_1 hold. If T_S increases from 15 mK to 100 mK, the heat absorbed is 2.4×10^4 erg.

The problem remains to find an environment in which ^{237}Np can be polarized and which will permit the nuclear spins to be in good thermal contact with the electronic system associated with a nuclear heat sink such as thallium metal. Neptunium-237 has two properties which should facilitate this. Its large magnetic moment (2.8 nm[4]) decreases the size of the effective field required to achieve a given polarization at a given temperature. In a metallic environment the high Z of the nucleus increases the coupling of the nuclear spins and conduction electrons and should decrease spin lattice relaxation time. There are ^{237}Np compounds and alloys which have hyperfine fields of several MG at the nucleus. At present a metallic matrix seems most desirable in order to establish sufficient thermal contact with a heat sink via conduction electrons.

An ultra low temperature system can also probably be adapted for use with pulsed neutron beams produced by linear accelerators, and other nuclei can be polarized for use as targets.

We thank Prof. J. C. Wheatley for valuable discussions about cryogenic aspects of the experiment.

References

1. B.C.Diven, Proc. of the Internatl. Conf. on the Study of Nuclear Structure with Neutrons, Antwerp, 1965 (North Holland, Amsterdam, 1966) p. 441
2. G. A. Keyworth and J. R. Lemley, "An Underground Nuclear Explosion as a Polarized Neutron Source," Proc. 3rd Internatl. Symp. Polarization Phenomena in Nuclear Reactions (to be published)
3. W. R. Abel et al., Physics 1 (1965) 337
4. J.A. Stone and W.L. Pillinger, Phys. Rev. 165 (1968) 1319

Performance of the LASL Polarized Source*

J. L. McKibben, G. P. Lawrence, and Gerald G. Ohlsen

Los Alamos Scientific Laboratory, University of California
Los Alamos, New Mexico 87544

Our construction of a source of polarized negative ions based on charge exchange reactions in cesium and argon was initiated in 1965; the initial design was reported five years ago at Karlsruhe. We have made many changes from the early design. A description of the source as of the end of 1968 has been published;[1] this description is still fairly accurate.

Installation. The source was installed and delivered its first beam through the tandem accelerator on July 4, 1969, and experiments commenced soon after. Experience soon showed that we needed remote control of a number of variables and this was incorporated during late 1969. During the first half of 1970 a total of 700 hours of operating time has been accumulated. The installation layout is shown in Fig. 1.

The beam is inflected 58° by a special double focusing magnet; the choice of angle was dictated by space and focusing considerations. Rotation of the direction of spin from the axial direction to any required direction is done by means of a crossed-field device which we call a spin precessor. The precessor can be mechanically rotated about its axis. The beam is brought to focus at the middle of the precessor by means of an electrostatic quadrupole doublet; a cup can intercept the beam there for measurement of the source intensity. A quadrupole singlet which follows the precessor is used to correct for cylindrical focusing effects of the spin precessor fields. The beam is brought to a second focus about ½ meter ahead of the accelerating tube by means of the 58° magnet and the einzel lens. A special viewer near the second focus has proven useful in finding the proper adjustments of focus and of the several steering elements.

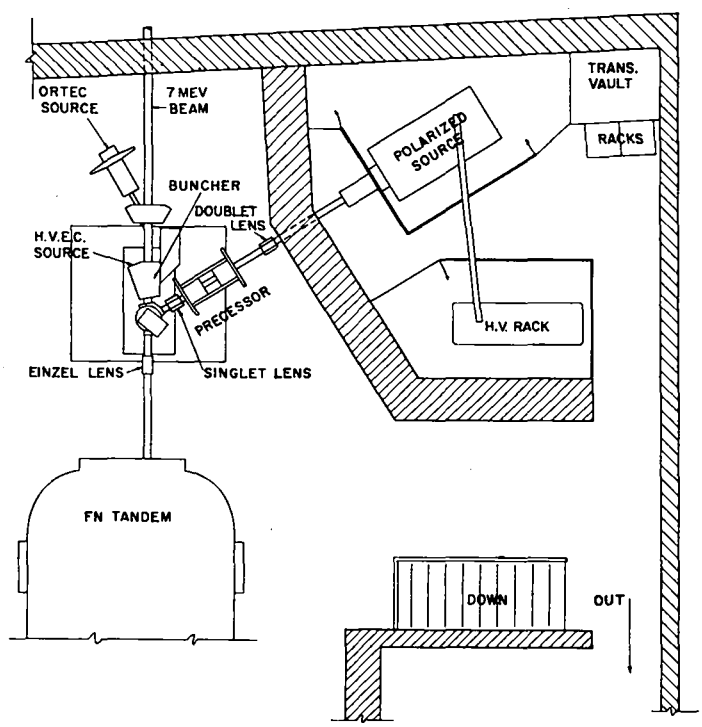

Fig. 1. Installation Arrangement for the LASL Polarized Ion Source

Transmission. The emittance of the beam as it leaves the source is known from the geometry of the source, and by measurement, to be approximately 1.0 cm rad $eV^{\frac{1}{2}}$. This is substantially smaller than the acceptance of the tandem Van de Graaff. However, the best transmission we have seen is 65% (from the precessor

* Work performed under the auspices of the U. S. Atomic Energy Commission.

cup to the target through a 2.5x2.5 mm aperture) for deuterons and 50% for protons.

Polarization and Intensity. The quenchable fraction of the beam varies in the range 86 to 90% for protons and 74-80% for deuterons under normal operating conditions. Better polarization values are obtained by rotating the smallest aperture into position at the focal point of the first acceleration lens and using about 1/3 the normal argon flow rates; under these conditions, polarizations of 93% for protons and 86% for deuterons have been measured. The best proton current delivered so far to a useful target is 107 nA; the best deuteron current so far observed is 208 nA with 74% polarization. Most of our usage has been with deuterons for which 60-100 nA is usually available while the available proton current is usually only about 25% less than the deuteron current.

Spin States Available. Certain spin states require a strong field (with respect to the hyperfine interaction) in the negative-ion-formation region, in order that large nuclear polarization can be maintained. However, too strong a field produces a low intensity beam with poor emittance. Our practice has been to use 6G for protons and 60G for deuterons; fortunately 60G does not cause a serious loss of intensity for deuterons. The polarizations of ions produced by a pure metastable beam are, for the magnetic fields of interest:

Ion	m_I	P_3	P_{33}	Field (in G)
H^-	$+\frac{1}{2}$	1	—	6
H^-	$-\frac{1}{2}$	-0.12	—	6
D^-	+1	1	1	6 (or 60)
D^-	0	0.012	-1.966	60
D^-	-1	-0.984	0.952	60

Actual polarizations are obtained by multiplying these numbers by the quenchable percentage value. This is the fraction of the negative ion beam produced through the metastable process, and is measured by quenching the metastable portion. For proton or deuteron vector polarization experiments, the spin is usually precessed to the vertical and the precessor is mechanically rotated to reverse the spin direction. To reverse the vector polarization in the case of deuterons it is often better to turn to the m_I=-1 state since mechanical rotation of the precessor may lose some of the beam; the steering elements can be adjusted to compensate for the beam shift effect but it takes time. For experiments involving tensor polarization, the spin axis is usually precessed in the horizontal plane and rotation of the counters is used instead of rotation of the precessor.

Stability and Intensity. The source runs unattended for many hours at a time. The polarization is quite stable; deviations of less than a percent during a run are common. The temperature of the cesium cell and its reservoir are each thermostatically controlled. The loss of cesium is <0.1 gram per hour and its cleanup during servicing has been easy. Good current stability does require finding stable operating conditions; in this respect we have been greatly aided by a transverse adjustment on the accel electrode which may be operated while the source is at high voltage. That this source is capable of much greater output we have little doubt, but recently our time has been spent mainly on its installation and utilization.

Reference

1. G. P. Lawrence, G. G. Ohlsen and J. L. McKibben, Phys. Lett. 28B, 594 (1969).

Absolute Beam Polarization Determination for the LASL Lamb-Shift Source by the Quench Ratio Method

Gerald G. Ohlsen, G. P. Lawrence, P. W. Keaton, Jr.,
J. L. McKibben, and D. D. Armstrong

Los Alamos Scientific Laboratory, University of California
Los Alamos, New Mexico 87544

In conjunction with a Lamb-shift polarized ion source, a "nuclear spin filter" provides an extremely clean way to select single hyperfine states of either hydrogen or deuterium metastable atoms. The spin filter action takes place in a ∿1600-MHz rf field (∿10 V/cm) parallel to the atomic beam, a (perpendicular) dc electric field (∿10 V/cm), and a (parallel) magnetic field whose strength is adjusted to correspond to resonance for the state desired. The output ion current versus spin filter magnetic field is schematically shown in Fig. 1. The current which remains when the magnetic field does not correspond to a resonance arises from the intense ground-state atomic beam which is also present. For state-1 selection of either hydrogen or deuterium, the metastable contribution is 100% polarized ($P = 1$ for hydrogen, $P_3 = P_{33} = 1$ for deuterium) while the background current has approximately zero polarization; thus, the actual beam polarization is approximately given by

$$p = \frac{I - I_o}{I} \equiv 1 - \frac{1}{Q} , \qquad (1)$$

where the quenching ratio, Q, is defined by I/I_o, and where p represents either P, P_3, or P_{33}. (If other than state-1 atoms are selected, the strength of the magnetic field in the region of ionization must be taken into account in computing the polarization.)

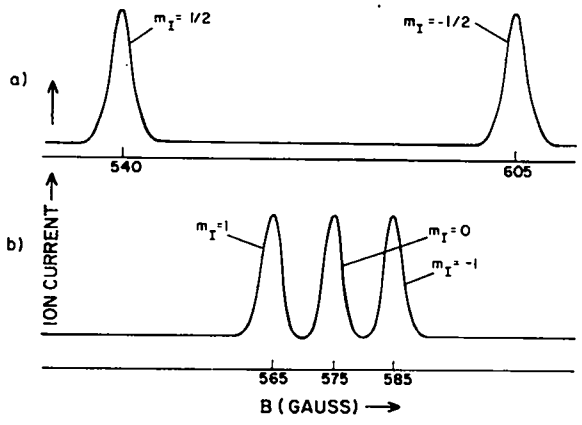

Fig. 1. a) Ion current versus B for H atoms. b) Ion current versus B for D atoms.

It is the purpose of the present paper to describe our efforts to evaluate the accuracy of the quench ratio method. We describe two small corrections and list a number of conditions which must be met for the results to be precise. Our conclusion is that the method is capable of ∿1/2% absolute accuracy, with about 1% reliability achieved to date. Most of our tests made use of $^4He(p,p)^4He$ scattering at 12 MeV and 112° (lab) where its analyzing power is ∿1.0.

First, we have noted that the quenched beam is actually slightly polarized (P or $P_3 \approx -0.03$). For typical hydrogen quench ratios of ∿10, Eq. (1) therefore overestimates the polarization by about 0.3%; for a typical deuterium quench ratio of 5, Eq. (1) overestimates the vector polarization about 0.6%. The precise mechanism that produces this effect is still under investigation. It appears to be associated with the fact that $m_J = -1/2$ metastable atoms are quenched much earlier than the $m_J = 1/2$ atoms. For more detail, see Ref. 1.

---

*Work performed under the auspices of the U. S. Atomic Energy Commission.

Second, the polarized component of the beam has better emittance than the unpolarized component; thus transmission through the accelerator can increase the beam polarization with respect to the value determined by quench ratio measurements made at the source. We have recently determined that this effect can be several percent and depends both on the design of the source output ion-optical systems and on the particular trajectory followed by the beam in the remaining transport elements and the accelerator itself. With one ion source lens design, for example, the effect was never greater than 1% (except for deliberately chosen transport parameters which led to poor transmission); with a recent lens modification, 5% effects (for deuterons) have been observed. This polarization enhancement can be taken into account with the relation $P_T = P_S/[P_S(1-\alpha)+\alpha]$, where P_T and P_S are the polarizations as measured at the target and at the source, respectively, and α is the accelerator transmission ratio for the unpolarized beam component and polarized component; α can be estimated in various ways and need only be crudely known to achieve $\sim$1% accuracy in the derived value of P_T. Alternatively, the quenching ratio can be measured with a faraday cup situated as close to the target as permits accurate beam current measurements (probably at a point just ahead of the tandem regulating slit jaws). Present data indicate that essentially no further polarization enhancement occurs from this point on, so that quench ratio measurements taken here would yield the true on target beam polarization to within 1% accuracy.

Probably the largest uncertainty arises from the requirement that no conditions in the source change between the filtered and quenched beam current measurements. Experience has shown that the ion source stability is such that at least 0.5-1% reproducibility is obtained. The measurements are usually made under computer control, and require about 7 sec to complete. Other conditions, which appear to be well satisfied, for the method to be absolute are 1) the spin filter parameters must be such that there is no overlap of states; 2) there must be no depolarization of the atomic beam between the spin selection and ionization region; 3) there must be no depolarization of the beam by charge exchange in a poor vacuum region (e.g., in the tandem accelerator terminal); and 4) no contaminant beam (e.g., electrons, heavy ions) may reach the current measuring device. With regard to 4), we have seen as much as 20 nA of unidentified heavy ions in a cup close to the source. A suitable magnetic field, such as the first section of our spin precessor, removes any such component. Finally, good current measurement practices should be used. More detail on these matters is given in Ref. 1.

The direction of the spin axis at the target must also be known accurately for some types of experiments. Unwanted bends of 1° or 2° can easily arise if the beam goes through bending magnets off the midplane or if a great deal of steering is used. These effects are discussed from a formal point of view elsewhere[2]. Our experience shows that somewhat better than 1° accuracy for deuterons and 2° accuracy for protons can be obtained with present techniques; better accuracy can be obtained by left-right and up-down polarization monitoring techniques.

References

1. G. G. Ohlsen, "The Los Alamos Lamb-Shift Polarized Ion Source: A Users Guide," Los Alamos Scientific Laboratory Report LA-4451 (unpublished)

2. R. R. Stevens, Jr., and G. G. Ohlsen, "Transfer Matrix Method for Polarized Beam Transport Calculations," Proc. 3rd International Symposium on Polarization Phenomena in Nuclear Reactions (to be published)

A Rapid Method for the Measurement of Analyzing Tensors in Reactions Induced by Polarized Deuterons*

G. P. Lawrence, Gerald G. Ohlsen, J. L. McKibben,
P. W. Keaton, Jr., and D. D. Armstrong

Los Alamos Scientific Laboratory, University of California
Los Alamos, New Mexico 87544

The cross section for a reaction induced by polarized deuterons may be written in the form

$$I(\theta,\phi) = I_o(\theta)\{1+\frac{3}{2}\langle P_y\rangle P^o_y(\theta)+\frac{2}{3}\langle P_{xz}\rangle P^o_{xz}(\theta)+\frac{1}{6}\langle P_{xx}-P_{yy}\rangle[P^o_{xx}(\theta)-P^o_{yy}(\theta)]+\frac{1}{2}\langle P_{zz}\rangle P^o_{zz}(\theta)\},$$

where the quantities in brackets represent the beam polarization quantities while $P^o_y(\theta)$, $P^o_{xz}(\theta)$, $P^o_{xx}(\theta)$, $P^o_{yy}(\theta)$, and $P^o_{zz}(\theta)$ represent the analyzing tensors for the reaction. The y axis is along $\vec{k}_{in} \times \vec{k}_{out}$, the z axis is along $\vec{k}_{in}$, and the x axis is chosen to make a right-handed coordinate system.

A beam produced by a polarized ion source is characterized by its vector and tensor polarization with respect to its quantization axis, p_Z and p_{ZZ}, together with the polar and azimuthal angles (β,ϕ), which describe the orientation of the quantization axis with respect to the x,y,z coordinate system described above. The angle ϕ is defined such that scattering to the "left" if the particle has spin "up" corresponds to $\phi = 0$, with positive ϕ corresponding to a rotation of the x axis toward the y axis. With this convention, the beam polarization quantities are

$$\langle P_y\rangle = p_Z \sin\beta\cos\phi \qquad \langle P_{xx}-P_{yy}\rangle = -\frac{3}{2} p_{ZZ} \sin^2\beta\cos 2\phi$$

$$\langle P_{xz}\rangle = -\frac{3}{2} p_{ZZ} \sin\beta\cos\beta\sin\phi \qquad \langle P_{zz}\rangle = \frac{1}{2} p_{ZZ} (3\cos^2\beta-1) \ .$$

If we adopt the convention that "up" describes the half-plane containing the quantization axis $(\hat{S})$ and the incident momentum $(\vec{k}_{in})$, then left, right, up, and down will correspond to $\phi = 0$, 180°, 270°, and 90°, respectively. Using the notation L, R, U, and D to denote the counts observed in the left, right, up, and down detectors, we can form the three observable asymmetries:

$$A_1 = \frac{2(L-R)}{L+R+U+D} = \left[\frac{3}{2} p_Z \sin\beta\ P^o_y\right] \Big/ \left[1 + \frac{1}{4} p_{ZZ} (3\cos^2\beta-1)\ P^o_{zz}\right]$$

$$A_2 = \frac{2(U-D)}{L+R+U+D} = \left[p_{ZZ} \sin\beta\cos\beta\ P^o_{xz}\right] \Big/ \left[1 + \frac{1}{4} p_{ZZ} (3\cos^2\beta-1)\ P^o_{zz}\right]$$

$$A_3 = \frac{(L+R)-(U+D)}{L+R+U+D} = \left[-\frac{1}{4} p_{ZZ} \sin^2\beta\ (P^o_{xx}-P^o_{yy})\right] \Big/ \left[1 + \frac{1}{4} p_{ZZ} (3\cos^2\beta-1)\ P^o_{zz}\right] ,$$

and the observable ratio

$$R = \frac{T^{(1)}}{T^{(2)}} = \left[1 + \frac{1}{4} p^{(1)}_{ZZ} (3\cos^2\beta-1)\ P^o_{zz}\right] \Big/ \left[1 + \frac{1}{4} p^{(2)}_{ZZ} (3\cos^2\beta-1)\ P^o_{zz}\right] ,$$

where the superscripts 1 and 2 refer to two runs taken with different values of the polarization p_{ZZ}, and where T = L+R+U+D. The two runs in this case are assumed to correspond to the same integrated current, target thickness, etc. If $\beta = 0$ is chosen, the four detectors may set at different angles so that P^o_{zz} at 4 angles may be obtained simultaneously.

*Work performed under the auspices of the U. S. Atomic Energy Commission.

The four quantities above suffice for the determination of all four observables. In particular, if β is chosen equal to 54.7°, we obtain

$$A_1 = \frac{3}{2} p_Z \sin\beta \, P^o_y \qquad A_3 = -\frac{1}{4} p_{ZZ} \sin^2\beta \, (P^o_{xx} - P^o_{yy})$$

$$A_2 = p_{ZZ} \sin\beta\cos\beta \, P^o_{xz} \qquad R = 1 \quad .$$

That is, the ratios determine three of the four tensors in a monitor-free manner exactly analogous to the two-detector scheme long used for accurate spin-½ analyzing power measurements. The fourth tensor is determined by choosing $\beta = 0$, in which case

$$A_1 = A_2 = A_3 = 0 \qquad R = \left[1 + \frac{1}{2} p^{(1)}_{ZZ} \, P^o_{zz}\right] \Big/ \left[1 + \frac{1}{2} p^{(2)}_{ZZ} \, P^o_{zz}\right] \quad ;$$

all of the dependence of the measurements on current integration and the like is thus thrown into this term.

At Los Alamos we have applied this technique successfully in a large number of experiments; we use a 4-detector reaction chamber which can be rotated azimuthally and set at any of the quadrant angles with 0.1° accuracy by means of a microswitch-controlled 2-speed motor. For the ratio measurements we sequentially rotate each of the four counters into each of the four azimuthal positions and use geometric means for L, R, U, D; that is, for example, $L = (L_1 L_2 L_3 L_4)^{1/4}$; where L_1 is the number of counts observed by detector 1 during the run in which it was in the left position, and so on. We use an $\sim$80% $m_I = 1$ beam for the ratio measurements; that is, a beam with $p_Z = p_{ZZ} = \sim 0.8$. Occasionally we use an $\sim$80% $m_I = 0$ beam as a check ($p_Z = 0$, $p_{ZZ} = \sim -1.6$). This ensures, for example, that the P^o_{xz} measurement is not contaminated by a P^o_y contribution because of misalignment and that left-right asymmetries vanish when $\langle P_y \rangle = 0$, etc.

For the measurement of P^o_{zz}, no azimuthal rotation of the detectors is used since there is no azimuthal cross section dependence. For this ratio we use an $m_I = 1$ followed by $m_I = 0$ polarized beam, so that $p^{(1)}_{ZZ} = \sim 0.8$ and $p^{(2)}_{ZZ} = \sim -1.6$.

Application of this technique requires good control and knowledge of the actual direction of the quantization axis, which calls for some care with respect to the effects of bending magnets, electrostatic steerers, etc. We have found reproducibility to one degree or better in β; a ± 0.5-degree uncertainty contributes an error of $\pm 0.75\%$ in the observed asymmetry in the least favorable case.

Due to the high rate of data acquisition it has been necessary to automate the described measurement procedure as much as possible. The LASL tandem on-line computer controls the reaction chamber rotation sequence, and is interfaced with the polarized ion source to automatically measure beam polarization (one measurement for each ϕ angle change); it accumulates and stores the data at each of the designated angles, and at the end of each sequence calculates the appropriate geometric means, averages beam polarization, and computes the relevant analyzing tensors. In "fully automatic" mode the computer runs through the entire 4-fold sequence without operator intervention (once the appropriate gates and indices have been set). With the available beam intensities and the degree of automation noted, it is usually possible to measure one complete angular distribution of the four tensors (5° intervals) in a 24-hour period.

NEUTRON POLARIZATION IN THE T(d,n)^{4}He REACTION USING A POLARIZED INCIDENT BEAM*

W. B. Broste,† G. P. Lawrence, J. L. McKibben, G. G. Ohlsen, and J. E. Simmons
Los Alamos Scientific Laboratory, University of California,
Los Alamos, New Mexico 87544

Measurements have been made of the neutron polarization from the T(d,n)^{4}He reaction with polarized deuterons incident. This type of polarization transfer measurement was the first of its kind at Van de Graaff energies. The experiments were made possible by the recent initial operation of a high performance Lamb-shift polarized ion source on the Los Alamos FN tandem Van de Graaff accelerator, together with the availability of an efficient liquid helium neutron polarimeter.

The polarization of the outgoing neutrons was measured when the incident deuteron beam was 76% in the $m_I = +1$ state with respect to a quantization axis perpendicular to the horizontal reaction plane. Gammel et al.[1] have provided a formalism for the description of polarization observables in the T(d,n)^{4}He reaction; in their notation, the outgoing neutron polarization for the beam used is given by

$$\langle \sigma_y \rangle = \frac{\left(P(\theta) + \frac{3}{2}\langle P_y \rangle P_y^y(\theta) + \frac{1}{2}\langle P_{yy} \rangle P_{yy}^y(\theta)\right)}{\left(1 + \frac{3}{2}\langle P_y \rangle P_y^o(\theta) + \frac{1}{2}\langle P_{yy} \rangle P_{yy}^o(\theta)\right)} \qquad (1)$$

The quantities $\langle \sigma_y \rangle$, $P(\theta)$, $P_y^y(\theta)$, $P_{yy}^y(\theta)$, $P_y^o(\theta)$ and $P_{yy}^o(\theta)$ describing the reaction are given in a coordinate system with its y-axis along the normal $\vec{n} = \vec{k}_d \times \vec{k}_n$, where $\vec{k}_d$ and $\vec{k}_n$ are the directions of the deuteron and neutron momenta. For the beam chosen for the experiments $\langle P_y \rangle = \langle P_{yy} \rangle = .76$. $P(\theta)$, $P_y^o(\theta)$ and $P_{yy}^o(\theta)$ were measured in separate experiments.

The deuteron beam was accelerated onto a 3-cm long gas target filled with T_2 gas at 5 atm. The neutrons were collimated and had their spins precessed ±90° before scattering from a 5.9 cm x 6.1 cm cylindrical volume of liquid helium either 99 cm or 139 cm from the target. Neutrons scattered at angles of 117° or 125°, depending on their energy, were detected in 5.1 cm x 17.8 cm x 7.6 cm NE102 proton recoil scintillators at a distance of 25.4 cm. The measured asymmetries were corrected for the effects of multiple scattering and finite geometry, then divided by n-helium polarization analyzing powers calculated from the phase shifts of Hoop and Barschall[2] to determine $\langle \sigma_y \rangle$.

For $\theta = 0$, formula (1) simplifies to

$$\langle \sigma_y \rangle = \frac{3}{2}\langle P_y \rangle P_y^y(0)/\left(1 + \frac{1}{2}\langle P_{yy} \rangle P_{yy}^o(0)\right) \qquad (2)$$

Using independent measurements of P^{o}_{yy}, the polarization transfer coefficient $P^{y}_{y}(0)$ was determined for deuteron energies of 3.9, 7.0, 9.0, 11.4, 13.0, and 15.0 MeV. The results are given in Fig. 1. Above 7.0 MeV, $P^{y}_{y}(0)$ approaches the value 2/3 as might be expected from a simplified stripping picture for the interaction. As the deuteron energy decreases, the influence of the 107 keV $J^{\pi} = 3/2^{+}$ resonance, where $P^{y}_{y}(0) = -2/3$, begins to be felt, and $P^{y}_{y}(0)$ drops to -0.015 ± 0.028 at $E_d = 3.9$ MeV. The dashed curve on Fig. 1 indicates the neutron polarization $\langle \sigma_y \rangle$ which would be obtained for a 100% polarized beam. Actual values of $\langle \sigma_y \rangle$ measured for $\langle P_y \rangle = .76$ reached a maximum of 0.565 ± 0.036 for $E_d = 15$ MeV.

The neutron polarization was measured as a function of θ at 7.0 and 11.4 MeV incident deuteron energy. Figure 2 illustrates the results at 11.4 MeV. Neutron polarization is reckoned positive in the direction along the deuteron spin quantization axis. The data at 7 MeV are very similar to the 11.4 MeV results shown. Although the quantities $P(\theta)$, $P^{o}_{y}(\theta)$ and $P^{y}_{y}(\theta)$ have been determined, further measurements would be required to obtain values for $P^{y}_{y}(\theta)$ and $P^{y}_{yy}(\theta)$. Nevertheless, the appearance of the very large negative polarization $\theta^{yy} = 37\frac{1}{2}^{\circ}$ right leads one to believe that at this point the reaction is dominated by a spin flip mechanism, in contrast to the almost complete non-spin flip at zero degrees.

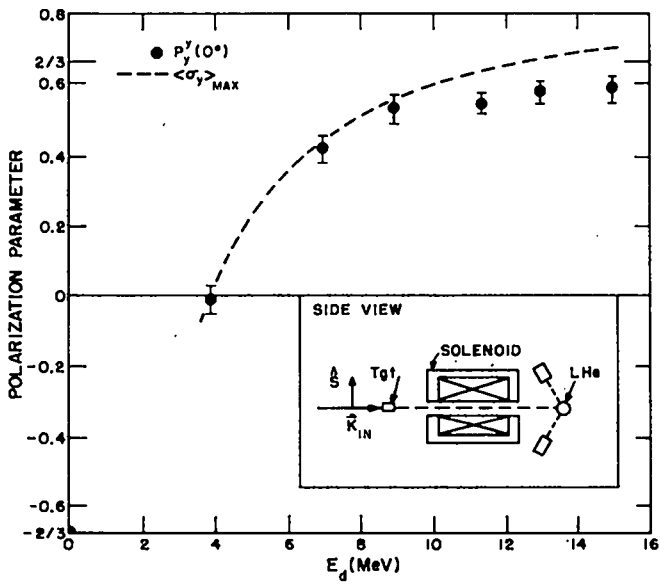

Figure 1

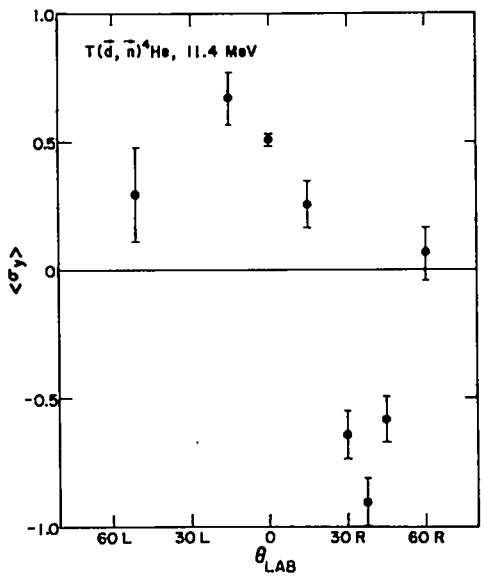

Figure 2

*Work performed under the auspices of the U.S. Atomic Energy Commission.
†Associated Western Universities Fellow from University of Wyoming.
1) J. L. Gammel, P. W. Keaton, and G. G. Ohlsen, these proceedings.
2) B. Hoop and H. H. Barschall, Nucl. Phys. 83 (1966) 65.

PRELIMINARY MEASUREMENTS OF NEUTRON POLARIZATION FROM THE $D(\vec{d},\vec{n})^3He$ REACTION USING A POLARIZED INCIDENT BEAM*

J. E. Simmons, W. B. Broste†, George P. Lawrence, and Gerald G. Ohlsen

Los Alamos Scientific Laboratory, University of California,
Los Alamos, New Mexico 87544

The $D(d,n)^3He$ reaction has long been an important neutron source. At zero degrees (lab) the differential cross section,[1] I(0) is large varying from approximately 30 mb/sr at E_d = 1 MeV to 90 mb/sr at E_d = 10 MeV, with a Q-value of 3.26 MeV. Much effort has been given to measurements of neutron polarization from this reaction; a summary of existing measurements[2] indicates that the polarization at θ = 30° lab varies from -0.1 at 2 MeV to +0.3 at 12 MeV. Recent measurements[3] on the outgoing proton polarization show increased values at higher energies namely ≈ 0.5 at 12 MeV. However, the differential cross section is sharply peaked forward which results in an unfavorable cross section at the angles for which the neutrons have a significant polarization. At E_d = 10 MeV,[4] for example, the cross section ratio, I(0)/I(30), has the value 12. Backgrounds would also be serious under such conditions. The net result is that the d-d reaction has not been very attractive as a polarized neutron source.

It is clearly of interest to measure the extent to which neutron polarization may be generated by transfer from an incident polarized deuteron beam. A preliminary experiment has been performed at the Los Alamos FN tandem accelerator, as a continuation of comparable measurements on the $T(d,n)^4He$ reaction.[5] The beam was accelerated onto a 3-cm gas target with beam quantization axis pointing in the vertical direction, here denoted as the y-direction. The deuteron beam was ∿78% in the m_I = +1 spin state (as measured at the source), that is, with vector and tensor polarization given by $p_3 = p_{33} = 0.78$ with deviations of order ± .01 depending on ion source conditions. Beam intensities on target varied in the range 10-45 nA.

The y-component of outgoing neutron polarization was measured at 0° by means of a liquid helium polarimeter, including a precession solenoid for which a diagram is given elsewhere.[5] Equations[6] relating the observables and beam polarization read as follows:

$$\langle \sigma_y \rangle = \frac{3}{2} p_3 P_y^y(0)/[1 + \frac{1}{2} p_{33} P_{yy}^o(0)] = e/P_2(\theta_2),$$

where $\langle \sigma_y \rangle$ is the measured neutron polarization, e and $P_2(\theta_2)$ are the observed asymmetry and the analyzing power in n-^{4}He scattering, p_3 and p_{33} are the vector and tensor beam polarizations, $P_y^y(0)$ is the polarization transfer parameter and $P_{yy}^o(0)$ is a polarization efficiency tensor in the reaction.

The preliminary results show large polarization effects. Measurements were made at 0° lab for 6 deuteron energies in the range 4.0 to 13.5 MeV. The raw asymmetries had values near 0.63 with statistical errors of order ± .015; little if any dependence on energy is discernible. These results may be contrasted with results from the $T(\vec{d},\vec{n})^4$He reaction,[5] where a spin flip mechanism causes $\langle \sigma_y \rangle$ at 0° to cross zero near 3.9 MeV. It is estimated that multiple scattering and geometry corrections of order 10% will be applicable to these asymmetries, which would result in values of $\langle \sigma_y \rangle$ near 0.70. Auxiliary intensity measurements made during the experiment gave values of $P_{yy}^o(0) \approx 1/4$, roughly independent of energy. These results lead to estimates for $P_y^y(0)$ near .66, which would lead to neutrons with ~ 90% polarization for a 100% polarized ($m_I = 1$) beam of deuterons. The process behaves very much as if the neutron spin was virtually unaffected by the interaction at 0°. This qualitatively is what might be expected from a stripping process. Light as the reaction particles are, good fits to the differential cross section have been obtained[7] by an exchange stripping model.

This preliminary work demonstrates that the $D(\vec{d},\vec{n})^3$He reaction is an excellent source of polarized neutrons at 0° for neutron energies in the range 7 to 16 MeV.

*Work performed under the auspices of the U.S. Atomic Energy Commission.
†Associated Western Universities Fellow from University of Wyoming.

1) J.E. Brolley and J.L. Fowler, Fast Neutron Physics, Vol. I, (Interscience Pub., N.Y., 1960) Chapter I.C.
2) H. Barschall, Proc. 2nd International Symp. on Polarization Phenomena (Birkhäuser Verlag, 1966) p. 393.
3) L.E. Porter and W. Haeberli, Phys. Rev. 164 (1967) 1229.
4) S.T. Thornton, Nucl. Phys. A136 (1969) 25.
5) W.B. Broste, et al. these proceedings.
6) J.L. Gammel, P.W. Keaton, Jr., and G.G. Ohlsen, these proceedings.
7) M.D. Goldberg and J.M.LeBlanc, Phys. Rev. 119 (1960) 1992.

Asymmetries in Deuteron Scattering from a Polarized ^{3}He Target*

Bob E. Watt and W. T. Leland

Los Alamos Scientific Laboratory, University of California
Los Alamos, New Mexico 87544

The experiment described herein was performed on the Los Alamos tandem Van de Graaff using a polarized ^{3}He gas target and an unpolarized deuteron beam. Figure 1 shows schematically the target cell arrangement. Basically, the cell consists of a pyrex vessel to which appropriate aluminum windows have been attached to permit passage of the primary beam and allow scattered or reaction particles to exit. The primary deuteron beam is collimated to a diameter of 1/8-in. by means of apertures ahead of the cell, passes through entrance and exit windows of 0.0003-in. aluminum, and is stopped and monitored with a deep faraday cup. Scattered deuterons exit through 0.0005-in. aluminum windows and are detected with silicon solid state detectors. The angular position of the scattered deuterons is defined by slits, one near the exit window (not shown) and the other at the detector. Polarization of the ^{3}He was accomplished by an optical pumping technique which was developed by Colegrove et al.[1]. The degree of polarization was calculated from the relation

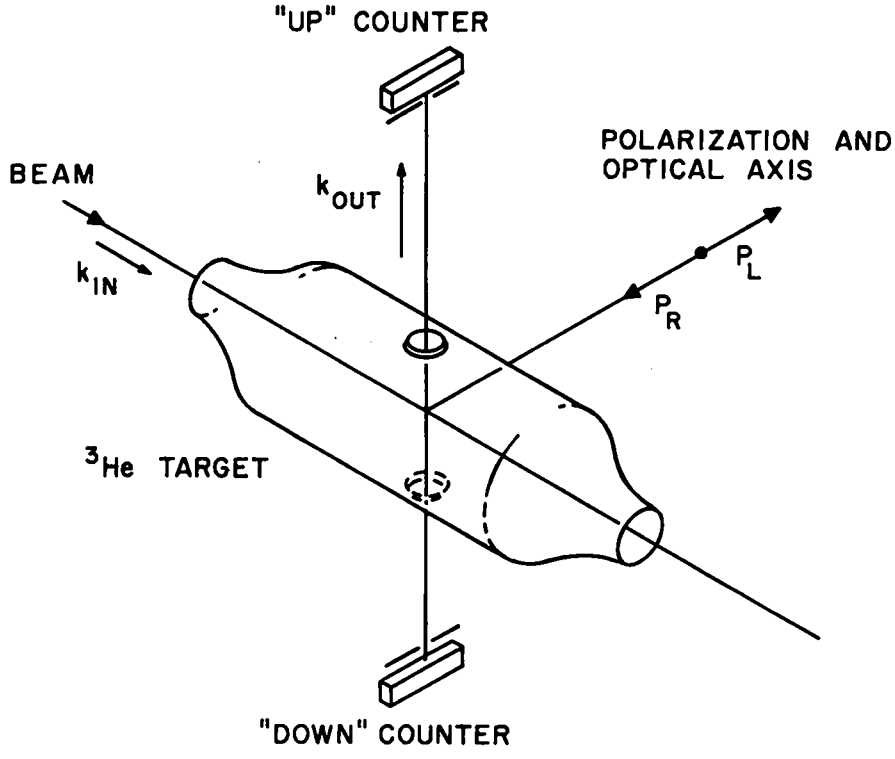

Fig. 1. Polarized ^{3}He target cell.

$$\frac{\Delta I}{I} = \frac{P}{3+P^2}\,[6-2P+3(1-P^2)k] \ ,$$

where ΔI is the difference in amount of light absorbed by ^{3}He metastables with and without polarization, I is the amount of light absorbed by ^{3}He metastables, P is the nuclear polarization, and k is a constant which depends on various transition probabilities and the relative degree of illumination of the F = 1/2 and F = 3/2 levels. Several investigators[1-5] have discussed the relation between P and the observed optical signals. We have chosen k = 0.3 which agrees with the measurements made by Hauer and Klinger[3].

A typical point was obtained by positioning the up and down counters at the appropriate angle and then making two runs with a reversal of the polarization between runs. The scattering asymmetry was then calculated from the formula

$$A_S = [(1-R)/(1+R)]\,\frac{1}{2}\,\left(\frac{1}{P_L} + \frac{1}{P_R}\right) \ ,$$

*Work performed under the auspices of the U. S. Atomic Energy Commission.

where $R \equiv \sqrt{U_L D_R / D_L U_R}$

U_L = "up" detector count with left circular polarization,

U_R = "up" detector count with right circular polarization,

D_L = "down" detector count with left circular polarization,

D_R = "down" detector count with right circular polarization,

P_L = ^{3}He target polarization, left,

P_R = ^{3}He target polarization, right.

By combining measurements where only the direction of the polarization is changed we are able to cancel out any asymmetries that are spin independent. Typical target polarization were in the range 0.17 to 0.20. Table 1 and 2 tabulate our results for 9.9 MeV and 11.9 MeV deuterons, respectively. Positive asymmetry is reported when a majority of the scattered particles have $\vec{k}_{in} \times \vec{k}_{out}$ parallel to P. Error estimates are based entirely on counting statistics.

Table 1. Deuteron scattering asymmetries for 9.9 MeV.

$\theta_{c.m.}$	A_S
78.2	0.139±0.02
83.5	0.087±0.019
88.6	0.004±0.015
94.1	-0.059±0.014
102	-0.121±0.014
109	-0.209±0.018
115	-0.273±0.022
121	-0.242±0.022

Table 2. Deuteron scattering asymmetries for 11.9 MeV.

$\theta_{c.m.}$	A_S
78.2	0.258±0.031
	0.29 ±0.06
83.4	0.079±0.028
89	0.030±0.019
94	-0.030±0.015
100	-0.11 ±0.026
102	-0.159±0.022
	-0.164±0.038
109	-0.188±0.027
115	-0.282±0.026
121	-0.361±0.031
127	-0.327±0.077

References

1. F. D. Colegrove, L. D. Schearer and G. K. Walters, Phys. Rev. 132 (1963) 2561
2. R. C. Greenhow, Phys. Rev. 136 (1964) A660
3. W. Klinger, Ph.D. Thesis, Friedrich-Alexander-Universität, Erlingen-Nürnberg (May, 1968)
4. N. Hauer and W. Klinger, Jahresbericht der Arbeitsgruppen am Institut Glückstrasse, pp. 105-106, Physikalisches Institut Universität, Erlangen-Nürnberg (1967/68)
5. S. D. Baker, D. H. McSherry, and D. O. Findley, Phys. Rev. 178 (1969) 1616

Polarization of 22-MeV Neutrons Elastically Scattered from Liquid Tritium and Deuterium*

J. D. Seagrave, J. C. Hopkins, E. C. Kerr, R. H. Sherman, A. Niiler, and R. K. Walter

Los Alamos Scientific Laboratory, University of California
Los Alamos, New Mexico 87544

The asymmetries from $T(\vec{n},\hat{n})T$ elastic scattering of 22.1-MeV incident neutrons have been measured for 11 laboratory angles between 40° and 118.5°. Heretofore, information about this interaction has been limited to one measurement[1] at 1.1 MeV and to predictions from phase-shift analysis[2] of the cross section data below 6.0 MeV. A cryogenic system provided a one-mole cylindrical sample of liquid tritium.

The Los Alamos vertical Van de Graaff accelerator and Mobley buncher were used with the T(d,n) reaction at a deuteron energy of 6 MeV. The 22.1-MeV neutrons produced at 29.8° (lab) were (+47.4 ± 1.45)% polarized[3].

Two detectors placed at 2.5 meters from the sample were massively shielded with copper, polyethylene, and tungsten. In addition, n-γ discrimination was employed to reduce the gamma-ray background. Corrections for differences in detector efficiencies were based on measurements with the detectors interchanged. The data were corrected for various other artificial asymmetries.

The results are shown in fig. 1 and tabulated in table 1. The $^3He(\vec{p},\hat{p})^3He$ polarization data at 21.3 MeV of Tivol[4] are sketched for comparison. Small corrections were applied for multiple scattering. The solid curve is a phase shift fit to the polarization data and the differential cross section[6].

Table 3: $T(\vec{n},\hat{n})T$ Polarizations $P_2(\theta_2)$ at 22.1 MeV

$\theta_2$lab (deg)	θ_2c.m. (deg)	$\cos\theta_2$ c.m.	ε	$P_2(\theta_2)^\dagger$	δP_2 absolute	$(\delta P_2/P_2)$ percent statistics
40	52.4	0.610	-0.095	-0.20	0.058	5.5
55	70.9	0.327	-0.14	-0.30	0.059	5.0
70	88.3	0.029	-0.19	-0.40	0.061	5.2
80	99.2	-0.160	-0.22	-0.47	0.071	8.6
85	104.5	-0.250	-0.24	-0.52	0.080	11.0
90	109.5	-0.334	-0.21	-0.45	0.085	13.0
95	114.5	-0.414	0.13	0.27	0.070	21.0
100	119.2	-0.488	0.24	0.59	0.098	14.0
105	123.8	-0.557	0.35	0.82	0.110	11.0
110¼	128.5	-0.623	0.36	0.83	0.096	8.6
118½	135.6	-0.714	0.31	0.69	0.078	6.2

†Based on a source polarization of 0.474 ± 0.015.
††Also includes ±0.026 uncertainty in artificial asymmetries.

*Work performed under the auspices of the U. S. Atomic Energy Commission.

In preparation for the tritium measurements, observations of $D(\vec{n},\hat{n})D$ asymmetries were made at the same energy. These results are consistent with the earlier work of Malanify et al.[5]. Details of this experiment will be found in the thesis by R. K. Walter[6] and in two review papers by Seagrave[7,8]. A paper combining all LASL work on n-D and n-T cross sections and polarization work is in preparation.

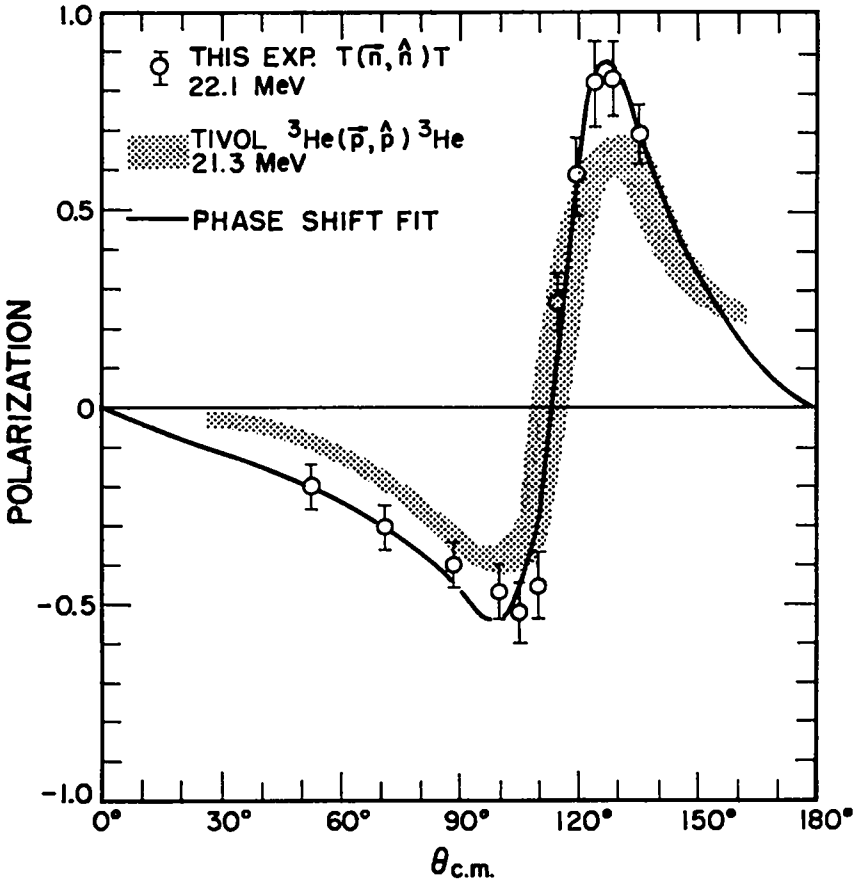

Fig. 1. $T(\vec{n},\hat{n})$ polarizations at 22.1 MeV. Comparison is made with the charge-conjugate reaction studied by Tivol[4], and with a phase-shift fit to both polarization and differential cross section[6,7].

References

1. J. D. Seagrave, L. Cranberg, and J. E. Simmons, Phys. Rev. 119 (1960) 1981
2. T. A. Tombrello, Phys. Rev. 143 (1966) 772
3. W. Broste and J. E. Simmons, private communication
4. W. F. Tivol, Thesis (1968) UCRL-18137
5. J. J. Malanify, J. E. Simmons, R. B. Perkins, and R. L. Walter, Phys. Rev. 146 (1966) 632
6. R. K. Walter, Ph.D. Thesis, Brigham Young University (1969); Los Alamos Scientific Report LA-4334
7. J. D. Seagrave, Proceedings of the Symposium on Light Nuclei, Few Body Problems, and Nuclear Forces, Brela, Jugoslavia, 1967 (Gordon & Breach, London, 1969) Vol. II, p. 787
8. J. D. Seagrave, Proceedings of the Internatl. Conf. on Three-Body Problem, Birmingham, England, 1969 (North Holland, Amsterdam, 1970) p. 41

Polarization in Nucleon-Deuteron Scattering at Medium Energies*

Victor Franco
Department of Physics, Brooklyn College of the City University of New York,
Brooklyn, New York 11210**
and
Los Alamos Scientific Laboratory, University of California
Los Alamos, New Mexico 87544

New techniques[1] have created the possibility of performing detailed measurements on recoil deuterons in nucleon-deuteron (N-d) collisions at medium energies and at recoil angles near 90° (laboratory system). Such collisions correspond to nucleons being scattered through small angles and should be well described by the Glauber approximation[2] in which single and double collisions are treated. To describe spin-dependent properties such as polarizations, it is necessary to use the spin-dependent N-N elastic scattering amplitudes in the calculations. Analyses above 800 MeV suffer from the paucity of n-p data. The situation below 800 MeV is more favorable since significant n-p data exist there. Consequently we have calculated cross sections and polarizations for p-d collisions at and below 800 MeV.

Our calculations include single and double scattering effects. To facilitate obtaining a first estimate of the cross sections and polarizations, we assume the deuteron to be a pure S-state. In the double scattering amplitude (only) we neglect those terms which vanish in the forward direction and Coulomb effects and we approximate the N-N amplitudes by Gaussian functions of momentum transfer q (i.e., by $a_i \exp(-b_i q^2)$, where a_i and b_i are complex), or by q or q^2 multiplying such functions. Calculations in which these approximations are not made are in progress. In the present analysis we use the Dubna phase shifts[3] for the N-N amplitudes, and the Moravcsik III wave function[4] for the deuteron.

In fig. 1 we show the angular distribution of protons for an unpolarized incident beam. For protons polarized 100% normal to the scattering plane, the intensities differ from that shown by ±33% near 10° and by virtually 0% below 1°. Near 5° $d\sigma/d\Omega$ exhibits a small Coulomb-nuclear destructive interference. The effect of double scattering on $d\sigma/d\Omega$ is negligible below 1°, but increases rapidly with increasing angle above 1°. Near 10° its neglect leads to a cross section that is more than 20% too large.

In fig. 2 we present the vector polarization $\langle T_{11}/i \rangle$ of the deuteron. We show results for unpolarized protons and for protons polarized 100% normal to the scattering plane. The direction $\hat{n}$ denotes $\hat{k}\times\hat{k}'/|\hat{k}\times\hat{k}'|$, where $\hat{k}$ and $\hat{k}'$ give the directions of the incident and scattered protons, respectively. For $\theta_{cm}<2°$, $\langle T_{11}/i \rangle < 0.025$ for unpolarized protons. However, use of polarized protons could yield vector polarizations as large as 0.07 near 1.5°. Furthermore, use of polarized protons reveals structure in $\langle T_{11} \rangle$ for $\theta_{cm}<2°$. The curves for $\vec{P}_{inc}=\pm\hat{n}$ form the envelope of the curves for arbitrary incident-nucleon polarizations along a direction parallel to $\hat{n}$. To prove this, note that for incident polarizations parallel to $\hat{n}$, $\langle T_{11}/i \rangle$ is a monotonic function of $\vec{P}_{inc}\cdot\hat{n}$ for fixed θ_{cm}. It therefore attains its physically allowable maximum and minimum values at $\vec{P}_{inc}=\pm\hat{n}$. For $d\sigma/d\Omega$ the relative importance of double scattering increases with increasing θ_{cm}, but for $\langle T_{11}/i \rangle$ no such statement can be made for $\theta_{cm}<10°$. For $\vec{P}_{inc}=0$

*Work supported in part by the National Science Foundation, the City University of New York Faculty Research Program, and the U. S. Atomic Energy Commission.
**Present address.

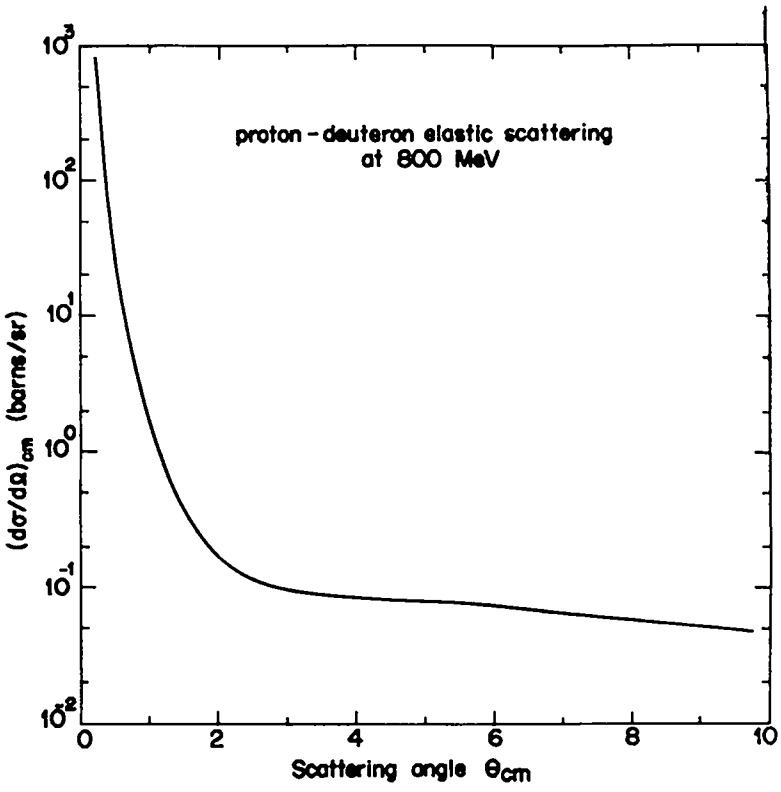

Fig. 1. Angular distribution for scattering of 800-MeV unpolarized protons by deuterium.

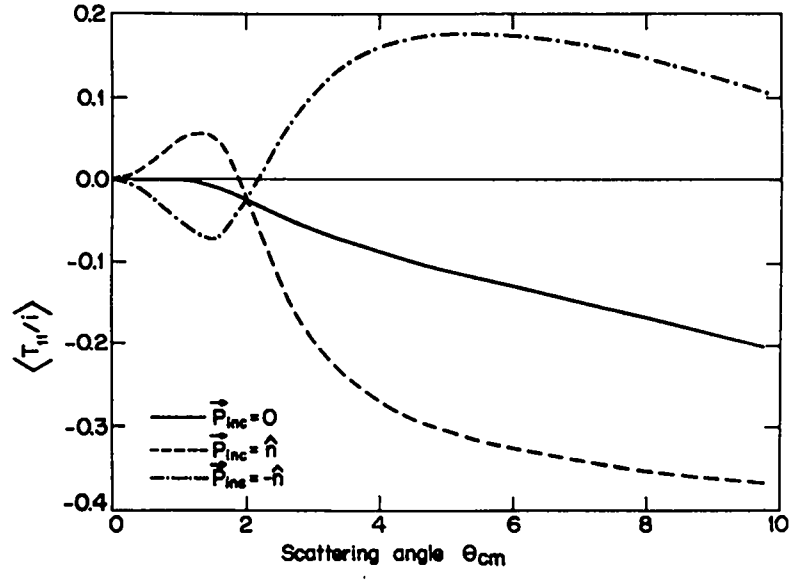

Fig. 2. Angular variation of the vector polarization of the deuteron in 800-MeV p-d scattering. The angle θ_{cm} is the scattering angle of the proton. The solid curve corresponds to unpolarized incident protons. The dashed and dot-dash curves correspond to incident protons fully polarized normal to the scattering plane.

double scattering effects change $\langle T_{11}/i \rangle$ by less than 0.002 for $\theta_{cm}<10°$, and show no tendency to increase with increasing θ_{cm}. For $\vec{P}_{inc}=\pm\hat{n}$ these effects are significant for $\theta_{cm}\gtrsim 2°$, producing changes in $\langle T_{11}/i \rangle$ that are typically $\sim\pm 0.02$, and showing some tendency to increse with angle for $\theta_{cm}\gtrsim 7°$.

References

1. J. E. Brolley, G. G. Ohlsen, and G. P. Lawrence, "Proposal for a Lamb-Shift Polarimeter," Proc. 3rd International Symp. on Polarization Phenomena in Nuclear Reactions (to be published)
2. V.Franco and R.J.Glauber, Phys. Rev. 142 (1966) 1195; V.Franco, Phys. Rev. Lett. 21 (1968) 1360, and references cited therein.
3. Z. Janout et al., Nucl. Phys. A127 (1969) 449
4. M.J. Moravcsik, Nucl. Phys. 7 (1958) 113

Proposal for a Lamb-shift Polarimeter*

J. E. Brolley, G. P. Lawrence, and Gerald G. Ohlsen

Los Alamos Scientific Laboratory, University of California
Los Alamos, New Mexico 87544

Spin polarization measurements on low energy charged particles have not, in general, been technically feasible to date. In this note we suggest a novel procedure which should prove useful for H, D, (and T) ions in the energy range 0-500 keV.[1] The particular applications proposed[2] for the device include the study of spin polarization of recoil protons and deuterons near 90°, corresponding to very small angle scattering of 800 MeV protons (LAMPF H^- beam) from H_2 and D_2 jet targets presently being developed. Polarization occurring in small angle (p,p) and (p,d) scattering is not well fitted by predictions calculated from phase shifts. The existing data, however, are meager since this is a region not readily accessible by conventional techniques; using the jet targets and the proposed polarimeter it should be possible to considerably augment small angle polarization measurements.

The design aim for the polarimeter is to construct a device which can measure all polarization components for either protons or deuterons in the energy range 0-500 keV, with an overall efficiency of 1%. In Fig. 1 we show a schematic diagram of a device which could reasonably be expected to meet this aim. The steps in the process would be as follows.

Scattered particles are first bent by a wedge magnet; this selects the energy of the particles to be analyzed and thus the effective scattering angle. A 50.3° bend rotates proton spins 90°, which is a useful feature; no reasonable bend angle seems better than another in the deuteron case.

The spin measurement system is expected to work well only in the range 500 eV to 50 keV, so the incident particles must be decelerated or accelerated to the desired energy; 10 keV is the probable design figure. If the accepted energy spread is not too great (∿1%), a crossed field device which rotates around the beam direction would appear very desirable in that arbitrary spin orientation could be provided for ions entering the spin filter.

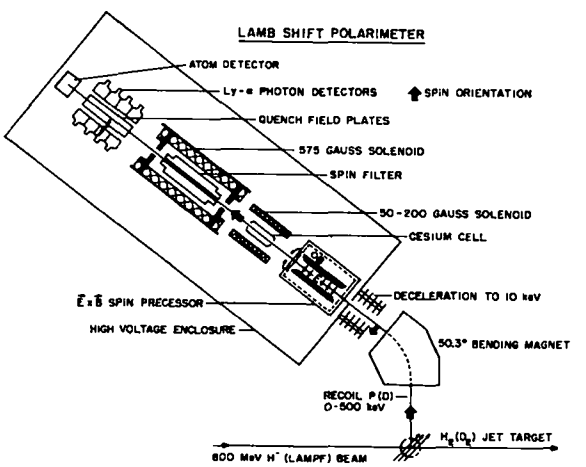

Fig. 1. Schematic Drawing of Proposed Polarimeter

A large fraction of the beam (∿10%) is converted to 2S atoms in a cesium vapor cell. The charge transfer needs to be carried out in a "strong" magnetic field (∿200 gauss for H, and ∿50G for D) in order to avoid significant depolarization. The 2S atoms now enter a spin filter which is tuned to pass those in a particular m_I state and quench the rest. For the case of protons it can be shown[2] that the number of $m_I=+\frac{1}{2}$ atoms passed is $n_+ \propto (1+\langle\sigma_z\rangle)$ where $\langle\sigma_z\rangle$ is the polarization component along the polarimeter (z) axis. Similarly if the device is tuned to transmit $m_I=-\frac{1}{2}$ atoms, the number passed is $n_- \propto (1-\langle\sigma_z\rangle)$ so that the polarization component along the

* Work performed under the auspices of the U. S. Atomic Energy Commission.

z axis is: $\langle\sigma_z\rangle = (n_+-n_-)/(n_++n_-)$, in exact analogy to nuclear scattering methods (with a 100% efficient analyzing reaction). Other polarization components in the incoming beam can be measured with the aid of the spin orientation device.

For deuterons, with the filter set to pass $m_I=1$, 0, and -1 atoms, respectively we find: $n_+ \propto [1+3/2\langle P_z\rangle+1/2\langle P_{zz}\rangle]$, $n_o \propto [1-\langle P_{zz}\rangle]$, and $n_- \propto [1-3/2\langle P_z\rangle+1/2\langle P_{zz}\rangle]$, so that

$$\langle P_z\rangle = \frac{2}{3}\left(\frac{n_+-n_-}{n_++n_o+n_-}\right) \qquad 1+\frac{1}{2}\langle P_{zz}\rangle = \left(\frac{n_++n_--n_o}{n_++n_o+n_-}\right) ,$$

again in direct analogy to a nuclear analyzer with 100% vector and/or tensor analyzing powers. Experimentally, one would cycle between the spin filter magnetic field values which tune for the various states. The desired quantities are all ratios so that no absolute efficiencies are involved, although one must ensure that no efficiency factors change as a function of magnetic field.

For the applications discussed above, the rate of arrival of particles in the polarimeter will probably be on the order of 10/sec or less. With 10% conversion efficiency to 2S atoms and 25% typical pass efficiency in the spin filter (protons), the arrival rate of the selected 2S atoms in the detection volume is $\leq$0.25/sec. Detection of the metastable atoms must therefore employ single event counting techniques, with particular emphasis on suppression of background events by coincidence and pulse discrimination procedures.

The filtered 2S atoms are passed through a transverse electric field strong enough (500 V/cm) to induce a transition to the ground state with emission of a Lyman-α photon (1216°A). The photons are then detected in coincidence with the associated 10 keV atoms which are incident on a particle detector downstream from the quenching region. The Lyman-α photons can be detected with 10% efficiency by existing image intensifier photomultiplication devices. With a suitable number of such instruments stacked around the quenching region, approximately half the emitted photons can be intercepted, leading to a total photon detection efficiency of 5%, for an overall count rate of $\leq$1 count/minute. The associated 10 keV atoms can be detected with nearly 100% efficiency, by a gas gain proportional counter.

Pulses from the photon and atom detectors will be fed to a fast coincidence unit (<10 nsec time resolution), with the photon pulse suitably delayed to allow for the finite atom transit time. Internally generated noise events will arise mainly from random coincidences between dark counts in the photon detectors and non-selected 10 keV particles incident on the atom detector. With photocathode cooling the dark rate can be reduced to <20 counts/sec. Coupled with an unwanted atom count rate of $\approx$10/sec, the accidental coincidence rate is $\approx 10^{-4}$/min. It is clear that the polarimeter will be usable even if the externally induced random coincidence rates (due to nuclear interactions in the target area) are 3 or 4 orders of magnitude higher, particularly since a large fraction of such events can be eliminated by pulse-height and shape discrimination and anti-coincidence techniques.

References

1) A process several orders of magnitude less efficient has been suggested by G. Clausnitzer and D. Fick [Nucl. Instr. & Methods 47, 171 (1967)].

2) See the extended version of this paper in LA-4465-MS.

APPENDIX I: Applications for the Lamb-Shift Polarimeter

There is a paucity of polarization measurements for proton-proton scattering in the small angle region. The smallest angle measurements we are aware of are at 142[1], 147[2], and 310[3] MeV. All three of these experiments indicate negative polarizations. The difficulties associated with such measurements are attested to by the large errors indicated in fig. 1. Clearly, a different approach, such as envisioned in this paper, is desirable to see if it will generate smaller errors. In fig. 1 we note polarizations kindly calculated by J. C. Hopkins from the phase shifts of MacGregor, Arndt, and Wright[4].

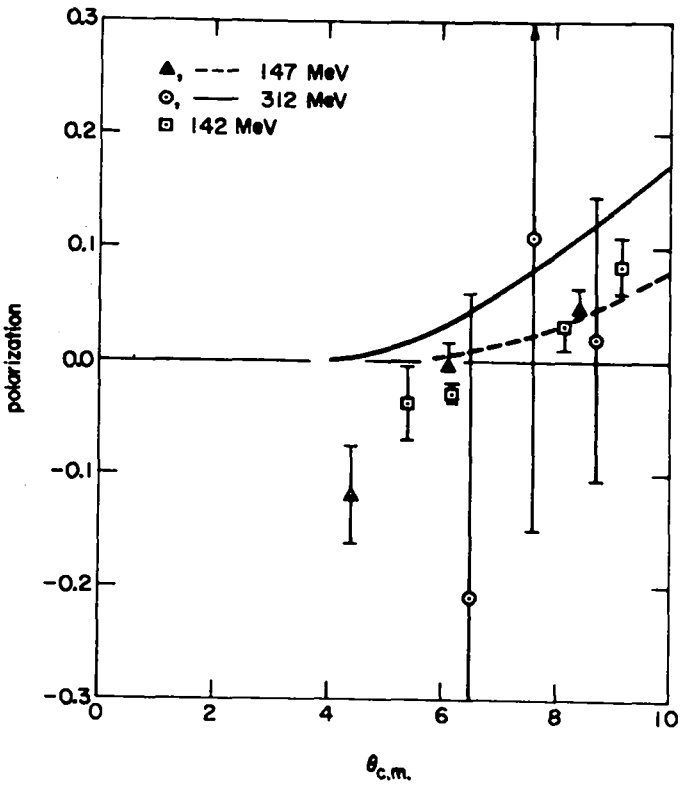

Fig. 1. Plot of existing small scattering angle p-p polarization data. The solid and dashed lines are calculated values.

It is, of course, desirable to extend the small angle measurements to such quantities as A, A', R, and R'[5]. Since the polarized proton beam planned for LAMPF can be prepared with its quantization axis in any desired direction, it suffices to perform an appropriate spin rotation on the recoil particle prior to transmitting it through the polarimeter spin filter in order to execute any of these measurements.

There do not appear to be any existing measurements of these quantities for small scattering angles. Such measurements would undoubtedly help to firm up our knowledge of p-p phase shifts. Additionally, it might extend our picture of T invariance by testing the relativistic Sprung[6] relation

$$\tan\theta = \frac{A+R'}{A'-R}$$

where θ is the laboratory scattering angle.

Polarization measurements on the recoil deuteron associated with 800 MeV small angle (p,d) scattering are nonexistent. However, Franco[7] has shown that Glauber theory predicts quite appreciable polarizations even at very small angles. His results are shown in fig. 2. For a plot of cross sections the reader is referred to the paper by Franco[7] in this report.

Glauber theory connects our knowledge of both bound and unbound states of the nucleon-nucleon system, and for this as well as other reasons it is desirable to

to examine all aspects of it. Clearly, the LAMPF polarized beam and deuterium jet-target could be employed in conjunction with the proposed polarimeter to approach the deuteron polarization measurements in the small angle region.

The bound state of the two nucleons can be studied in another fashion. Photodisintegration of the deuteron near threshold produces protons of low energy and appreciable polarization. Earle Lomon has kindly calculated the results shown in fig. 3 from the Lomon-Partovi theory. The polarization of the few hundred kilovolt protons is quite appreciable. Experimental measurements would be highly desirable, and could readily be obtained by utilizing the deuterium jet target, the polarimeter, and the LAMPF electron prototype accelerator (or its next generation) to provide the bremmstrahlung photons.

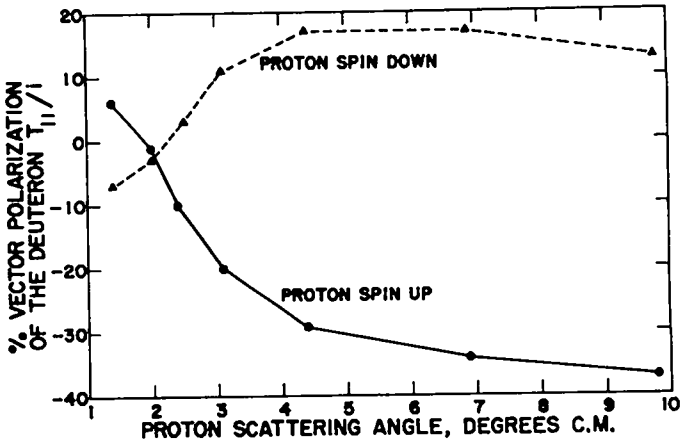

Fig. 2. Vector polarization calculated from Glauber theory. The points are calculated values; the lines are visual guides only.

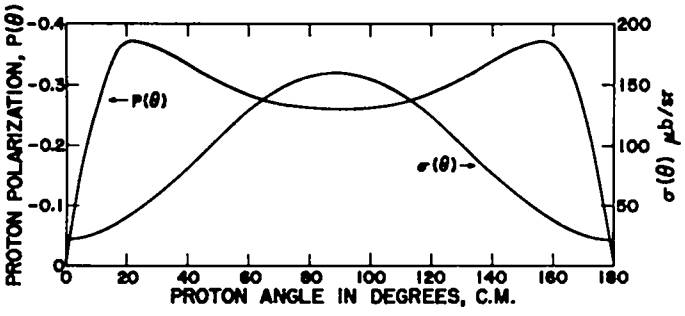

Fig. 3. Polarization and cross section of the proton from d(γ,p)n for 2.757-MeV photons.

APPENDIX II: Polarimeter Spin Analysis Formalism

In this appendix we demonstrate the parallel between the function of the polarimeter spin filter and polarization analysis by nuclear scattering.

1. Spin 1/2 Case. When the spin filter is turned to pass $m_I = +1/2$ hydrogen atoms, atoms with $m_I = -1/2$ are rejected. This amounts to saying that the transfer matrix has the form

$$\begin{pmatrix} b_1 \\ b_2 \end{pmatrix} = \begin{pmatrix} \alpha & 0 \\ 0 & 0 \end{pmatrix} \begin{pmatrix} b_1^o \\ b_2^o \end{pmatrix} \quad \text{where} \quad \begin{pmatrix} b_1^o \\ b_2^o \end{pmatrix} \quad \text{and} \quad \begin{pmatrix} b_1 \\ b_2 \end{pmatrix} \quad \text{are}$$

the initial and final spinors, respectively, in a representation with the z axis along the spin filter solenoidal magnetic field direction. If we use a density matrix representation, the most general initial density matrix is

$$\rho^i = \frac{1}{2}(1+\langle\sigma_x\rangle\sigma_x+\langle\sigma_y\rangle\sigma_y+\langle\sigma_z\rangle\sigma_z) \ .$$

The trace of the final density matrix is

$$n_+ = Tr\rho^f = TrM\rho^i M^\dagger = \frac{\alpha}{2}(1+\langle\sigma_z\rangle) \ ,$$

where $M = \begin{pmatrix} \alpha & 0 \\ 0 & 0 \end{pmatrix}$. Similarly, if the device is tuned to transmit $m_I = -1/2$ atoms, we obtain $M = \begin{pmatrix} 0 & 0 \\ 0 & \alpha \end{pmatrix}$ and $n_- = Tr\rho^f = \frac{\alpha}{2}(1-\langle\sigma_z\rangle)$, so that the polarization component along the z axis is $\langle\sigma_z\rangle = (n_+-n_-)/(n_++n_-)$, in exact analogy to nuclear scattering using a hypothetical 100% efficient analyzing reaction.

2. Spin-1 Case. For deuterons the transfer matrices for $m_I = 1$, 0, and -1 tuning of the spin filter are

$$M_1 = \begin{pmatrix} \alpha & 0 & 0 \\ 0 & 0 & 0 \\ 0 & 0 & 0 \end{pmatrix} \qquad M_o = \begin{pmatrix} 0 & 0 & 0 \\ 0 & \alpha & 0 \\ 0 & 0 & 0 \end{pmatrix} \qquad M_{-1} = \begin{pmatrix} 0 & 0 & 0 \\ 0 & 0 & 0 \\ 0 & 0 & \alpha \end{pmatrix} \ .$$

The most general initial density matrix for spin-1 particles is

$$\rho^i = \frac{1}{3}[1+\frac{3}{2}\langle P_x\rangle P_x+\frac{3}{2}\langle P_y\rangle P_y+\frac{3}{2}\langle P_z\rangle P_z+\frac{2}{3}\langle P_{xz}\rangle P_{xz}+\frac{2}{3}\langle P_{yz}\rangle P_{yz}+\frac{2}{3}\langle P_{xy}\rangle P_{xy}$$
$$+\frac{1}{3}\langle P_{xx}\rangle P_{xx}+\frac{1}{3}\langle P_{yy}\rangle P_{yy}+\frac{1}{3}\langle P_{zz}\rangle P_{zz}] \ .$$

For $m_I = 1$, 0, and -1 spin filter tuning, respectively, we find

$n_+ = \frac{1}{3}(1+\frac{3}{2}\langle P_z\rangle+\frac{1}{2}\langle P_{zz}\rangle)$, $n_o = \frac{1}{3}(1-\langle P_{zz}\rangle)$, $n_- = \frac{1}{3}(1-\frac{3}{2}\langle P_{zz}\rangle+\frac{1}{2}\langle P_{zz}\rangle)$, so that $\langle P_z\rangle = \frac{2}{3}[(n_+-n_-)/(n_++n_o+n_-)]$, $1+\frac{1}{2}\langle P_{zz}\rangle = (n_++n_--n_o)/(n_++n_o+n_-)$, and again we have a direct analogy with a nuclear analyzer having 100% vector and/or tensor analyzing power.

References

1. A. E. Taylor, E. Wood, and L. Bird, Nucl. Phys. 16 (1960) 320

2. J. N. Palmieri, A. M. Cormack, N. F. Ramsey, and R. Wilson, Ann. Phys. 5 (1958) 299

3. W. N. Hess, Rev. Mod. Phys. 30 (1958) 368

4. M. H. MacGregor, R. A. Arndt, and R. M. Wright, Phys. Rev. 182 (1969) 1714

5. M. J. Moravcsik, The Two Nucleon Interaction (Oxford, 1963)

6. D. W. L. Sprung, Phys. Rev. 121 (1961) 925

7. V. Franco, "Polarization in Nucleon Deuteron Scattering at Medium Energies," Proc. 3rd Internatl. Symp. Polarization Phenomena in Nuclear Reactions (to be published)

TRANSFER MATRIX METHOD FOR CALCULATING SPIN ABERRATIONS IN THE TRANSPORT OF POLARIZED BEAMS*

by

Ralph R. Stevens, Jr. and Gerald G. Ohlsen

Los Alamos Scientific Laboratory
University of California
Los Alamos, New Mexico

Transfer matrix methods have long been a useful tool for the design and evaluation of beam transport systems. When the beams are polarized, the effect of the transport elements on the spin axis is also of interest. We here generalize the usual beam transport matrix calculations so as to determine the spin axis orientation in a beam transport system. This development was motivated by experimental observations with the LASL polarized ion source on the tandem Van de Graaff installation where it has been found that "spin aberrations" induced by the transport system can be as large as several degrees with improper adjustment of the various transport elements.

In this treatment, we follow closely Penner's[1] development of first-order beam transport matrices for determining particle trajectories. We assume a coordinate system with the z-axis taken along the beam line, the y-axis vertical, and the x-axis taken to make a right-handed coordinate system. The beam line is a straight line in focusing and drift elements and a circular arc of radius ρ in a bending element. The effect of the beam transport elements is characterized by operators which rotate the spin axis, $\vec{S}_o$, to a new orientation $\vec{S}$. In the Cartesian representation, we have:

$$\begin{pmatrix} S_x \\ S_y \\ S_z \end{pmatrix} = \begin{pmatrix} a_{11} & a_{12} & a_{13} \\ a_{21} & a_{22} & a_{23} \\ a_{31} & a_{32} & a_{33} \end{pmatrix} \begin{pmatrix} S_{x_o} \\ S_{y_o} \\ S_{z_o} \end{pmatrix}$$

The rotations induced by these transport elements are determined by the equation of motion for the spin vector $\vec{S}$ in a magnetic field $\vec{B}$:

$$\frac{d\vec{S}}{dt} = \frac{ge}{2m_p}\left(\vec{S} \times \vec{B}\right)$$

where g is the gyromagnetic ratio and m_p is the proton mass. The matrix elements for several beam transport elements of interest are presented in Table I.

In order to use this formalism one must first carry out the usual beam transport calculations to determine the coordinates and slopes at the entrance and exit of each transport element for the particle trajectories of interest. With this information, one can then determine the rotation of the spin axis for these trajectories with the transfer matrices described above. Using this procedure, it has been found that one of the more important sources of spin aberrations is associated with polarized particles entering and leaving a bending magnet off the median plane.[2] This same

* Work supported by the U. S. Atomic Energy Commission.

Transfer Matrix Method for Calculating Spin Aberrations in the Transport of Polarized Beams (cont.)

type of transfer matrix calculation can also be used to determine spin aberrations in the transport of polarized neutron beams.

In conclusion, we find that suitable care is required with the alignment and steering in a beam transport system to obtain undistorted transport of polarized beams.

TABLE I: POLARIZATION TRANSPORT MATRICES

Beam Transport Element	a_{11}	a_{22}	a_{33}	a_{12}	a_{13}	a_{23}
Inclined Magnet Pole Face (entry angle β_1)	1	1	1	$\mp \frac{y}{\rho}\left[\frac{gM}{2m_p}\right]\frac{\alpha}{\lvert\alpha\rvert}$	0	$\frac{y}{\rho}\tan\beta_1\left[\mp\frac{gM}{2m_p}\right]$
Inclined Magnet Pole Face (exit angle β_2)	1	1	1	$\pm \frac{y}{\rho}\left[\frac{gM}{2m_p}\right]\frac{\alpha}{\lvert\alpha\rvert}$	0	$\frac{y}{\rho}\tan\beta_2\left[\mp\frac{gM}{2m_p}\right]$
Horizontal Bending Magnet (bend angle α)	$\cos\delta_y$	1	$\cos\delta_y$	0	$\sin\delta_y$	0
Quadrupole Lens (focusing in x-plane)	1	1	1	0	Δ_c	Δ_d
Quadrupole Lens (focusing in y-plane)	1	1	1	0	Δ_d	Δ_c
Drift	1	1	1	0	0	0

Where $\delta_y = \alpha\left[-1 \pm \frac{gM}{2m_p}\right] \pm \left(\theta-\theta_o\right)\frac{gM}{2m_p}$

$\Delta_c = \pm\left[\left(\theta-\theta_o\right)_c\left(\frac{gM}{2m_p}\right)\right]$

$\Delta_d = \pm\left[\left(\theta-\theta_o\right)_d\left(\frac{gM}{2m_p}\right)\right]$

ρ = bending radius.

M = polarized ion mass.

θ_o = entrance angle to a transport element.

θ = exit angle from a transport element.

$\left(\theta-\theta_o\right)_c$ = angular divergence imparted in the converging plane of a quadrupole lens.

$\left(\theta-\theta_o\right)_d$ = angular divergence imparted in the diverging plane of a quadrupole lens.

The upper sign is for a positive beam while the lower sign is for a negative beam. For a horizontal bending magnet, a positive bend angle α is assumed to be in the sense that rotates the z-axis into the x-axis. The off-diagonal elements not listed may be found from the relation $a_{ij} = -a_{ji}$.

(1) S. Penner, Review of Scientific Instruments, 32(1961) 150.

(2) Additional details are presented in LA-4465-MS.

APPENDIX I: BENDING MAGNETS

Consider entering a horizontal bending magnet perpendicular to the pole face but off the midplane a distance Y. In the fringe field region there will be Y and Z components of magnetic field. Using Maxwell's equations, we can relate these components:

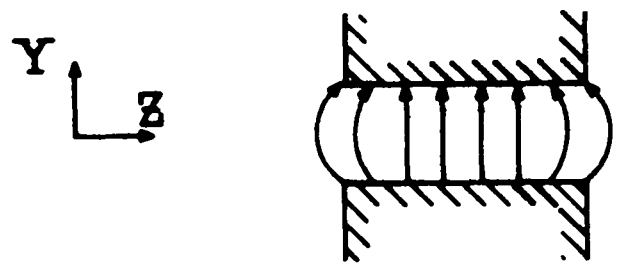

$$\frac{\partial B_Z}{\partial Y} = \frac{\partial B_Y}{\partial Z},$$

so that, defining $\partial B_Y/\partial Z = B'(Z)$ (an easily measured quantity for any magnet), we can write, to first order,

$$B_Z = B'(Z)Y.$$

Now, assume that the pole edge is rotated by an angle β_1 such as to effect vertical focusing. Looking from the top view, we can resolve B_z into components:

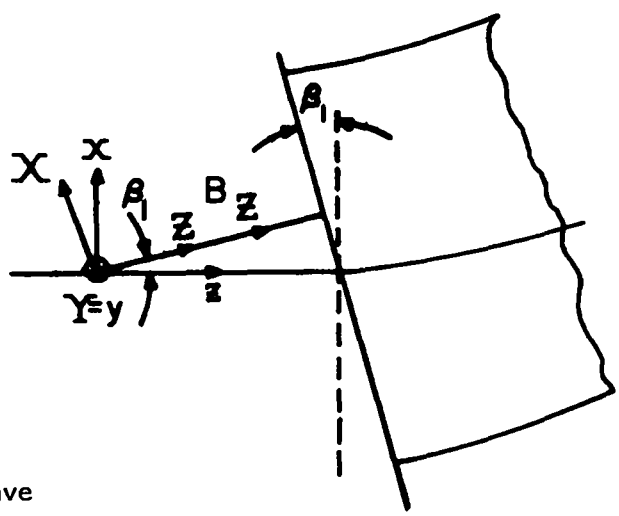

$$B_x = B'(Z)Y \sin \beta_1$$
$$B_z = B'(Z)Y \cos \beta_1.$$

Putting $Y = y$ and $z = Z \cos \beta_1$, we have

$$B_x = B'(z \cos \beta_1)y \sin \beta_1$$
$$B_z = B'(z \cos \beta_1)y \cos \beta_1.$$

Now the net angle of bend of the beam induced by the x component is given by

$$\Delta\theta_x = \int \frac{e}{MV_z} B_x(S)dS.$$

where the integration extends over the entrance fringe field region.

Appendix I (cont.)

Now, we define $\rho = \frac{MV_z}{eB}$

$$\Delta\theta_x = \frac{1}{\rho B}\int B_x(S)dS = \frac{1}{\rho B}\int B'(z\cos\beta_1)y\sin\beta_1\, dz$$

$$= \frac{y\tan\beta_1}{\rho}\,.$$

which is the usual vertical focusing expression obtained for a rotated pole edge. For spin precession, the angle is given by the same calculation except e/m is replaced by $g(e/2m_p)$ so that

$$|\delta_x| = \left(\frac{gM}{2m_p}\right)\frac{\tan\beta_1}{\rho}\,y;$$

the proper sense of the rotation can be deduced by recognizing that spins are precessed the same way as positively charged beams for all of the particles of interest to us, e.g., H, D, and T.

The B_z field component has no first-order effect on the orbit but does have a first order effect on the spin direction. We obtain

$$|\delta_z| = \int g\left(\frac{e}{2m_pV}\right)B'(z\cos\beta_1)y\cos\beta_1\, dz$$

$$= \left(\frac{gM}{2m_p}\right)\frac{1}{\rho}\,y.$$

where again the integration extends over the entrance fringe field region. The sense of the spin precession angle δ_z will also depend on the sense of the bend angle, since the sign of B_z changes as the sense of the bend angle reverses.

For typical bending magnets, we may regard these rotations as infinitesimal[3] so that the rotations together produce the transfer matrix $U(\beta_1)$:

---

(3) This condition will be met as long as the focal length of the rotated pole face is large compared to the beam size since the angular convergence imparted to the beam and hence the spin precession induced by the rotated pole face will then be small.

Appendix I (cont.)

$$U(\beta_1) = \begin{pmatrix} 1 & 0 & 0 \\ 0 & 1 & \delta_x \\ 0 & -\delta_x & 1 \end{pmatrix} \begin{pmatrix} 1 & \delta_z & 0 \\ -\delta_z & 1 & 0 \\ 0 & 0 & 1 \end{pmatrix} = \begin{pmatrix} 1 & \delta_z & 0 \\ -\delta_z & 1 & \delta_x \\ 0 & -\delta_x & 1 \end{pmatrix}$$

$$U(\beta_1) = \begin{pmatrix} 1 & \mp \frac{gM}{2m_p} \frac{y_o}{\rho} \frac{\alpha}{|\alpha|} & 0 \\ \pm \frac{gM}{2m_p} \frac{y_o}{\rho} \frac{\alpha}{|\alpha|} & 1 & \frac{y_o}{\rho} \tan \beta_1 \left(\mp \frac{gM}{2m_p} \right) \\ 0 & -\frac{y_o}{\rho} \tan \beta_1 \left(\mp \frac{gM}{2m_p} \right) & 1 \end{pmatrix}$$

In the central region of the bending magnet, we consider the precession induced by the main vertical field; we must now relate the precessed spin direction to the new transformed coordinate system at the exit of the magnet. The angle of bend for a given trajectory is $\left[\alpha + \left(\theta-\theta_o\right)\right]$ where α is the main bend angle and where θ_o and θ and the entrance and exit slopes defined by Penner.[1] (In this definition, $\theta_o = \theta = 0$ for normal entry and exit if $\beta_1 = \beta_2 = 0$.) The spin is precessed by an amount $\pm \frac{gM}{2m_p} \left[\alpha + \left(\theta-\theta_o\right)\right]$ depending on whether the beam is positive or negative respectively. The sign of the precession angle reverses as the sign of the beam reverses since the direction of the main magnetic field must reverse to keep the same sense for the main bending angle. Thus, the precession of the spin axis relative to the new transformed exit coordinate system is:

$$\delta_y = \pm \frac{gM}{2m_p} \left(\alpha + \theta-\theta_o\right) - \alpha$$

$$= \alpha\left(-1 \pm \frac{gM}{2m_p}\right) \pm\left(\theta-\theta_o\right)\left(\frac{gM}{2m_p}\right).$$

Note, a bend angle in the sense that the z-axis rotates towards the x-axis is considered a positive bend regardless of whether the beam is negative or positive. For a positive beam, the spin precesses in the same direction as the trajectory is bent, while for a negative beam the spin precesses in the opposite sense to which the trajectory is bent.

The operator corresponding to this bend is given by:

Appendix I (cont.)

$$U(\alpha) = \begin{pmatrix} \cos\delta_y & 0 & \sin\delta_y \\ 0 & 1 & 0 \\ -\sin\delta_y & 0 & \cos\delta_y \end{pmatrix}$$

For the exit pole face with a pole face rotation β_2, we have a similar expression as that at the entrance pole face except for a reversal of sign in the a_{12} element, due to the fact that the B_z field reverses sign in the exit fringe field. Thus:

$$U(\beta_2) = \begin{pmatrix} 1 & \pm\frac{y}{\rho}\left[\frac{gM}{2m_p}\right]\frac{\alpha}{|\alpha|} & 0 \\ \mp\frac{y}{\rho}\left[\frac{gM}{2m_p}\right]\frac{\alpha}{|\alpha|} & 1 & \frac{y}{\rho}\tan\beta_2\left[\pm\frac{gM}{2m_p}\right] \\ 0 & -\frac{y}{\rho}\tan\beta_2\left[\pm\frac{gM}{2m_p}\right] & 1 \end{pmatrix}$$

where y is now the distance from the midplane at the exit face of the bending magnet.

Then, the overall transfer matrix, U, for this case is:

$$U = U(\beta_2)U(\alpha)U(\beta_1).$$

As an example, consider the transport of a polarized $\vec{H}^-$ beam through a 58° horizontal inflection magnet having a rotated entrance pole face of 32°.

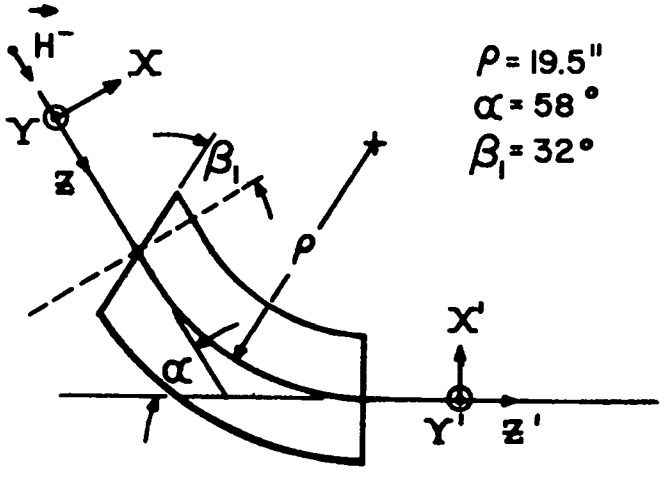

58° HORIZONTAL BENDING MAGNET

Appendix I (cont.)

The spin vector precesses in the opposite direction to the angle of bend (since the beam is negative) so that as the beam is bent +58°(CCW), the spin component in the x-z plane $\vec{S}_o$ precesses $\left(\frac{g}{2}\right)(-58°) = -162°$(CW) to $\vec{S}_o'$ thus giving a total angle of spin precession in the new coordinate system at the exit of the magnet of -220° as indicated below.

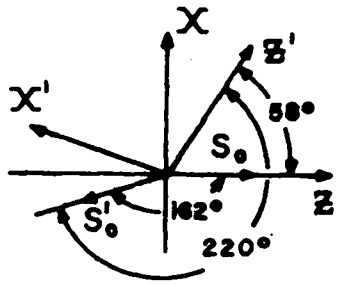

To calculate the total spin precession, we have:

(1) Entrance face:

$$\delta_x = \frac{y_o}{\rho} \tan \beta_1 \left(\frac{g}{2}\right) = 0.089 y_o \quad \text{where } y_o \text{ is in inches}$$

$$\delta_z = \frac{y_o}{\rho} \left(\frac{g}{2}\right) = 0.143 y_o.$$

Thus

$$U(\beta_1) = \begin{pmatrix} 1 & \delta_z & 0 \\ -\delta_x & 1 & \delta_x \\ 0 & -\delta_x & 1 \end{pmatrix} = \begin{pmatrix} 1 & .143y_o & 0 \\ -.143y_o & 1 & .089y_o \\ 0 & -.089y_o & 1 \end{pmatrix}$$

(2) Main bending field:

$$\delta_y = \alpha\left(-1 - \frac{g}{2}\right) = -220° \qquad \begin{aligned} \cos \delta_y &= -.767 \\ \sin \delta_y &= +.643 \end{aligned}$$

$$U(\beta) = \begin{pmatrix} \cos \delta_y & 0 & \sin \delta_y \\ 0 & 1 & 0 \\ -\sin \delta_y & 0 & \cos \delta_y \end{pmatrix} = \begin{pmatrix} -.767 & 0 & .643 \\ 0 & 1 & 0 \\ -.643 & 0 & -.767 \end{pmatrix}$$

Appendix I (cont.)

Exit face:

$$\delta_z = \frac{y}{\rho}(g/2)$$

To determine y at the exit face requires consideration of the particular trajectories involved. We assume now that $y_o' = \left(\frac{dy}{dz}\right)_{\text{(entrance face)}}$ is zero. Then $y = y_o + (y_o' - \Delta\phi)\rho\alpha$ where $\Delta\phi = \frac{y_o}{\rho}\tan\beta_1$

$$= y_o - y_o\,\alpha\tan\beta_1 + y_o'\rho\alpha$$

Thus, for these trajectories ($y_o' = 0$), we have

$$y = y_o\left[1 - \alpha\tan\beta_1\right] = 0.37y_o.$$

Then

$$\delta_z = \frac{0.37\,y_o}{\rho}(2.79) = 0.053y_o$$

$$U(\beta_2=0) = \begin{pmatrix} 1 & -\delta_z & 0 \\ \delta_z & 1 & 0 \\ 0 & 0 & 1 \end{pmatrix} = \begin{pmatrix} 1 & -.053y_o & 0 \\ .053y_o & 1 & 0 \\ 0 & 0 & 1 \end{pmatrix}.$$

Thus, $U = U(\beta_2=0)\;U(\alpha)\;U(\beta_1)$

$$= \begin{pmatrix} -.767 & -.220y_o & .643 \\ -.183y_o & 1 & .123y_o \\ -.643 & -.024y_o & -.767 \end{pmatrix}.$$

Thus if $S_{y_o} = o$ initially, we have

$S_x = -.220y_o \Rightarrow -12.6y_o$ degrees rotation (y_o in inches)

$S_y = 1$

$S_z = -.0235y_o \Rightarrow -1.35y_o$ degrees rotation (y_o in inches).

Assuming a beam displacement of 0.1" from the median plane, we find a 1.3° rotation is imparted to the spin vector as the beam traverses the bending magnet. This rotation constitutes a "spin aberration" and it is

Appendix I (cont.)

therefore important to insure that polarized beams traverse a bending magnet near the median plane to preclude this effect.

APPENDIX II: QUADRUPOLE LENSES

To first order, the fields in a magnetic quadrupole lens are given by

$$B_y = \frac{\partial B_y}{\partial x} \cdot x = Gx$$

$$B_x = \frac{\partial B_x}{\partial y} \cdot y \equiv -\frac{\partial B_y}{\partial x}\, y = Gy.$$

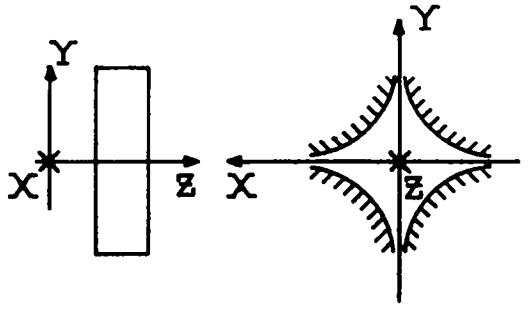

QUADRUPOLE LENS COORDINATE SYSTEM

so that the equations of motion are

$$m\ddot{x} = -eV_z B_y,$$

$$m\ddot{y} = eV_z B_x,$$

or using $\ddot{x} = V_z^2\left(dx/dz\right)^2 = V_z^2 x'$,

$$x'' + k^2 x = 0 \qquad k^2 = \left(\frac{e}{mV_z}\frac{\partial By}{\partial x}\right) \equiv \left(\frac{1}{B\rho}\frac{\partial B_y}{\partial x}\right) \equiv \left(\frac{G}{B\rho}\right)$$

where $B\rho$ is the magnetic rigidity of the particle and where we assume that $G = \partial B_y/\partial x$ is positive; i.e., focusing occurs in the x plane. Similarly, in the defocusing plane,

$$y'' - k^2 y = 0.$$

For electrostatic quadrupole lenses, the equations of motion are the same except the parameter k^2 is given by

$$k^2 = \frac{eV}{\varepsilon R^2},$$

where 2R is the diameter of the quadrupole, V the voltage applied to an element, and ε is the beam energy.

In the central region of a quadrupole lens, there is no axial component of magnetic field so spin precessions are directly related to either the focusing or defocusing angular deflections of the particle trajectory in the lens. Solution of the trajectory equations gives:

$$\left[\theta - \theta_o\right]_c = -\left(k \sin kL\right) x_o - \left(1 - \cos kL\right)\theta_o$$

in the converging plane where θ_o is the slope of the trajectory at the entrance to the lens and θ is the slope at the exit.

If the lens is defocusing in the x - z plane, a similar analysis gives

$$\left[\theta - \theta_o\right]_d = \left(k \sinh kL\right)x_o - \left(1 - \cosh kL\right)\theta_o$$

for the diverging case. The same trajectory equations hold in the y - z plane.

In both the focusing and defocusing cases, it follows from the equation of motion of the spin vector that the angle of precession imparted to the spin vector by a quadrupole lens is given by:

$$\pm\left[\left(\theta - \theta_o\right)\left(\frac{gM}{2m_p}\right)\right] \qquad \begin{array}{rl} \text{Top Sign:} & \text{Positive Beam} \\ \text{Bottom Sign:} & \text{Negative Beam} \end{array}$$

where the value of $\left(\theta - \theta_o\right)$ for a given trajectory can be calculated by the appropriate expressions given above or can be determined from other transport calculations.

In the fringe field of a quadrupole lens, there are first order transverse components of magnetic field, which are taken into account in the effective length of the central region, and second order axial components which are given by:

$$B_z = xy\,\frac{\partial^2 B_y}{\partial y \partial z} = xy\left(\frac{\partial G}{\partial z}\right).$$

The axial components of magnetic field will result in spin precession of the transverse components of the spin vector and may be significant in some cases. Using the equation of motion for the spin vector, we have:

$$\frac{d\vec{S}}{dt} = \frac{ge}{2m_p}\left(\vec{S} \times \vec{B}\right)$$

$$\Delta S_x = \frac{ge}{2m_p}\int S_y B_z dt = \frac{gM}{2m_p}\left(\frac{e}{MV_z}\right)S_y \int xy\,\frac{\partial G}{\partial z}\,dz$$

$$= \frac{gM}{2m_p}\left(\frac{e}{MV_z}\right)S_y \int x_o y_o\,\frac{\partial G}{\partial z}\,dz$$

$$= \left[\frac{gM}{2m_p}\left(\frac{eG}{MV_z}\right)x_o y_o\right]S_y$$

$$= \delta_1 S_y$$

$$\text{and } \Delta S_y = -\delta_1 S_x$$

where $\delta_1 = \frac{gM}{2m_p} x_o y_o \left(\frac{eG}{MV_z}\right) = \frac{gM}{2m_p} x_o y_o \left(\frac{G}{B\rho}\right)$

$= \frac{gM}{2m_p}$.

Thus, at the entrance to a quadrupole lens, we have:

$$\begin{pmatrix} S_x \\ S_y \\ S_z \end{pmatrix} = \begin{pmatrix} 1 & \delta_1 & 0 \\ -\delta_1 & 1 & 0 \\ 0 & 0 & 1 \end{pmatrix} \begin{pmatrix} S_{x_o} \\ S_{y_o} \\ S_{z_o} \end{pmatrix}$$

A similar matrix holds at the exit where δ_1 is replaced by $-\delta_2 = -\frac{gM}{2m_p} k^2 xy$. The spin rotation matrix for the entire quadrupole lens is:

$$U_Q = U(\delta_2)\, U(\theta_c, \theta_d)\, U(\delta_1) \cdot$$

We note that $\frac{\delta_1}{(\theta - \theta_o)_c}$ is approximately $\frac{gM}{2m_p} \frac{k^2 x_o y_o}{k^2 L x_o}$ which basically is the ratio of the beam size to the effective length of the lens. Thus, the effect of the quadrupole fringing fields is significant only for quadrupole lenses where the beam size is large and the effective length of the lens is small, i.e., for large bore short lenses. In first order calculations we may, therefore, neglect the axial fringe fields as long as the beam size is small compared to the effective length of the lens.

For electrostatic quadrupole lenses, there is, of course, no precession of the spin axis relative to the beam line.

APPENDIX III: SOLENOIDS

Consider a charged particle which enters a solenoid at a radial position $r = \sqrt{x_o^2 + y_o^2}$. Assume the beam is positive and that the solenoidal field is parallel to the z axis of the beam line. Upon entering the fringe field on the solenoid, the particle experiences both radial and axial components of magnetic field. We assume here that the axial components are taken into account in the effective length of the solenoid and that only radial components operate at the entrance and exit of the field region. As a result of this radial magnetic field, a charged particle acquires a "transverse" velocity V_ϕ:

$$V_\phi = \frac{e}{M}\frac{Br_o}{2}$$

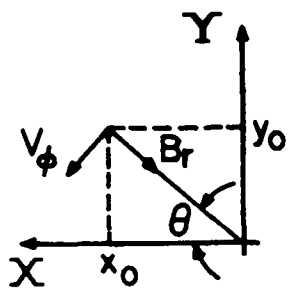

where B is the strength of the main field in the solenoid. In terms of the x and y components,

$$V_x = \frac{e}{M}\frac{By_o}{2}$$

$$V_y = -\frac{e}{M}\frac{Bx_o}{2}\,.$$

The spin vector $\vec{S}$ is precessed through an angle $\left(\frac{gM}{2m_p}\right)$ times as much as the velocity vector. Now the rotations imparted to the velocity vector are V_x/V_z and V_y/V_z where V_z is the axial velocity of the particles. Thus, at the entrance to the solenoid, the spin precessions imparted to the spin vector $\vec{S}$ are:

$$\delta_{x_o}(a_{23}\text{ element}) = \frac{gM}{2m_p}\frac{V_y}{V_z}$$

$$\delta_{z_o}(a_{13}\text{ element}) = \frac{gM}{2m_p}\frac{V_x}{V_z}\,.$$

To write these precessions in a more convenient form, we define ρ_z as the z displacement during which one complete cyclotron orbit of the transverse velocity components occurs:

$$\rho_z = \frac{MV_z}{eB} .$$

Then $\frac{V_x}{V_z} = \frac{V_\phi \sin\theta}{V_z} = \frac{eB}{MV_z}\frac{r_o \sin\theta}{2} = \frac{y_o}{2\rho_z}$ and $\frac{V_y}{V_z} = -\frac{x_o}{2\rho_z}$, so that:

$$\delta_{x_o} = -\frac{gM}{2m_p}\frac{x_o}{2\rho_z}$$

$$\delta_{y_o} = +\frac{gM}{2m_p}\frac{y_o}{2\rho_z} .$$

Since these rotations are small, we may consider the total rotation matrix to be the product of a rotation about the x and then the y axis.

Now, consider the effect of the main solenoidal field. We consider first the orbit of a particle that enters at (x_o, y_o) and will restrict our consideration here to particles which have only an axial velocity. The orbit of such particles is a helix which when projected onto the x - y plane is a circle of radius $\rho = r_o/2$ which passes through the origin:

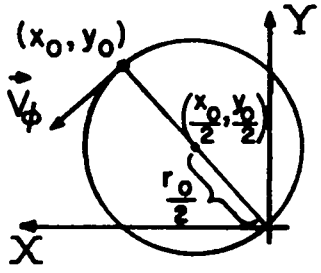

$$\vec{r} = \left[\frac{x_o}{2} + \frac{r_o}{2}\cos\left(\frac{z}{\rho_z} + \theta_o\right)\right]\hat{i} + \left[\frac{y_o}{2} + \frac{r_o}{2}\sin\left(\frac{z}{\rho_z} + \theta_o\right)\right]\hat{j} + z\hat{k}$$

$$\text{where } \theta_o = \arctan\frac{y_o}{x_o}$$

$$\text{and } z = V_z t.$$

The spin vector $\vec{S}$ is precessed through an angle $\frac{gM}{2m_p}$ times the amount the projection of the orbit of the x - y plane is rotated.

Thus:

$$\delta_z = \frac{gM}{2m_p}\frac{\ell}{\rho_z}$$

where ℓ is the effective length of the solenoid. More detailed orbit calculations are required for other trajectories and may be carried out by transport codes such as TRANSPORT, but the spin precession imparted is still the same. The rotation matrix for precession is therefore:

$$U(\ell) = \begin{pmatrix} \cos\delta_z & \sin\delta_z & 0 \\ -\sin\delta_z & \cos\delta_z & 0 \\ 0 & 0 & 1 \end{pmatrix}$$

Finally, we consider the effect of the fringing field at the solenoid exit. This field is of the same form as the entrance fringing field except for a reversal of sign due to the reversal of the radial magnetic field. Thus:

$$\delta_x(a_{23}\text{ component}) = +\frac{gM}{2m_p}\frac{x}{2\rho_z}$$

$$\delta_x(a_{13}\text{ component}) = -\frac{gM}{2m_p}\frac{y}{2\rho_z}$$

where x and y are the transverse coordinates of the trajectory being considered at the exit of the solenoid.

Overall, the transfer matrix is given by:

$$\begin{pmatrix} 1 & 0 & \delta_y \\ 0 & 1 & \delta_x \\ -\delta_y & -\delta_x & 1 \end{pmatrix} \begin{pmatrix} \cos\delta_z & \sin\delta_z & 0 \\ -\sin\delta_z & \cos\delta_z & 0 \\ 0 & 0 & 1 \end{pmatrix} \begin{pmatrix} 1 & 0 & \delta_{y_o} \\ 0 & 1 & \delta_{x_o} \\ -\delta_{y_o} & \delta_{x_o} & 1 \end{pmatrix}$$

$$= \begin{pmatrix} \cos\delta_z & \sin\delta_z & \delta_{y_o}\cos\delta_z+\delta_{x_o}\sin\delta_z+\delta_y \\ -\sin\delta_z & \cos\delta_z & -\delta_{y_o}\sin\delta_z+\delta_{x_o}\cos\delta_z+\delta_x \\ -\delta_y\cos\delta_z+\delta_x\sin\delta_z-\delta_{y_o} & -\delta_y\sin\delta_z-\delta_x\cos\delta_x-\delta_{x_o} & 1 \end{pmatrix}$$

Note that this matrix depends on whether the beam is positive or negative only through the orbit equations which connect x_o, y_o to x, y.

TABLE I
(continued)

Element	a_{11}	a_{22}	a_{33}	a_{12}	a_{13}	a_{23}
Solenoid Entrance $(\vec{B}\|\|\vec{V}_z)$	1	1	1	0	δ_{y_o}	δ_{x_o}
Solenoid Main Field $(\vec{B}\|\|\vec{V}_z)$	$\cos\delta_z$	$\cos\delta_z$	1	$\sin\delta_z$	0	0
Solenoid Exit $(\vec{B}\|\|\vec{V}_z)$	1	1	1	0	δ_y	δ_x

where $\delta_{x_o} = -\frac{gM}{2m_p}\frac{x_o}{2\rho_z}$

$$\delta_{y_o} = \frac{gM}{2m_p}\frac{y_o}{2\rho_z}$$

$$\delta_x = \frac{gM}{2m_p}\frac{x}{2\rho_z}$$

$$\delta_y = -\frac{gM}{2m_p}\frac{y}{2\rho_z}$$

$$\rho_z = \frac{MV_z}{eB}$$

The Absolute Polarization Determination of Mass-3 Nuclei*

P. W. Keaton, Jr., D. D. Armstrong, and L. R. Veeser
Los Alamos Scientific Laboratory, University of California
Los Alamos, New Mexico 87544

The polarizations of tritons[1] and ^{3}He nuclei[2] elastically scattered from ^{4}He at several energies and angles have been measured using double-scattering techniques. Absolute polarization values are deduced from the measurements of three asymmetries at appropriate energies and angles.

Nuclei scattered from the primary target are focused 2 m away onto the secondary target with a three-element magnetic quadrupole lens system. The lens system and secondary chamber can be rotated to positive or negative primary angles so that dependence on detector efficiencies can be eliminated. Nuclei scattered from the secondary target are detected by E-ΔE silicon-detector pairs and particle identified with an on-line computer code[3]. Typical target thicknesses were 200 keV for tritons and 800 keV for ^{3}He. Angular spreads were ±1.5°, and primary and secondary beam currents were about 1 μA and 1 pA, respectively.

Absolute values (but not signs) for polarizations can be obtained by measuring left-right asymmetries, A_{ij}, in a set of three double-scattering experiments such that only three different polarizations (assuming time reversal invariance) are involved:

$$A_{12} = P(\theta_1,E_1)P(\theta_2,E_2)$$
$$A_{23} = P(\theta_2,E_2)P(\theta_3,E_3)$$
$$A_{13} = P(\theta_1,E_1)P(\theta_3,E_3) \ ,$$

where θ_i and E_i (i = 1,2,3) are scattering angles and energies, respectively. An aluminum foil was inserted between the first and second scatterings to slow the nuclei to the correct energy so that A_{13} could be measured. The signs of the polarization values were determined by phase shift analyses[4].

The results of these measurements are given in Table 1. The energy and angular spreads are presented here so that the values in Table 1 can be used as standards by other groups until more precise absolute determinations are made. (See also Ref. 5.)

---

*Work performed under the auspices of the U. S. Atomic Energy Commission.

References

1. P. W. Keaton, Jr., D. D. Armstrong, and L. R. Veeser, Phys. Rev. Letters 20 (1968) 1392

2. D. D. Armstrong, L. L. Catlin, P. W. Keaton, Jr., and L. R. Veeser, Phys. Rev. Letters, 23 (1969) 135

3. D. D. Armstrong, J. G. Beery, E. R. Flynn, W. S. Hall, P. W. Keaton, Jr., and M. P. Kellogg, Nucl. Instr. Meth. 70 (1969) 69

4. R. J. Spiger and T. A. Tombrello, Phys. Rev. 163 (1967) 964

5. D. D. Armstrong, P. W. Keaton, Jr., and L. R. Veeser, "Elastic Scattering of Polarized Tritons," Proceedings of the 3rd International Symposium on Polarization Phenomena in Nuclear Reactions (to be published)

Table 1: Absolute Polarization Values

Reaction	Incident Energy (MeV)	Scattering Angle lab	Scattering Angle cm	Designation	Polarization
$^4He(t,\vec{t})^4He$	12.25	23°	40.1°	P_1	0.923±0.027
"	12.25	16.5°	28.9°	P_1'	0.825±0.042
"	10.28	30°	52.1°	$P_2(69)$	0.406±0.013
"	9.5	30°	52.1°	$P_2(68)$	0.370±0.016
"	7.2	30°	52.1°	P_{3A}	-0.724±0.027
"	6.6	30°	52.1°	P_{3B}	-0.615±0.029
"	6.0	30°	52.1°	$P_3(68)$	-0.378±0.020
$^3He(^4He,\vec{^3He})^4He$	13.0	19°	142°	P_1	-0.606±0.033
$^4He(^3He,\vec{^3He})^4He$	13.0	23°	40.1°	P_2	0.639±0.035
"	8.3	23°	40.1°	P_3	-0.604±0.033

Formalism for $A(\vec{d},\vec{n})B$ or $A(\vec{d},\vec{p})B$ Polarization Transfer Reactions*

J. L. Gammel, P. W. Keaton, Jr., and Gerald G. Ohlsen

Los Alamos Scientific Laboratory, University of California
Los Alamos, New Mexico 87544

If one assumes the conservation of parity, the formal expression for the cross section and nucleon polarization for reactions of the form $A(\vec{d},\vec{n})B$ or $A(\vec{d},\vec{p})B$ may be written in terms of the Goldfarb cartesian spin-1 operators[1] for the deuteron and in terms of the Pauli operators for the nucleon as follows:

$$I(\theta,\phi) = I_o(\theta)[1+\tfrac{3}{2}\langle P_y\rangle P^o_{\underline{y}}+\tfrac{2}{3}\langle P_{xz}\rangle P^o_{\underline{xz}}+\tfrac{1}{6}\langle P_{xx}-P_{yy}\rangle (P^o_{xx}-P^o_{yy})+\tfrac{1}{2}\langle P_{zz}\rangle P^o_{zz}]$$

$$\langle\sigma_{x'}\rangle I(\theta,\phi) = I_o(\theta)[\tfrac{3}{2}\langle P_x\rangle P^{x'}_{x}+\tfrac{3}{2}\langle P_z\rangle P^{x'}_{\underline{z}}+\tfrac{2}{3}\langle P_{xy}\rangle P^{x'}_{\underline{xy}}+\tfrac{2}{3}\langle P_{yz}\rangle P^{x'}_{yz}]$$

$$\langle\sigma_{y'}\rangle I(\theta,\phi) = I_o(\theta)[P^{y'}_{\underline{o}}+\tfrac{3}{2}\langle P_y\rangle P^{y'}_{y}+\tfrac{2}{3}\langle P_{xz}\rangle P^{y'}_{xz}+\tfrac{1}{6}\langle P_{xx}-P_{yy}\rangle (P^{y'}_{\underline{xx}}-P^{y'}_{\underline{yy}})+\tfrac{1}{2}\langle P_{zz}\rangle P^{y'}_{\underline{zz}}]$$

$$\langle\sigma_{z'}\rangle I(\theta,\phi) = I_o(\theta)[\tfrac{3}{2}\langle P_x\rangle P^{z'}_{\underline{x}}+\tfrac{3}{2}\langle P_z\rangle P^{z'}_{z}+\tfrac{2}{3}\langle P_{xy}\rangle P^{z'}_{xy}+\tfrac{2}{3}\langle P_{yz}\rangle P^{z'}_{\underline{yz}}] \quad . \qquad (1)$$

$I_o(\theta)$ is the cross section for an unpolarized beam at the scattering angle θ. The quantities in brackets represent the beam polarization referred to a right-handed (xyz) coordinate system with z along $\vec{k}_{in}$ and y along $\vec{k}_{in} \times \vec{k}_{out}$, while the remaining parameters are polarization transfer coefficients. The symbol zero is used in cases where nothing about the polarization is measured, so that P^o_y is the ordinary vector analyzing power and $P^{y'}_o$ is the nucleon polarization produced by an unpolarized deuteron beam. From the present point of view, the analyzing tensors are special cases of polarization transfer coefficients. The nucleon polarization is referred to a right-handed (x'y'z') coordinate system where y' is along $\vec{k}_{in} \times \vec{k}_{out}$. The z' axis may be chosen arbitrarily, but is usually most conveniently taken to be the outgoing laboratory nucleon direction. (If z' is the outgoing c.m. nucleon direction, the coefficients are simply related to parameters which describe the inverse reaction[2].)

A beam produced by a polarized ion source may be characterized by a vector polarization p_Z and a tensor polarization p_{ZZ} in a coordinate system with z axis along a quantization axis, $\hat{S}$, together with two angles which specify the quantization axis orientation with respect to the reaction initial (xyz) coordinate system. In terms of the angle between $\hat{S}$ and $\vec{k}_{in}$ (which we call β) and the angle between $\hat{S} \times \vec{k}_{in}$ and the x axis (which we call ϕ), the beam polarization quantities in the xyz coordinate system are

$$\langle P_x\rangle = -p_Z \sin\beta\sin\phi \qquad \langle P_{xy}\rangle = -\tfrac{3}{2} p_{ZZ} \sin^2\beta\sin\phi\cos\phi \qquad \tfrac{1}{2}\langle P_{xx}-P_{yy}\rangle = -\tfrac{3}{4} p_{ZZ} \sin^2\beta\cos 2\phi$$

$$\langle P_y\rangle = p_Z \sin\beta\cos\phi \qquad \langle P_{xz}\rangle = -\tfrac{3}{2} p_{ZZ} \sin\beta\cos\beta\sin\phi \qquad \langle P_{zz}\rangle = \tfrac{1}{2} p_{ZZ} (3\cos^2\beta-1)$$

$$\langle P_z\rangle = p_Z \cos\beta \qquad \langle P_{yz}\rangle = \tfrac{3}{2} p_{ZZ} \sin\beta\cos\beta\cos\phi \qquad (2)$$

If we define "up" scattering to be in the half-plane defined by $\hat{S}$ and $\vec{k}_{in}$, and left scattering to be in the half plane defined by $\hat{S} \times \vec{k}_{in}$ and $\vec{k}_{in}$, then left, right, up, and down directions correspond to the use of $\phi = 0°$, $180°$, $270°$, and $90°$, respectively, in Eq. (2).

---

*Work performed under the auspices of the U. S. Atomic Energy Commission.

For clarity, we write a typical observable, $P^{x'}_{xy}$, in terms of the scattering matrix, M:

$$P^{x'}_{xy} = (\mathrm{Tr}MP_{xy}M^{\dagger}\sigma_{x'})/(\mathrm{Tr}MM^{\dagger}) \ .$$

The cross section is given in terms of M by $I_o(\theta) = (\mathrm{Tr}MM^{\dagger})/3(2s_A+1)$.* The subscript always refers to the initial deuteron polarization, and the superscript to the final nucleon polarization.

The beam polarization quantities and polarization transfer coefficients vary between +1 and -1 (vector-type quantities), +1 and -2 (P_{xx}, P_{yy}, or P_{zz} type quantities) or +3/2 and -3/2 (P_{xy}, P_{xz}, P_{yz} or $1/2(P_{xx}-P_{yy})$ type quantities). Each of the coefficients defined is either an even function or an odd function of θ; the odd functions are underlined in Eq. (1). It is quite possible to separately measure all of the defined quantities at each scattering angle.

Finally, we rewrite Eq. (1) in terms of the spherical tensor spin-1 operators for the incident deuteron:

$$\begin{aligned}
I(\theta,\phi) &= I_o(\theta)[1+2\mathrm{Im}\langle T_{11}\rangle \underline{\mathrm{Im}T^{o}_{11}} + \langle T_{20}\rangle T^{o}_{20} + 2\mathrm{Re}\langle T_{21}\rangle \underline{\mathrm{Re}T^{o}_{21}} + 2\mathrm{Re}\langle T_{22}\rangle \mathrm{Re}T^{o}_{22}] \\
\langle\sigma_{x'}\rangle I(\theta,\phi) &= I_o(\theta)[\langle T_{10}\rangle \underline{T^{x'}_{10}} + 2\mathrm{Re}\langle T_{11}\rangle \mathrm{Re}T^{x'}_{11} + 2\mathrm{Im}\langle T_{21}\rangle \mathrm{Im}T^{x'}_{21} + 2\mathrm{Im}\langle T_{22}\rangle \underline{\mathrm{Im}T^{x'}_{22}}] \\
\langle\sigma_{y'}\rangle I(\theta,\phi) &= I_o(\theta)[P^{y'}_{o} + 2\mathrm{Im}\langle T_{11}\rangle \mathrm{Im}T^{y'}_{11} + \langle T_{20}\rangle \underline{T^{y'}_{20}} + 2\mathrm{Re}\langle T_{21}\rangle \mathrm{Re}T^{y'}_{21} + 2\mathrm{Re}\langle T_{22}\rangle \underline{\mathrm{Re}T^{y'}_{22}}] \\
\langle\sigma_{z'}\rangle I(\theta,\phi) &= I_o(\theta)[\langle T_{10}\rangle T^{z'}_{10} + 2\mathrm{Re}\langle T_{11}\rangle \underline{\mathrm{Re}T^{z'}_{11}} + 2\mathrm{Im}\langle T_{21}\rangle \underline{\mathrm{Im}T^{z'}_{21}} + 2\mathrm{Im}\langle T_{22}\rangle \mathrm{Im}T^{z'}_{22}] \ . \qquad (3)
\end{aligned}$$

The functions which are odd in θ are again underlined. The beam quantities are expressed in terms of the initial beam vector polarization (t_{10}), tensor polarization (t_{20}), and the angles, β and ϕ, as follows:

$$\begin{aligned}
\mathrm{Re}\langle T_{11}\rangle &= \frac{1}{\sqrt{2}}\sin\beta\sin\phi\ t_{10} & \mathrm{Im}\langle T_{22}\rangle &= -\sqrt{\frac{3}{8}}\sin^2\beta\sin 2\phi\ t_{20} \\
\mathrm{Im}\langle T_{11}\rangle &= -\frac{1}{\sqrt{2}}\sin\beta\cos\phi\ t_{10} & \mathrm{Re}\langle T_{21}\rangle &= \sqrt{\frac{3}{2}}\sin\beta\cos\beta\sin\phi\ t_{20} \\
\langle T_{10}\rangle &= \cos\beta\ t_{10} & \mathrm{Im}\langle T_{21}\rangle &= -\sqrt{\frac{3}{2}}\sin\beta\cos\beta\cos\phi\ t_{20} \\
\mathrm{Re}\langle T_{22}\rangle &= -\sqrt{\frac{3}{8}}\sin^2\beta\cos 2\phi\ t_{20} & \langle T_{20}\rangle &= \frac{1}{2}(3\cos^2\beta-1)\ t_{20} \ . \qquad (4)
\end{aligned}$$

These matters are treated at greater length in Ref. 3.

*s_A is the arbitrary spin for target A.

References

1. L. J. B. Goldfarb, Nucl. Phys. 7 (1958) 622

2. Gerald G. Ohlsen and P. W. Keaton, Jr., "Formalism for $A(\vec{p},\vec{p})A$ and $A(\vec{d},\vec{d})A$ Polarization Transfer," Proceedings of the 3rd International Symposium on Polarization Phenomena in Nuclear Reactions (to be published)

3. J. L. Gammel, P. W. Keaton, Jr., and G. G. Ohlsen, to be published

Formalism for $A(\vec{p},\vec{p})A$ and $A(\vec{d},\vec{d})A$ Polarization Transfer

Gerald G. Ohlsen and P. W. Keaton, Jr.

Los Alamos Scientific Laboratory, University of California
Los Alamos, New Mexico 87544

The formalism presented here is valid for the reaction $A + \vec{B} \rightarrow \vec{C} + D$, where B is any polarized spin-one (one-half) particle (photons excluded) in the entrance channel and C is any polarized spin-one (one-half) particle in the exit channel, and where A and D have arbitrary spins. Thus we treat not only elastic and inelastic deuteron and proton scattering, but also such reactions as $^{11}B(\vec{d},p)^{12}\vec{B}_{g.s.}$ and $^{7}Li(\vec{p},n)^{7}Be$. However, for simplicity we will refer to these cases hereafter as "deuteron" ("proton") scattering. The structure of the expressions which appear here is the most general allowed by the assumption that parity is conserved.

The form of the observables for deuteron scattering is given in table 1 in terms of the Goldfarb tensor operators[1] for spin one. $I_o(\theta)$ is the cross section for an unpolarized incident deuteron beam at the scattering angle θ. Initial spin-one polarization of the beam is designated $\langle P^i_k \rangle$ and $\langle P^i_{k\ell} \rangle$ and final spin-one polarization is designated $\langle P^f_k \rangle$ and $\langle P^f_{k\ell} \rangle$. The polarization transfer coefficients are written, for example, $P^{y'z'}_{xy} \equiv P^{y'z'}_{xy}(\theta)$, and are the quantities which are to be measured. We use the coordinate systems described in an accompanying paper.[2] The Goldfarb operators are overcomplete; the operator relation $P_{xx}+P_{yy}+P_{zz} = 0$ can be used to rewrite the terms involving these tensors in various ways (as done, for instance, in ref. 2)

Table 1

$$I(\theta,\phi) = I_o[1+\tfrac{3}{2}\langle P^i_y\rangle P^o_{\underline{y}}+\tfrac{2}{3}\langle P^i_{xz}\rangle P^o_{\underline{xz}}+\tfrac{1}{3}\langle P^i_{xx}\rangle P^o_{xx}+\tfrac{1}{3}\langle P^i_{yy}\rangle P^o_{yy}+\tfrac{1}{3}\langle P^i_{zz}\rangle P^o_{zz}]$$

$$\sqrt{\tfrac{3}{2}}\langle P^f_{x'},\rangle I = I_o[\tfrac{3}{2}\langle P^i_x\rangle P^{x'}_x+\tfrac{3}{2}\langle P^i_z\rangle P^{x'}_{\underline{z}}+\tfrac{2}{3}\langle P^i_{xy}\rangle P^{x'}_{\underline{xy}}+\tfrac{2}{3}\langle P^i_{yz}\rangle P^{x'}_{yz}]$$

$$\sqrt{\tfrac{3}{2}}\langle P^f_{y'},\rangle I = I_o[\sqrt{\tfrac{3}{2}}P^{y'}_{\underline{o}}+\tfrac{3}{2}\langle P^i_y\rangle P^{y'}_y+\tfrac{2}{3}\langle P^i_{xz}\rangle P^{y'}_{xz}+\tfrac{1}{3}\langle P^i_{xx}\rangle P^{y'}_{\underline{xx}}+\tfrac{1}{3}\langle P^i_{yy}\rangle P^{y'}_{\underline{yy}}+\tfrac{1}{3}\langle P^i_{zz}\rangle P^{y'}_{\underline{zz}}]$$

$$\sqrt{\tfrac{3}{2}}\langle P^f_{z'},\rangle I = I_o[\tfrac{3}{2}\langle P^i_x\rangle P^{z'}_{\underline{x}}+\tfrac{3}{2}\langle P^i_z\rangle P^{z'}_z+\tfrac{2}{3}\langle P^i_{xy}\rangle P^{z'}_{xy}+\tfrac{2}{3}\langle P^i_{yz}\rangle P^{z'}_{\underline{yz}}]$$

$$\sqrt{\tfrac{2}{3}}\langle P^f_{x'y'},\rangle I = I_o[\tfrac{3}{2}\langle P^i_x\rangle P^{x'y'}_{\underline{x}}+\tfrac{3}{2}\langle P^i_z\rangle P^{x'y'}_z+\tfrac{2}{3}\langle P^i_{xy}\rangle P^{x'y'}_{xy}+\tfrac{2}{3}\langle P^i_{yz}\rangle P^{x'y'}_{\underline{yz}}]$$

$$\sqrt{\tfrac{2}{3}}\langle P^f_{x'z'},\rangle I = I_o[\sqrt{\tfrac{2}{3}}P^{x'z'}_{\underline{o}}+\tfrac{3}{2}\langle P^i_y\rangle P^{x'z'}_y+\tfrac{2}{3}\langle P^i_{xz}\rangle P^{x'z'}_{xz}+\tfrac{1}{3}\langle P^i_{xx}\rangle P^{x'z'}_{\underline{xx}}+\tfrac{1}{3}\langle P^i_{yy}\rangle P^{x'z'}_{\underline{yy}}+\tfrac{1}{3}\langle P^i_{zz}\rangle P^{x'z'}_{\underline{zz}}]$$

$$\sqrt{\tfrac{2}{3}}\langle P^f_{y'z'},\rangle I = I_o[\tfrac{3}{2}\langle P^i_x\rangle P^{y'z'}_x+\tfrac{3}{2}\langle P^i_z\rangle P^{y'z'}_{\underline{z}}+\tfrac{2}{3}\langle P^i_{xy}\rangle P^{y'z'}_{\underline{xy}}+\tfrac{2}{3}\langle P^i_{yz}\rangle P^{y'z'}_{yz}]$$

$$\tfrac{1}{\sqrt{3}}\langle P^f_{x'x'},\rangle I = I_o[\tfrac{1}{\sqrt{3}}P^{x'x'}_o+\tfrac{3}{2}\langle P^i_y\rangle P^{x'x'}_{\underline{y}}+\tfrac{2}{3}\langle P^i_{xz}\rangle P^{x'x'}_{\underline{xz}}+\tfrac{1}{3}\langle P^i_{xx}\rangle P^{x'x'}_{xx}+\tfrac{1}{3}\langle P^i_{yy}\rangle P^{x'x'}_{yy}+\tfrac{1}{3}\langle P^i_{zz}\rangle P^{x'x'}_{zz}$$

$$\tfrac{1}{\sqrt{3}}\langle P^f_{y'y'},\rangle I = I_o[\tfrac{1}{\sqrt{3}}P^{y'y'}_o+\tfrac{3}{2}\langle P^i_y\rangle P^{y'y'}_{\underline{y}}+\tfrac{2}{3}\langle P^i_{xz}\rangle P^{y'y'}_{\underline{xz}}+\tfrac{1}{3}\langle P^i_{xx}\rangle P^{y'y'}_{xx}+\tfrac{1}{3}\langle P^i_{yy}\rangle P^{y'y'}_{yy}+\tfrac{1}{3}\langle P^i_{zz}\rangle P^{y'y'}_{zz}]$$

$$\tfrac{1}{\sqrt{3}}\langle P^f_{z'z'},\rangle I = I_o[\tfrac{1}{\sqrt{3}}P^{z'z'}_o+\tfrac{3}{2}\langle P^i_y\rangle P^{z'z'}_{\underline{y}}+\tfrac{2}{3}\langle P^i_{xz}\rangle P^{z'z'}_{\underline{xz}}+\tfrac{1}{3}\langle P^i_{xx}\rangle P^{z'z'}_{xx}+\tfrac{1}{3}\langle P^i_{yy}\rangle P^{z'z'}_{yy}+\tfrac{1}{3}\langle P^i_{zz}\rangle P^{z'z'}_{zz}]$$

*Work performed under the auspices of the U. S. Atomic Energy Commission.

The form of the observables for proton scattering is given in table 2. We use the Pauli spin-1/2 operators, σ_x, σ_y, and σ_z. The notation is analogous to that which was used for spin-one in table 1. The polarization transfer coefficients are the same as those defined by Wolfenstein[3] with $\sigma_o^{y'}(\theta) = P_2$, $\sigma_y^{y'}(\theta) = D$, $\sigma_x^{x'}(\theta) = R$, $\sigma_z^{x'}(\theta) = A$, $\sigma_x^{z'}(\theta) = R'$, $\sigma_z^{z'}(\theta) = A'$, and are included here for completeness.

Table 2

$$I(\theta,\phi) = I_o(\theta)[1+\langle\sigma_y^i\rangle\underline{\sigma_y^o(\theta)}] \qquad \langle\sigma_{x'}^f\rangle I = I_o[\langle\sigma_x^i\rangle\sigma_x^{x'}(\theta)+\langle\sigma_z^i\rangle\underline{\sigma_z^{x'}(\theta)}]$$

$$\langle\sigma_{y'}^f\rangle I = I_o[\underline{\sigma_o^{y'}(\theta)}+\langle\sigma_y^i\rangle\sigma_y^{y'}(\theta)] \qquad \langle\sigma_{z'}^f\rangle I = I_o[\langle\sigma_x^i\rangle\underline{\sigma_x^{z'}(\theta)}+\langle\sigma_z^i\rangle\sigma_z^{z'}(\theta)]$$

Finally, following the line of argument by Csonka et al.[4], we define the number of times x, y, and z appears in a polarization transfer coefficient as N_x, N_y, and N_z, respectively. We can then classify the coefficients in two useful ways. First, those which have N_x+N_y odd are odd functions of θ. All such terms are underlined in tables 1 and 2. All other transfer coefficients are even in θ. Second, if z' is chosen along the outgoing c.m. direction, those polarization transfer coefficients which have N_x odd reverse sign for the inverse reaction if one assumes time reversal invariance. This leads to, for example,

$$\overline{P_y^o(\theta)} = P_o^{y'}(\theta) \ , \quad \overline{P_{xz}^o(\theta)} = -P_o^{x'z'}(\theta), \text{ and } \overline{P_{xz}^{y'y'}(\theta)} = -P_{yy}^{x'z'}(\theta),$$

where the bars denote observables in the inverse reaction. For the case of proton elastic scattering we arrive at, for example,

$$\overline{\sigma_x^{z'}(\theta)} = -\sigma_z^{x'}(\theta) \ ,$$

which in the p-p scattering case is the well-known relation R' = -A. It should be emphasized that although the formalism of tables 1 and 2 are valid for any choice of the z' axis, statements regarding time reversal invariance hold only for particular coordinate system choices (one of which is cited above)[5].

References

1. L. J. B. Goldfarb, Nucl. Phys. 7 (1958) 622

2. J. L. Gammel, P. W. Keaton, Jr., and Gerald G. Ohlsen, "Formalism for $A(\vec{d},\vec{n})B$ or $A(\vec{d},\vec{p})B$ Polarization Transfer Reactions," Proceedings of the 3rd International Symposium on Polarization Phenomena in Nuclear Reactions" (to be published).

3. L. Wolfenstein, Ann. Rev. Nucl. Sci. 6 (1956) 43

4. P. L. Csonka and M. J. Moravcsik, Phys. Rev. 152 (1966) 1310

5. P. W. Keaton, Jr., "Time Reversal in Polarization Phenomena of Nuclear Reactions," Los Alamos Sci. Lab. Report LA-4373-MS (unpublished)

Quadratic Relations Between the $T(\vec{d},\vec{n})^4He$ Observables*

Gerald G. Ohlsen, J. L. Gammel, and P. W. Keaton, Jr.

Los Alamos Scientific Laboratory, University of California
Los Alamos, New Mexico 87544

There are altogether 18 observables which may be measured for the $T(\vec{d},\vec{n})^4He$ polarization transfer reaction, in the case of an unpolarized tritium target, at each energy and angle (if one assumes conservation of parity). These are the differential cross section $I_o(\theta)$, four analyzing tensors $P^o_y(\theta)$, $P^o_{xz}(\theta)$, $\frac{1}{2}[P^o_{xx}(\theta)-P^o_{yy}(\theta)]$, and $P^o_{zz}(\theta)$, the polarization produced by an unpolarized neutron beam, $P^{y'}_o(\theta)$, and twelve "polarization transfer coefficients" as defined in an accompanying paper[1]. In general, the lower subscript indicates the polarization of the incident deuteron and the superscript indicates the neutron polarization component. Two right-handed coordinate systems with $\vec{k}_{in} \times \vec{k}_{out}$ defining both the y and y' axes are assumed; the xz and x'z' axes are arbitrary but are usually chosen with z along $\vec{k}_{in}$ and z' along $\vec{k}_{out}$. Since the scattering matrix, M, which describes the reaction has only six complex elements, clearly these eighteen experiments are not independent. No linear relations between the observables exist; however, in table 1 twelve quadratic relations between the observables are presented, so that at most six of the experimental observables are truly independent.

These relations might be expected to serve several useful purposes. First, each relation is in itself a parity test. Second, these relations may be applied as consistency checks between sets and types of data when data of the polarization transfer type become more readily available. (The relations may be regarded as defining the volume in an eighteen dimensional hyperspace which can be physically "occupied" by the data sets.) Finally the relations may serve as a guide, in some cases, as to which of the various experiments that might be performed are least related to the experiments already completed and, therefore, contain the greatest amount of new information. Also, the relations show, at least in principle, that some of the experiments can be omitted altogether without sacrifice of information.

In table 1, the coefficients which are underlined are odd in the scattering angle, θ, and therefore vanish at 0° (180°). Using also the zero degree relations $P^{z'}_{xy} = 0$, $P^{y'}_{xz} = -P^{x'}_{yz}$, $P^{x'}_{x} = P^{y'}_{y}$, and $P^o_{xx} = P^o_{yy}$, these twelve equations reduce to only two independent relations at 0° (180°):

$$(\frac{3}{2}P^{y'}_{y})^2 + (P^{y'}_{xz})^2 = (1-P^o_{xx})(1-P^o_{zz}) \; ; \quad \frac{3}{2}P^{z'}_{z} = 1 - P^o_{xx} \equiv 1 + \frac{1}{2}P^o_{zz} \; .$$

---

*Work performed under the auspices of the U. S. Atomic Energy Commission.

The first relation shows that, at 0°, it would never be necessary to measure the geometrically complicated quantity $P^{y'}_{xz}$. The second relation can be shown to follow from angular momentum conservation alone; it is interesting in that it implies that the outgoing longitudinal neutron polarization is 100% for a 100% $m_I = 1$ ($\langle P_z \rangle = \langle P_{zz} \rangle = 1$) deuteron beam. This conclusion is independent of all dynamics.

Table 1: Quadratic Relations

1. $\left(\frac{3}{2}P^{x'}_{x}\right)^2+\left(P^{x'}_{yz}\right)^2+\left(\frac{3}{2}P^{z'}_{x}\right)^2+\left(P^{z'}_{yz}\right)^2 = (1-P^{o}_{yy})(1-P^{o}_{zz})-(P^{y'}_{o}-P^{y'}_{yy})(P^{y'}_{o}-P^{y'}_{zz})$

2. $\left(\frac{3}{2}P^{x'}_{z}\right)^2+\left(P^{x'}_{xy}\right)^2+\left(\frac{3}{2}P^{z'}_{z}\right)^2+\left(P^{z'}_{xy}\right)^2 = (1-P^{o}_{xx})(1-P^{o}_{yy})-(P^{y'}_{o}-P^{y'}_{xx})(P^{y'}_{o}-P^{y'}_{yy})$

3. $\left(\frac{3}{2}P^{o}_{y}\right)^2+\left(P^{o}_{xz}\right)^2+\left(\frac{3}{2}P^{y'}_{y}\right)^2+\left(P^{y'}_{xz}\right)^2 = (1-P^{o}_{xx})(1-P^{o}_{zz})+(P^{y'}_{o}-P^{y'}_{xx})(P^{y'}_{o}-P^{y'}_{zz})$

4. $\frac{3}{2}P^{x'}_{x}P^{z'}_{yz} - \frac{3}{2}P^{z'}_{x}P^{x'}_{yz} = -\frac{1}{2}(1-P^{o}_{yy})(P^{y'}_{o}-P^{y'}_{zz})-\frac{1}{2}(1-P^{o}_{zz})(P^{y'}_{o}-P^{y'}_{yy})$

5. $\left(\frac{3}{2}\right)^2 P^{o}_{y}P^{y'}_{y} + P^{o}_{xz}P^{y'}_{xz} = \frac{1}{2}(1-P^{o}_{zz})(P^{y'}_{o}-P^{y'}_{xx})+\frac{1}{2}(1-P^{o}_{xx})(P^{y'}_{o}-P^{y'}_{yy})$

6. $\frac{3}{2}P^{x'}_{z}P^{z'}_{xy} - \frac{3}{2}P^{z'}_{z}P^{x'}_{xy} = -\frac{1}{2}(1-P^{o}_{yy})(P^{y'}_{o}-P^{y'}_{xx})+\frac{1}{2}(1-P^{o}_{xx})(P^{y'}_{o}-P^{y'}_{yy})$

7. $\frac{3}{2}P^{x'}_{x}P^{o}_{xz} + \frac{3}{2}P^{o}_{y}P^{x'}_{yz} - \left(\frac{3}{2}\right)^2 P^{z'}_{x}P^{y'}_{y} + P^{z'}_{yz}P^{y'}_{xz} = -P^{z'}_{xy}(P^{y'}_{o}-P^{y'}_{zz})+\frac{3}{2}P^{x'}_{z}(1-P^{o}_{zz})$

8. $\left(\frac{3}{2}\right)^2 P^{x'}_{x}P^{o}_{y} - P^{x'}_{yz}P^{o}_{xz} + \frac{3}{2}P^{z'}_{x}P^{y'}_{xz} + \frac{3}{2}P^{y'}_{y}P^{z'}_{yz} = \frac{3}{2}P^{z'}_{z}(P^{y'}_{o}-P^{y'}_{zz})+P^{x'}_{xy}(1-P^{o}_{zz})$

9. $\left(\frac{3}{2}\right)^2 P^{x'}_{x}P^{x'}_{z} - P^{x'}_{yz}P^{x'}_{xy} + \left(\frac{3}{2}\right)^2 P^{z'}_{x}P^{z'}_{z} - P^{z'}_{yz}P^{z'}_{xy} = -P^{y'}_{xz}(P^{y'}_{o}-P^{y'}_{yy})+P^{o}_{xz}(1-P^{o}_{yy})$

10. $\frac{3}{2}P^{x'}_{x}P^{x'}_{xy} + \frac{3}{2}P^{x'}_{z}P^{x'}_{yz} + \frac{3}{2}P^{z'}_{x}P^{z'}_{xy} + \frac{3}{2}P^{z'}_{z}P^{z'}_{yz} = -\frac{3}{2}P^{y'}_{y}(P^{y'}_{o}-P^{y'}_{yy})+\frac{3}{2}P^{o}_{y}(1-P^{o}_{yy})$

11. $\frac{3}{2}P^{x'}_{z}P^{o}_{xz} + \frac{3}{2}P^{o}_{y}P^{x'}_{xy} + \left(\frac{3}{2}\right)^2 P^{y'}_{y}P^{z'}_{z} - P^{y'}_{xz}P^{z'}_{xy} = P^{z'}_{yz}(P^{y'}_{o}-P^{y'}_{xx})+\frac{3}{2}P^{x'}_{x}(1-P^{o}_{xx})$

12. $P^{o}_{xz}P^{x'}_{xy} - \left(\frac{3}{2}\right)^2 P^{o}_{y}P^{x'}_{z} + \frac{3}{2}P^{y'}_{y}P^{z'}_{xy} + \frac{3}{2}P^{z'}_{z}P^{y'}_{xz} = \frac{3}{2}P^{z'}_{x}(P^{y'}_{o}-P^{y'}_{xx})-P^{x'}_{yz}(1-P^{o}_{xx})$

Reference

1. J. L Gammel, P. W. Keaton, Jr., and Gerald G. Ohlsen, "Formalism for $A(\vec{d},\vec{n})B$ and $A(\vec{d},\vec{p})B$ Polarization Transfer Reactions," Proc. 3rd Internatl. Symp. on Polarization Phenomena in Nuclear Reactions" (to be published)

Figures of Merit for Polarized Deuteron Beams*

P. W. Keaton, Jr., and Gerald G. Ohlsen

Los Alamos Scientific Laboratory, University of California
Los Alamos, New Mexico 87544

The quantity p^2I, where I is the current and p is the polarization, has long been used as a figure of merit for polarized proton beams. We generalize this figure of merit to include the case of vector and tensor polarized deuteron beams.

For a spin-1/2 beam, one measures an asymmetry A, given by $A = (L-R)/(L+R)$, where L and R are the counts recorded in the left detector and in the right detector, respectively. In terms of the beam polarization and the analyzing power of the reaction, $P(\theta)$, we have $A = pP(\theta)$. The statistical error, $\Delta P(\theta)$, associated with such a determination of $P(\theta)$ is

$$\Delta P(\theta) = \frac{1}{p} \cdot \frac{\sqrt{1-A^2}}{\sqrt{L+R}} \propto \frac{\sqrt{1-A^2}}{p\sqrt{It}} , \tag{1}$$

since L+R is proportional to It, where t is the data acquisition time. In deriving Eq. (1), we have assumed that L and R contain no background counts. In the limit of small A, we find

$$\Delta P(\theta) \propto \frac{1}{p\sqrt{It}} . \tag{2}$$

We define the figure of merit to be inversely proportional to the counting time necessary to produce a given statistical error $\Delta P(\theta)$. Thus we see that the relevant figure of merit is in fact p^2I. Notice, however, that in the case of large $P(\theta)$ this figure underestimates considerably the advantage of large beam polarizations. (This will be true also for the deuteron quantities.)

For deuterons, we consider five asymmetries. These are, with the corresponding observables and (zero-background) statistical error expressions:

$$A_1 = \frac{(L+R)-(U+D)}{L+R+U+D} = \frac{-\frac{1}{4}p_{ZZ}\sin^2\beta[P^o_{xx}-P^o_{yy}]}{1+\frac{1}{4}p_{ZZ}(3\cos^2\beta-1)P^o_{zz}} \quad ; \quad \Delta A_1 = \sqrt{\frac{1-A_1^2}{L+R+U+D}}$$

$$A_2 = \frac{2(L-R)}{L+R+U+D} = \frac{\frac{3}{2}p_Z\sin\beta P^o_y}{1+\frac{1}{4}p_{ZZ}(3\cos^2\beta-1)P^o_{zz}} \quad ; \quad \Delta A_2 = \sqrt{\frac{\frac{4(L+R)}{L+R+U+D} - A_2^2}{L+R+U+D}}$$

$$A_3 = \frac{2(U-D)}{L+R+U+D} = \frac{p_{ZZ}\sin\beta\cos\beta P^o_{xz}}{1+\frac{1}{4}p_{ZZ}(3\cos^2\beta-1)P^o_{zz}} \quad ; \quad \Delta A_3 = \sqrt{\frac{\frac{4(U+D)}{L+R+U+D} - A_3^2}{L+R+U+D}}$$

$$A_4 = \frac{L-R}{L+R} = \frac{\frac{3}{2}p_Z\sin\beta P^o_y}{1+\frac{1}{2}p_{ZZ}[\sin^2\beta P^o_{yy}+\cos^2\beta P^o_{zz}]} \quad ; \quad \Delta A_4 = \sqrt{\frac{1-A_4^2}{L+R}}$$

$$A_5 = \frac{U-D}{U+D} = \frac{p_{ZZ}\sin\beta\cos\beta P^o_{xz}}{1+\frac{1}{2}p_{ZZ}[\sin^2\beta P^o_{xx}+\cos^2\beta P^o_{zz}]} \quad ; \quad \Delta A_5 = \sqrt{\frac{1-A_5^2}{U+D}}$$

*Work performed under the auspices of the U. S. Atomic Energy Commission.

where L, R, U, and D are the counts recorded in the left, right, up, and down detectors, respectively, and where p_Z and p_{ZZ} are the incident vector and tensor beam polarizations. (For definitions of β, ϕ, "up," etc., see Ref. 1.)

It is clear from Eq. (3) that one cannot simply divide out the beam polarization as in the spin-1/2 case. That is, except for the special case of $\cos\beta = 1/\sqrt{3}$ for A_1, A_2, and A_3 [2], the asymmetries are not linearly related to the beam polarization and analyzing tensors. We must first measure separately the denominator factor by means of a ratio of counts with different values of p_{ZZ}. Denoting the counts observed with beam polarization p_{ZZ} by T and with beam polarization p'_{ZZ} by T', we define

$$B = \frac{T-T'}{p_{ZZ}T'-p'_{ZZ}T} \quad ; \quad \Delta B = \frac{(p_{ZZ}-p'_{ZZ})}{(p_{ZZ}T'-p'_{ZZ}T)^2}\sqrt{T^2T'+T'^2T} \ ,$$

where B could be $\frac{1}{4}(3\cos^2\beta-1)\,P^o_{zz}$, $\frac{1}{2}[\sin^2\beta P^o_{yy}+\cos^2\beta P^o_{zz}]$, or $\frac{1}{2}[\sin^2\beta P^o_{xx}+\cos^2\beta P^o_{zz}]$, and T would be L+R+U+D, L+R, or U+D, respectively. In the limit of zero for the analyzing tensors, T→T', and

$$\Delta B = \frac{1}{(p_{ZZ}-p'_{ZZ})\sqrt{T}} \ .$$

The figure of merit relevant for measuring B is, therefore, given by $(\Delta p_{ZZ})^2 I$, where Δp_{ZZ} is the change in p_{ZZ} obtainable between the two modes of operation for the ion source.

Returning to the asymmetries A_1 through A_5, we see that if the denominator factor has already been determined, the figure of merit becomes $p_Z^2 I$ for A_2 and A_4, and $p_{ZZ}^2 I$ for A_1, A_3, and A_5. In summary, deuteron beams are described in terms of three figures of merit: $p_Z^2 I$ for $P^o_y(\theta)$ measurements, $p_{ZZ}^2 I$ for $P^o_{xx}(\theta)-P^o_{yy}(\theta)$ and $P^o_{xz}(\theta)$ measurements, and $(\Delta p_{ZZ})^2 I$ for $P^o_{zz}(\theta)$ measurements.

By way of example, we compare a pure vector polarized beam ($p_Z=2/3$, $p_{ZZ}=0$) to a pure $m_I=1$ beam ($p_Z=p_{ZZ}=1$). Measurement of A_2 or A_4 to a given accuracy takes 9/2 times as much time for the pure vector polarized beam; however, for the $m_I=1$ beam some additional time must be spent in the evaluation of the denominator expression. The amount of time required depends on the method used--for example, the use of an intense unpolarized beam might reduce time required markedly. Further, this time should not be charged against the measurement of $P^o_y(\theta)$, since one is measuring two quantities, not one. The ideal figures of merit for three methods are given in Table 1. The best mode of operation for each figure of merit is assumed.

Table 1. Ideal figures of merit for three methods of polarizing deuterons with Lamb-shift sources.

Method	$p_Z^2 I$	$p_{ZZ}^2 I$	$(\Delta p_{ZZ})^2 I$
spin filter ($p_Z = p_{ZZ} = 1$ or $p_Z = 0$, $p_{ZZ} = -2$)	I	4I	9I
zero field crossing ($p_Z = 2/3$, $p_{ZZ} = 0$ or $p_Z = 0$, $p_{ZZ} = -1$)	$\frac{4}{9}$I	I	I
adiabatic field reduction ($p_Z = 1/3$, $p_{ZZ} = -1/3$ or unpolarized)	$\frac{1}{9}$I	$\frac{1}{9}$I	$\frac{1}{9}$I

References

1. J.L.Gammel, P.W.Keaton, and G.G.Ohlsen, "Formalism for $A(\vec{d},\vec{n})B$ and $A(\vec{d},\vec{p})B$ Polarization Transfer Reactions," Proc. 3rd Internatl. Symp. Polarization Phenomena in Nuclear Reactions (to be published)
2. G.P.Lawrence, G.G.Ohlsen, J.L.McKibben, P.W.Keaton, and D.D.Armstrong, "A Rapid Method for the Measurement of Analyzing Tensors in Reactions Induced by Polarized Deuterons," same as above

A Study of $^3He(\vec{d},d)^3He$ Scattering at 10 and 12 MeV*

D. C. Dodder, D. D. Armstrong, P. W. Keaton, Jr.,
G. P. Lawrence, J. L. McKibben, and Gerald G. Ohlsen

Los Alamos Scientific Laboratory, University of California
Los Alamos, New Mexico 87544

We have measured the vector and tensor analyzing power for d-^{3}He elastic scattering at 10 and 12 MeV. A "cube" scattering chamber enabled us to measure the left, right, up, and down yield simultaneously for any polar angle in the range 20° to 160°. An angular resolution of 2° (FWHM) was used. A complete measurement consists of four counting periods with the chamber rotated around the beam direction by 90° between periods; this procedure removes detector efficiency problems. The deuteron quantization axis was at 54.7° with respect to the beam direction (in the horizontal plane) for the simultaneous P^o_y, P^o_{xz}, and $(P^o_{xx}-P^o_{yy})/2$ measurements and parallel to the beam direction for the P^o_{zz} measurements.[1] Only the P^o_{zz} measurements depend upon accurate current integration. m_I = 1 deuterons

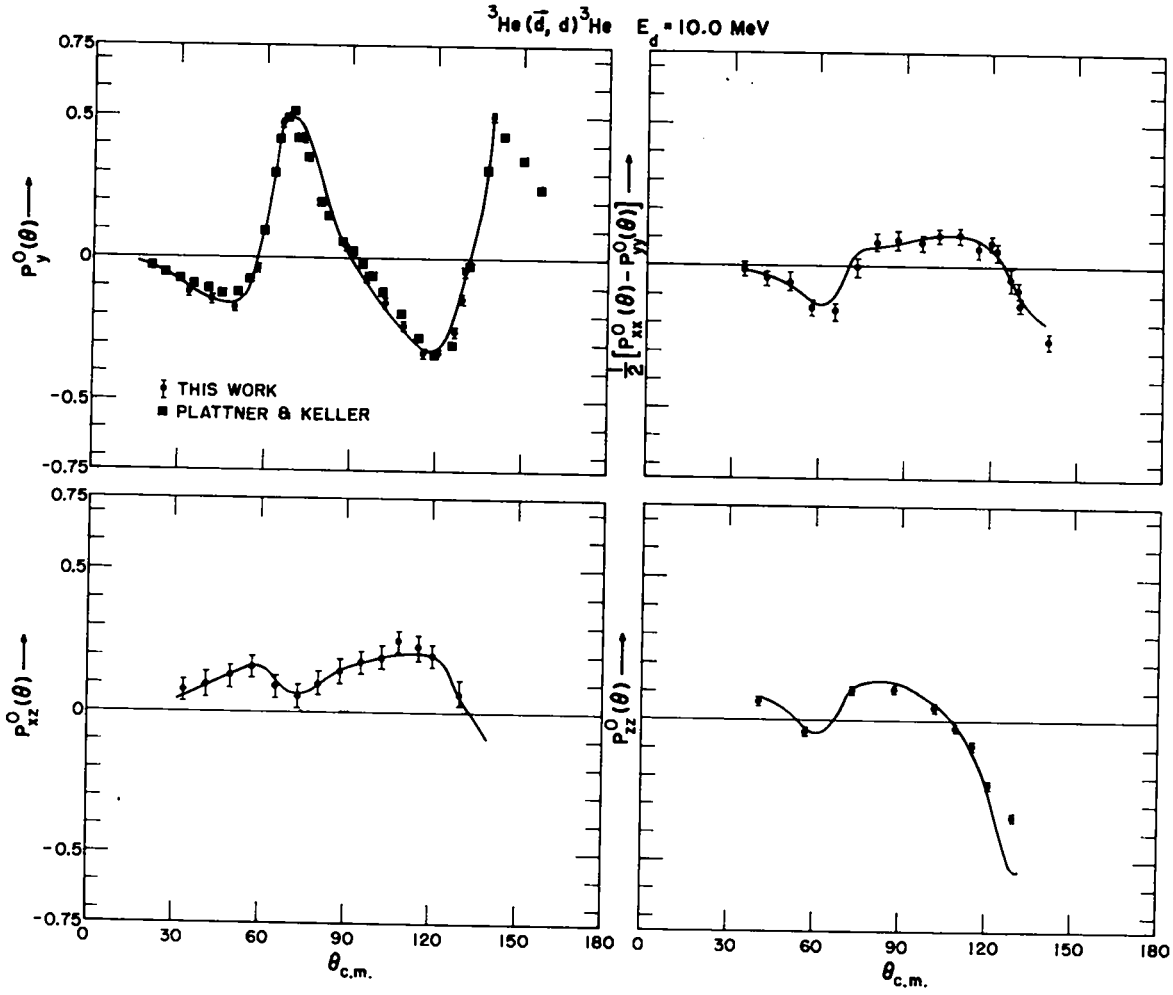

Fig. 1. Vector and tensor analyzing power for $^3He(\vec{d},d)^3He$ elastic scattering at 10 MeV.

*Work performed under the auspices of the U. S. Atomic Energy Commission.

($p_Z = p_{ZZ} \approx 0.8$) were used for most of the measurements; $m_I = 0$ deuterons ($p_Z \approx 0$, $p_{ZZ} \approx -1.6$) were used occasionally to check the alignment of the chamber. False asymmetries were kept small by minimizing the beam on a properly suppressed collimator which preceded the faraday cup. P^o_{xz} is about 2-1/2 times more sensitive to false asymmetries than is P^o_y; for this reason, larger errors are assumed for P^o_{xz}.

Silicon surface barrier E-ΔE detector telescopes were used to permit mass identification. An on-line computer recorded 512 channel spectra for one or two masses for each telescope. The computer also measured the beam polarization (quench method) periodically, rotated the cube, appropriately summed the spectra, and calculated the values of the analyzing vector and tensors.

The data obtained are shown in Figs. 1 and 2. All errors shown are the estimated systematic uncertainties. A preliminary phase shift fit for the 10-MeV data is also shown. Since 51 parameters are involved (77 data points) a meaningful fit can probably be obtained only if data of other types ($^3He(\vec{d},p)^4He$, $^3He(\vec{d},\vec{p})^4He$) is included. Such an analysis is in progress.

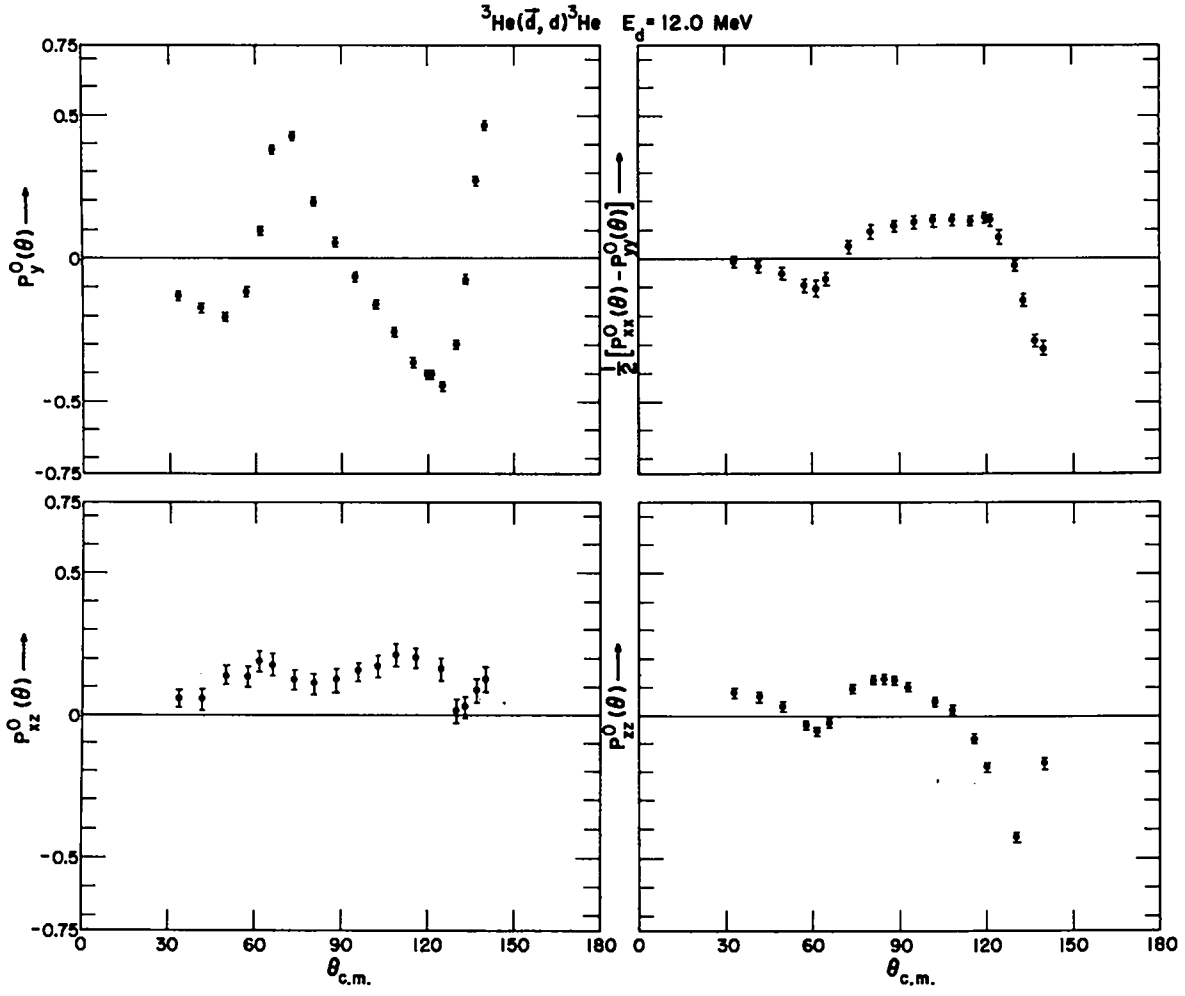

Fig. 2. Vector and tensor analyzing power for $^3He(\vec{d},d)^3He$ elastic scattering at 12 MeV.

Reference

1. G. P. Lawrence, Gerald G. Ohlsen, J. L. McKibben, P. W. Keaton, Jr., and D. D. Armstrong, "A Rapid Method for the Measurement of Analyzing Tensors in Reactions Induced by Polarized Deuterons" Proc. 3rd Internatl. Symp. on Polarization Phenomena in Nuclear Reactions (to be published)

Measurement of the Vector and Tensor Analyzing Power of d-^{4}He Elastic Scattering at 12 MeV*

G. P. Lawrence, D. C. Dodder, P. W. Keaton, Jr., D. D. Armstrong, J. L. McKibben, and Gerald G. Ohlsen

Los Alamos Scientific Laboratory, University of California
Los Alamos, New Mexico 87544

The vector and tensor analyzing powers of d-^{4}He elastic scattering at 12-MeV deuteron laboratory energy have been measured by means of methods and equipment described in other papers in this symposium[1,2]. The experimental results together with the phase shift fits to be discussed below are shown in Fig. 1.

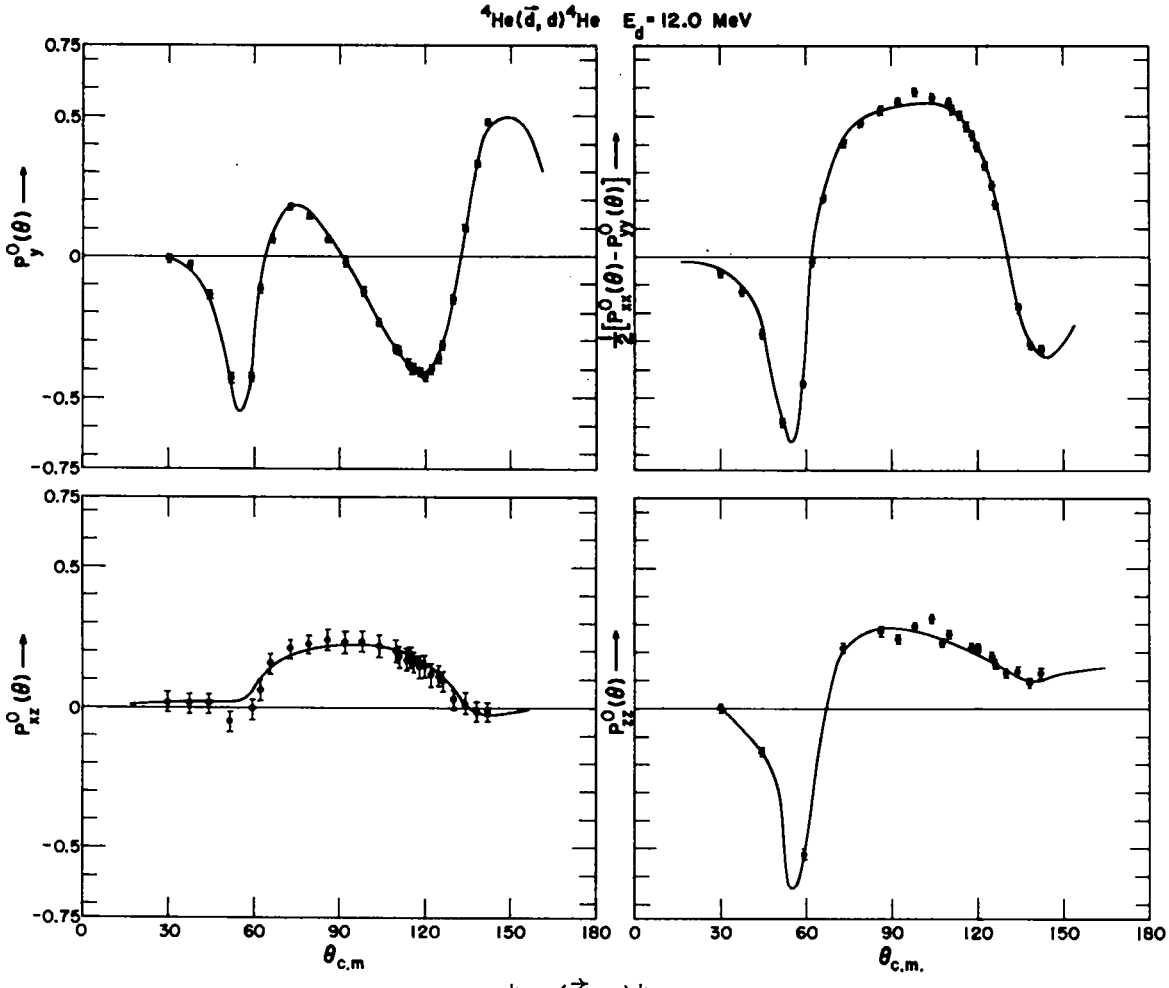

Fig. 1. Analyzing tensors for ^{4}He($\vec{d}$,d)^{4}He elastic scattering at 12 MeV.

The Cartesian tensors $P_i = S_i$ and $P_{ij} = 3(S_iS_j+S_jS_i)/2 - 2\delta_{ij}$ are used as a basis. Note that the observables must be bounded by $-2 < P^o_{zz} < 1$, $-3/2 < (P^o_{xx}-P^o_{yy})/2 < 3/2$, $-3/2 < P^o_{xz} < 3/2$, and $-1 < P^o_y < 1$, and that only a part of the range of possible variation is shown on the graphs. (As is well known, the observables are further related by certain inequalities.)

The tensor analyzing powers are well fit by parameters consistent with those obtained at lower energies by McIntyre and Haeberli[3], while the vector analyzing

*Work performed under the auspices of the U. S. Atomic Energy Commission.

power is only qualitatively fit. In an initial attempt to obtain an improved fit to the present data, the prediction for the cross section differed violently from the measured cross sections[4] at 11.5 MeV (the closest energy at which data is available). This convinced us that it would be necessary to include cross section data to obtain a meaningful fit; accordingly, the cross sections of Ref. 4 were extrapolated to 12 MeV and included in the analysis. Starting with phase shifts extrapolated from those of Ref. 3, a solution was obtained; the parameters are given in Table 1. The computer program used in the search was the Los Alamos General Energy Independent Reactance Matrix Analysis Code (ElA2)[5]. This code fits the data with a unitary collision matrix and a set of inelastic parameters which multiply the diagonal elements of the collision matrix. This nongeneral, nonunitary matrix differs from the nongeneral, nonunitary matrix used in Ref. 3, so the results are not strictly comparable for those states connected with nondiagonal elements of the collision matrix. The 2x2 submatrices of the nuclear unitary collision matrix are given in terms of the nuclear bar representation[6].

Table 1: Nuclear Bar Phase Shifts and Elastic Parameters

State	$\bar{\delta}_{LJ}$ or $\bar{\epsilon}_{L-L'}$ (degrees)	Inelastic Parameters
S_1	-134.0	0.95
S_1-D_1	6.0	
D_1	- 77.4	0.41
P_2	- 3.3	0.64
P_2-F_2	- 5.0	
F_2	3.8	0.97
P_1	- 14.9	0.93
P_0	- 28.1	1.0
D_3	- 28.9	0.68
D_3-G_3	0.47	
G_3	4.7	1.0
D_2	- 59.8	0.89
F_4	8.2	0.74
F_3	6.8	0.91
G_5	3.8	0.84
G_4	1.7	0.96

We have not obtained a fit to the extrapolated cross section of quality comparable to the fits of polarization data shown in Fig. 1. The overall weighted variance (χ^2 per degree of freedom) is 1.4. This is subject to change, since the estimated errors for the polarization data were preliminary, and since the errors on the extrapolated cross sections are somewhat crudely estimated.

The solution given here should not be taken as evidence that the presently available data at this energy give a unique set of parameters. Some 15 starts from random sets of parameters have not led to this solution, but have instead led to solutions with larger weighted variance (ranging from 4 to 13). This is not a sufficient search of the space to ensure that other solutions do not exist; the only evidence for that conclusion at present comes from the connection to the lower energy analysis.

References

1. G.P.Lawrence, G.G.Ohlsen, J.L.McKibben, P.W.Keaton,Jr., and D.D.Armstrong, "A Rapid Method for the Measurement of Analyzing Tensors in Reactions Induced by Polarized Deuterons," Proc. 3rd Internatl. Symp. on Polarization Phenomena in Nuclear Reactions (to be published)
2. D.C.Dodder, D. D. Armstrong, P.W.Keaton,Jr., G.P.Lawrence, J.L.McKibben, and G.G. Ohlsen, "A Study of ^{3}He(d,d)^{3}He Scattering at 10 and 12 MeV," same as above
3. L. C. McIntyre and W. Haeberli, Nucl. Phys. A91 (1967) 382
4. L.S.Senhouse and T.A.Tombrello, Nucl. Phys. 57 (1964) 624
5. D.C.Dodder and K.Witte (to be published)
6. H.P.Stapp, T.J.Ypsilantis, and N.Metropolis, Phys. Rev. 105 (1957) 302

Considerations on Polarized Neutron Production by $(\vec{d},\vec{n})$ Polarization Transfer Reactions at 0°*

Gerald G. Ohlsen, P. W. Keaton, Jr., and J. E. Simmons

Los Alamos Scientific Laboratory, University of California
Los Alamos, New Mexico 87544

We consider various aspects of zero-degree polarization transfer for $(\vec{d},\vec{n})$ reactions with a view toward the practical production of polarized fast neutrons. We use a right-handed coordinate system (xyz) with the z axis along the incident deuteron direction, $\vec{k}_{in}$, and the y axis in any direction perpendicular to $\vec{k}_{in}$. The general expressions for the neutron intensity and polarization[1] at 0° are

$$I(0°) = I_o(0°)[1+\tfrac{1}{2}\langle P_{zz}\rangle P_{zz}(0°)]$$
$$\langle\sigma_x\rangle I(0°) = I_o(0°)[\tfrac{3}{2}\langle P_x\rangle P^x_x(0°)+\tfrac{2}{3}\langle P_{yz}\rangle P^x_{yz}(0°)]$$
$$\langle\sigma_y\rangle I(0°) = I_o(0°)[\tfrac{3}{2}\langle P_y\rangle P^y_y(0°)+\tfrac{2}{3}\langle P_{xz}\rangle P^y_{xz}(0°)]$$
$$\langle\sigma_z\rangle I(0°) = I_o(0°)[\tfrac{3}{2}\langle P_z\rangle P^z_z(0°)] \ . \qquad (1)$$

These relations follow from ref. 1 since all terms odd in the scattering angle, θ, become zero at $\theta = 0$. We have also used the restriction $P^z_{xy} \equiv 0$, which follows from the fact that the x and y axes may be defined arbitrarily. Other zero-degree conditions, which follow from the same requirement, are $P^o_{xx} = P^o_{yy} = -\tfrac{1}{2}P^o_{zz}$, $P^x_x = P^y_y$, and $P^y_{xz} = -P^x_{yz}$.

In the following, we specialize to cases in which the deuteron polarization possesses an axis of symmetry, as is obtained from a polarized ion source, and where this axis is oriented either along the y axis or the z axis. In these cases, eq. (1) reduces to

$$\langle\sigma_j\rangle = \frac{\tfrac{3}{2}\langle P_j\rangle P^j_j(0°)}{1+\tfrac{1}{2}\langle P_{jj}\rangle P^o_{jj}(0°)} \ ; \quad I(0°) = I_o(0°)[1+\tfrac{1}{2}\langle P_{jj}\rangle P^o_{jj}(0°)] \ , \qquad (2)$$

where j is either y or z, and where $\langle P_j\rangle$ and $\langle P_{jj}\rangle$ are the deuteron vector and tensor polarization, respectively, with respect to the j axis.

The intensities and polarizations for a pure $m_I = 1$ beam and for a pure vector polarized beam are summarized in Table 1. The "figure of merit", IP^2, is always larger for the $m_I = 1$ type of polarization.

Table 1

Beam Polarization	I/I_o	Neutron Polarization at 0°
$\langle P_y\rangle = \langle P_{yy}\rangle = 1$	$1+\frac{1}{2}P^o_{yy}$	$\langle\sigma_y\rangle = \frac{3}{2}P^y_y/(1+\frac{1}{2}P^o_{yy})$
$\langle P_y\rangle = \frac{2}{3}$, $\langle P_{yy}\rangle = 0$	1	$\langle\sigma_y\rangle = P^y_y$
$\langle P_z\rangle = \langle P_{zz}\rangle = 1$	$1+\frac{1}{2}P^o_{zz}$	$\langle\sigma_z\rangle = \frac{3}{2}P^z_z/(1+\frac{1}{2}P^o_{zz})$
$\langle P_z\rangle = \frac{2}{3}$, $\langle P_{zz}\rangle = 0$	1	$\langle\sigma_z\rangle = P^z_z$

The $T(\vec{d},\vec{n})^4He$ reaction has been shown to produce highly polarized neutrons[2] at 0°. For this case, where the spin structure is relatively simple ($1+\frac{1}{2} \rightarrow \frac{1}{2}+0$),

*Work performed under the auspices of the U. A. Atomic Energy Commission.

we can deduce several general properties of the transfer coefficients. First, P_y^y and P_{yy}^o are connected by an inequality[3],

$$(\tfrac{3}{2}P_y^y)^2 \leq (1-P_{yy}^o)(1+2P_{yy}^o) \quad . \tag{3}$$

This shows, for example, that P_{yy}^o is always between -1/2 and +1. Note that the allowed range of P_{yy}^o is such that the polarized cross sections may vary between the extremes $3I_o/4$ and $3I_o/2$, and that if $P_y^y(0°)$ is nonzero, an even smaller range is allowed. For the longitudinal polarization case, P_z^z and P_{zz}^o obey the relation[3] $3P_z^z(0°)/2 = 1+P_{zz}^o(0°)/2$, so that $\langle\sigma_z\rangle \equiv 1$ for any energy. In this case, however, the polarized cross section may vary between 0 and $3I_o/2$. In the range 0-15 MeV[2,4], $P_{zz}^o(0°) < 0$ so the longitudinal polarized cross section is less than I_o and the transverse polarized cross section is greater than I_o.

In the general (d,n) case, one would expect a stripping mechanism to dominate at higher energies. Ideal stripping requires $P_y^y(0°) = P_z^z(0°) = 2/3$ and $P_{yy}^o = P_{zz}^o = 0$. These limits appear to be closely approached in the $D(\vec{d},\vec{n})^3He$ case[5]. Effects of the deuteron D state are not taken into account in the above limits; we are currently considering this problem.

The cross section for both the $D(d,\vec{n})$ and $T(d,\vec{n})$ reactions at angles where appreciable polarization is obtained with unpolarized projectiles is ∿5 mb/sr. In contrast, the zero-degree cross section is ∿100 mb/sr and ∿20 mb/sr, respectively. In addition, the ability to reverse the neutron spin by controls at the ion source obviates the need for a spin precession solenoid, so that a tighter geometry is permitted for many experiments. Thus, in the transverse neutron polarization case, the present technique will yield a given neutron flux with a polarized deuteron current between 1 and 2 orders of magnitude lower than required in the unpolarized deuteron case. The lower deuteron energy required to deliver neutrons of a given energy would tend to reduce the background, as would the reduced incident flux of deuterons. Thus, the signal-to-noise ratio should also be substantially improved, except where the background comes primarily from break-up in the reaction itself. In addition, the zero-degree geometry often permits, from the background point of view, a more favorable location for the detectors. Thus, it would appear that the polarization transfer technique is a highly competitive method for obtaining polarized neutrons with presently available polarized deuteron beam intensities.

References

1. J.L. Gammel, P.W. Keaton, and G.G. Ohlsen, "Formalism for $A(\vec{d},\vec{n})B$ and $A(\vec{d},\vec{p})B$ Polarization Transfer Reactions," Proc. 3rd Internatl. Symp. Polarization Phenomena in Nuclear Reactions (to be published)
2. W.B. Broste, G.P. Lawrence, J.L. McKibben, G.G. Ohlsen, and J.E. Simmons, (to be published)
3. G.G. Ohlsen, J.L. Gammel, and P.W. Keaton, "Quadratic Relations Between the $T(\vec{d},\vec{n})^4He$ Observables," same as ref. 1
4. G.G. Ohlsen, Phys. Rev. 164 (1967) 1268
5. J.E. Simmons, W.B.Broste, G.P. Lawrence, and G.G. Ohlsen, "Preliminary Measurements of Neutron Polarization from the $D(\vec{d},\vec{n})^3He$ Reaction at 0° Using a Polarized Incident Beam" same as ref. 1

A Precise Method for the Determination of Secondary Standards for Deuteron Analyzing Tensors*

P. W. Keaton, Jr., D. D. Armstrong, G. P. Lawrence,
J. L. McKibben, and Gerald G. Ohlsen

Los Alamos Scientific Laboratory, University of California
Los Alamos, New Mexico 87544

Two-body nuclear reactions in which one of the initial particles has spin-1 and the remaining three particles have spin zero have uniquely determined analyzing tensors[1]. These are

$$P^o_y(\theta) = 0\ ,\ P^o_{xz}(\theta) = 0,\ P^o_{xx}(\theta) = 1,\ P^o_{yy}(\theta) = -2\ ,\ P^o_{zz}(\theta) = 1\ , \qquad (1)$$

where we use the right-handed coordinate system with y along $\vec{k}_{in} \times \vec{k}_{out}$ and z along $\vec{k}_{in}$. The general cross section expression is

$$I(\theta,\phi) = I_o(\theta)[1+\tfrac{3}{2}\langle P_y\rangle P^o_y+\tfrac{2}{3}\langle P_{xz}\rangle P^o_{xz}+\tfrac{1}{3}\langle P_{xx}\rangle P^o_{xx}+\tfrac{1}{3}\langle P_{yy}\rangle P^o_{yy}+\tfrac{1}{3}\langle P_{zz}\rangle P^o_{zz}]\ , \qquad (2)$$

where $I_o(\theta)$ is the cross section for an unpolarized beam. Substituting Eq. (1) in Eq. (2), and using the identity $\langle P_{xx}\rangle + \langle P_{yy}\rangle + \langle P_{zz}\rangle = 0$, we obtain

$$I(\theta,\phi) = I_o(\theta)[1-\langle P_{yy}\rangle]\ .$$

$\langle P_{yy}\rangle$ may be expressed in terms of the tensor polarization of the beam, p_{ZZ}, with respect to its quantization axis and the angles β,ϕ which describe the orientation of the quantization axis with respect to the xyz coordinate system[2]:

$$\langle P_{yy}\rangle = \tfrac{1}{2}\, p_{ZZ}\, [3\sin^2\beta\cos^2\phi-1]\ .$$

Thus, if we define the cross section for "left," "right," "up," and "down" as $L = I(\theta,0°)$, $R = I(\theta,180°)$, $U = I(\theta,270°)$, and $D = I(\theta,90°)$, we have

$$L = R = I_o[1+\tfrac{1}{2}\, p_{ZZ}\ (1-3\sin^2\beta)] \qquad U = D = I_o[1+\tfrac{1}{2}\, p_{ZZ}]\ .$$

The reaction $^{16}O(d,\alpha_1)^{14}N$ (2.31-MeV state) posseses the required spins and has been shown to have a cross section large enough to make its use feasible at deuteron energy 7.1 MeV and laboratory angle 35°.[3] Our purpose here was to find an angle and energy for which the (d,α) reaction has acceptably high yield, which coincides with an angle and energy at which the reaction to be calibrated has a sufficiently large analyzing power to be useful. If the target material for the reaction to be calibrated is gaseous, it may be mixed with the oxygen so that both reactions may be observed simultaneously. The analyzing power being determined may then be deduced from a ratio in which uncertainties or instabilities in the beam polarization and possible misalignments in the detection apparatus have no effect.

We have used this method to determine the analyzing tensors for $^4He(\vec{d},d)^4He$ elastic scattering at 9.80 MeV and at a laboratory scattering angle of 60°. Our results are as follows:

$$\sqrt{3}\ T_{22}(60°) = \tfrac{1}{2}[P^o_{xx}(60°) - P^o_{yy}(60°)] = +0.553 \pm 0.008$$

$$\sqrt{2}\ T_{20}(60°) = [P^o_{zz}(60°)] = +0.330 \pm 0.005\ .$$

---

*Work performed under the auspices of the U. S. Atomic Energy Commission.

$\beta = 54.7°$ and left, right, up, and down detectors were used for the $(P^o_{xx}-P^o_{yy})/2$ measurements. With this choice of β, we may write, for any analyzing reaction,

$$\frac{(L+R)-(U+D)}{L+R+U+D} = -\frac{1}{6} p_{ZZ} (P^o_{xx}-P^o_{yy}) .$$

Since $P^o_{xx}-P^o_{yy} = +3.0$ for $^{16}O(d,\alpha_1)^{14}N^*$, $P^o_{xx}-P^o_{yy}$ for d-^{4}He scattering can be obtained by a ratio of simultaneously observed asymmetries. For other choices of β the analysis is somewhat more complicated. The quantity P^o_{zz} was obtained by measuring $m_I = 1$ to $m_I = 0$ ratios[2] with $\beta = 0°$.

The principal uncertainty in the present calibration arises from the background contribution to the $^{16}O(d,\alpha_1)^{14}N^*$ yield. The beam polarization calculated from either the $\beta = 54.7°$ data or from the $\beta = 0°$ data is increased by about 1.5% when a reasonable estimate of the background is subtracted from the yields. The quoted errors assume a 70% uncertainty in the background subtraction which is combined quadratically with the statistical error.

A scan of the d-^{4}He analyzing powers versus energy (±200 keV) and angle (±3°) was made in order to establish the accuracy required in reproducing these parameters. We find that neither $(P^o_{xx}-P^o_{yy})/2$ nor P^o_{zz} varies by more than 1.5% if the angle remains within ±1° of the nominal value and if the energy remains within ±100 keV of the nominal value.

References

1. B. A. Jacobsohn and R. M. Ryndin, Nucl. Phys. 24 (1961) 505. For a simple derivation based on first principles, see the extended version of the present paper in LA-4465-MS.

2. G. P. Lawrence, Gerald G. Ohlsen, J. L. McKibben, P. W. Keaton, Jr., and D. D. Armstrong, "A Rapid Method for the Measurement of Analyzing Tensors in Reactions Induced by Polarized Deuterons," Proc. of 3rd Internatl. Symp. on Polarization Phenomena in Nuclear Reactions (to be published)

3. R. M. Prior, K. W. Corrigan, and S. E. Darden, Bull. Am. Phys. Soc. 15 (1970) 35

APPENDIX: Derivation of the Cross Section

The work presented here utilizes the unique properties of a reaction in which all interacting particles have zero spin except for one spin-one particle in the entrance channel. Such a reaction can be written symbolically as 1+0 → 0+0. It will be shown that this reaction has a tensor analyzing power for deuterons which is independent of bombarding energy and scattering angle. The polarization of a particle produced in a reaction of the form 0+0 → 1+0 may be obtained from a trivial modification of the calculation presented below, or from time reversal arguments.

A. Scattering Matrix and Coordinate System. The present formalism is similar to that of Csonka et al.* We begin by noting that the scattering matrix can be expanded in terms of the eigenfunctions of a spin-1 particle:

$$M = a_1\chi_1^\dagger + a_o\chi_o^\dagger + a_{-1}\chi_{-1}^\dagger \ , \tag{A1}$$

where a_1, a_o and a_{-1} are scalars. The spin-one eigenfunctions can be written as follows:

$$\chi_1 = \begin{pmatrix}1\\0\\0\end{pmatrix} \ , \qquad \chi_o = \begin{pmatrix}0\\1\\0\end{pmatrix} \ , \qquad \chi_{-1} = \begin{pmatrix}0\\0\\1\end{pmatrix} \ . \tag{A2}$$

For a spatial representation, we use the following unit vectors:

$$\hat{n} \text{ along } \vec{k}_{in} \times \vec{k}_{out} \ , \quad \hat{k} \text{ along } \vec{k}_{in} \ , \quad \hat{p} \text{ along } \hat{n} \times \hat{k} \ . \tag{A3}$$

Since the right-hand side of Eq. (A1) may be regarded as the dot product of two spherical vectors, it is clear that we can also write M as follows:

$$M = b_x\chi_x^\dagger + b_y\chi_y^\dagger + b_z\chi_z^\dagger \ , \tag{A4}$$

where $\vec{\chi} = \chi_x\vec{p} + \chi_y\vec{n} + \chi_z\vec{k}$ is a pseudovector and where b_x, b_y, and b_z have even parity In this representation the components of $\vec{\chi}$ may be written

$$\chi_x = \frac{1}{\sqrt{2}}\begin{pmatrix}-1\\0\\1\end{pmatrix} \ , \qquad \chi_y = \frac{i}{\sqrt{2}}\begin{pmatrix}1\\0\\1\end{pmatrix} \ , \qquad \chi_z = \begin{pmatrix}0\\1\\0\end{pmatrix} \ . \tag{A5}$$

Conservation of parity requires the scattering matrix to obey the relation

$$M(\vec{k}_{in},\vec{k}_{out},\vec{\chi}) = M(-\vec{k}_{in},-\vec{k}_{out},\vec{\chi}) \ , \tag{A6}$$

which can only be satisfied if $b_x = b_z = 0$. Therefore, the most general M matrix

*P. L. Csonka, M. J. Moravcsik, M. D. Scadron, Ann. of Phys. 41 (1967) 1

which describes a reaction of the form 1+0 → 0+0 and which conserves parity may be written

$$M = b_y \chi_y \quad . \tag{A7}$$

It can be shown that b_y is an odd function of the scattering angle θ.

B. Density Matrix and Cross Section. The initial density matrix, ρ^i, may be expanded in terms of the properly normalized Cartesian tensors*

$$I, \sqrt{\frac{3}{2}} P_j \ , \ \sqrt{\frac{2}{3}} P_{jk} \ , \ \sqrt{\frac{1}{3}} P_{jj} \ , \tag{A8}$$

where I is the (3x3) unit matrix, the P_j's are the three spin-one matrices S_x, S_y, and S_z, and P_{jk} can be written

$$P_{jk} = \frac{3}{2} (S_j S_k + S_k S_j) - 2\delta_{jk} \ , \tag{A9}$$

where j,k take on values x, y, and z. The matrices are explicitly given in Table A1. Thus, the initial density matrix expansion is

$$\rho^i = \frac{1}{3} \left\{ I + \sum \left[\frac{3}{2} \langle P_j \rangle^i P_j + \frac{2}{3} \langle P_{jk} \rangle^i P_{jk} + \frac{1}{3} \langle P_{jj} \rangle^i P_{jj} \right] \right\} \ , \tag{A10}$$

where the bracketed quantities indicate expectation values for the incident deuteron beam.

The cross section for an arbitrarily polarized incident beam is

$$I(\theta,\phi) = \mathrm{Tr}[M \rho^i M^\dagger] \ . \tag{A11}$$

The cross section, I_o, for an unpolarized incident beam (i.e., for $\rho^i = (1/3) I$) can be calculated directly:

$$I_o = \frac{1}{3} \mathrm{Tr}[MM^\dagger] = \frac{1}{3} \cdot \frac{(b_y)^2}{2} \cdot \mathrm{Tr}\ (1,0,1) \begin{pmatrix} 1 \\ 0 \\ 1 \end{pmatrix} = \frac{|b_y|^2}{3} \quad . \tag{A12}$$

Thus, b_y is determined to within an arbitrary phase factor. We may require b_y to be real. Therefore, the M matrix may be written as follows:

$$M = (3I_o)^{1/2} \chi_y \ . \tag{A13}$$

Since b_y is an odd function of θ, I_o vanishes as $\sin^2\theta$ near $\theta = 0$.

---

*J. L. Gammel, P. W. Keaton, Jr., and Gerald G. Ohlsen (to be published)

C. Analyzing Power. The cross section for an incident polarized beam may now be calculated by substituting Eq. (A10) into Eq.(A11). Using the matrix form of the Cartesian tensors (see Table A1) one may calculate all of the components of $Tr(m\rho^i M^\dagger)$ and show that

$$I_o \equiv \frac{1}{3} Tr[MM^\dagger]$$

$$\frac{1}{3} I_o P^o_j \equiv \frac{1}{2} Tr[MP_j M^\dagger] = 0$$

$$\frac{1}{3} I_o P^o_{jk} \equiv \frac{2}{9} Tr[MP_{jk} M^\dagger] = 0 \ , \quad j \neq k$$

$$\frac{1}{3} I_o P^o_{xx} \equiv \frac{1}{9} Tr[MP_{xx} M^\dagger] = \frac{1}{3} I_o$$

$$\frac{1}{3} I_o P^o_{yy} \equiv \frac{1}{9} Tr[MP_{yy} M^\dagger] = -\frac{2}{3} I_o$$

$$\frac{1}{3} I_o P^o_{zz} \equiv \frac{1}{9} Tr[MP_{zz} M^\dagger] = \frac{1}{3} I_o \ . \qquad (A14)$$

Substituting Eqs. (A14) and (A10) into Eq. (A11), we find

$$I(\theta,\phi) = I_o[1+\frac{1}{3}\langle P_{xx}\rangle^i - \frac{2}{3}\langle P_{yy}\rangle^i + \frac{1}{3}\langle P_{zz}\rangle^i] \ . \qquad (A15)$$

An incident deuteron beam with tensor polarization p_{ZZ} and symmetry axis making an angle β with $\vec{k}_{in}$ and with an angle ϕ between $\vec{n}$ and $\vec{k}_{in} \times \vec{S} \times \vec{k}_{in}$ has the following beam quantities in the reaction coordinate system,

$$\langle P_{xx}\rangle^i = \frac{1}{2}[3\sin^2\beta\sin^2\phi - 1]\ p_{ZZ}$$

$$\langle P_{yy}\rangle^i = \frac{1}{2}[3\sin^2\beta\cos^2\phi - 1]\ p_{ZZ}$$

$$\langle P_{zz}\rangle^i = \frac{1}{2}[3\cos^2\beta - 1]\ p_{ZZ} \ . \qquad (A16)$$

Substituting Eq. (A16) into Eq. (A15), we obtain the analyzing cross section for any reaction of the form 1+0 → 0+0

$$I(\theta,\phi) = I_o[1+\frac{1}{2}\ p_{ZZ}\ (1-3\sin^2\beta\cos^2\phi)] \ . \qquad (A17)$$

Note that there is no cross section dependence on the beam vector polarization p_Z, and that the entire θ dependence is contained in the factor $I_o(\theta)$.

Table A1: I, P_j and $P_{jk} = \frac{3}{2}(S_jS_k+S_kS_j)-2\delta_{jk}$

$$I = \begin{pmatrix} 1 & 0 & 0 \\ 0 & 1 & 0 \\ 0 & 0 & 1 \end{pmatrix}$$

$$P_x = \frac{1}{\sqrt{2}} \begin{pmatrix} 0 & 1 & 0 \\ 1 & 0 & 1 \\ 0 & 1 & 0 \end{pmatrix}$$

$$P_y = \frac{1}{\sqrt{2}} \begin{pmatrix} 0 & -i & 0 \\ i & 0 & -i \\ 0 & i & 0 \end{pmatrix}$$

$$P_z = \begin{pmatrix} 1 & 0 & 0 \\ 0 & 0 & 0 \\ 0 & 0 & -1 \end{pmatrix}$$

$$P_{xy} = \frac{3}{2} \begin{pmatrix} 0 & 0 & -i \\ 0 & 0 & 0 \\ i & 0 & 0 \end{pmatrix}$$

$$P_{yz} = \frac{3}{\sqrt{8}} \begin{pmatrix} 0 & -i & 0 \\ i & 0 & i \\ 0 & -i & 0 \end{pmatrix}$$

$$P_{xz} = \frac{3}{\sqrt{8}} \begin{pmatrix} 0 & 1 & 0 \\ 1 & 0 & -1 \\ 0 & -1 & 0 \end{pmatrix}$$

$$P_{xx} = \frac{1}{2} \begin{pmatrix} -1 & 0 & 3 \\ 0 & 2 & 0 \\ 3 & 0 & -1 \end{pmatrix}$$

$$P_{yy} = \frac{1}{2} \begin{pmatrix} -1 & 0 & -3 \\ 0 & 2 & 0 \\ -3 & 0 & -1 \end{pmatrix}$$

$$P_{zz} = \begin{pmatrix} 1 & 0 & 0 \\ 0 & -2 & 0 \\ 0 & 0 & 1 \end{pmatrix}$$

THE SCATTERING OF POLARIZED PROTONS BY TRITONS AT 13.6 MeV*

J. L. Detch, Jr., J. H. Jett, and Nelson Jarmie

Los Alamos Scientific Laboratory, University of California
Los Alamos, New Mexico 87544

The asymmetries in the $T(\vec{p},\hat{p})T$ reaction were measured at 13.600 ± 0.015 MeV. The polarized protons were supplied by the LASL Lamb shift polarized ion source and accelerated by a tandem Van de Graaff. Previous measurements of proton asymmetries in this energy region were made by Rosen and Leland[1] at 14.5 MeV.

The experiment was performed with a single detector telescope using the same apparatus previously used for high accuracy (0.4% relative accuracy) cross section measurements. Basically, the equipment consisted of a thin-window (2.3 micrometers Havar) gas scattering cell which was pressurized to 0.25 atmosphere with tritium. The detector system has a 1° angular acceptance (or a G-factor of 1.06×10^{-4}). The included angle between left and right detector settings was known to ± 0.03° and the beam was constrained by slits so that it could not wander more than ±0.06° between left and right measurements. The beam was integrated in a standard way to an absolute accuracy of ±0.2%. A more detailed description of the apparatus used and error discussion is contained in ref. 2.

The data were taken at two different times. The majority of the data were taken during the first run and without an independent measurement of the beam polarization other than by the quench ratio method. The second data set consisted of 3 data points on the back angle peak and followed an extensive check of the beam polarization using p-α scattering as an analyzer. For this last run, the beam polarization was known to ±1.0% and the two sets of data were consistent.

The resulting data are shown in fig. 1 along with the data of Leland and Rosen[1]. For all but two of the data points, four measurements were made, being two measurements on each side of the chamber with the proton spin up and down. This method eliminates certain geometrical systematic errors.

The results are listed in table 1 along with the total error which includes the error in the knowledge of the beam polarization. The statistical uncertaintity was the predominant contribution to the errors except for the largest asymmetries.

---

*Work performed under the auspices of the U.S. Atomic Energy Commission.

[1] L. Rosen and W. T. Leland, Phys. Rev. Letters 8, 379 (1967).

[2] Nelson Jarmie, Ronald E. Brown, R. L. Hutson, and J. L. Detch, Jr., Phys. Rev. Letters 24, 240 (1970); J. H. Jett, J. L. Detch, Jr., R. L. Hutson, and Nelson Jarmie, to be published.

Table 1

Asymmetries in $T(\vec{p},\hat{p})T$ scattering at 13.6 MeV

θ_{Lab}	θ_{CM}	A	δA	θ_{Lab}	θ_{CM}	A	δA
15.0	20.0	-0.012	0.004	90.0	109.7	0.122	0.025
20.0	26.6	-0.031	0.005	97.5	116.9	0.626	0.020
30.0	39.7	-0.051	0.006	105.0	123.9	0.690	0.030
40.0	52.5	-0.097	0.008	105.0	123.9	0.712	0.018
50.0	65.0	-0.156	0.012	120.0	136.9	0.405	0.012
60.0	77.0	-0.224	0.012	140.0	152.5	0.205	0.021
70.0	88.5	-0.296	0.015	150.0	159.7	0.111	0.013
80.0	99.4	-0.263	0.020	160.0	166.1	0.075	0.011

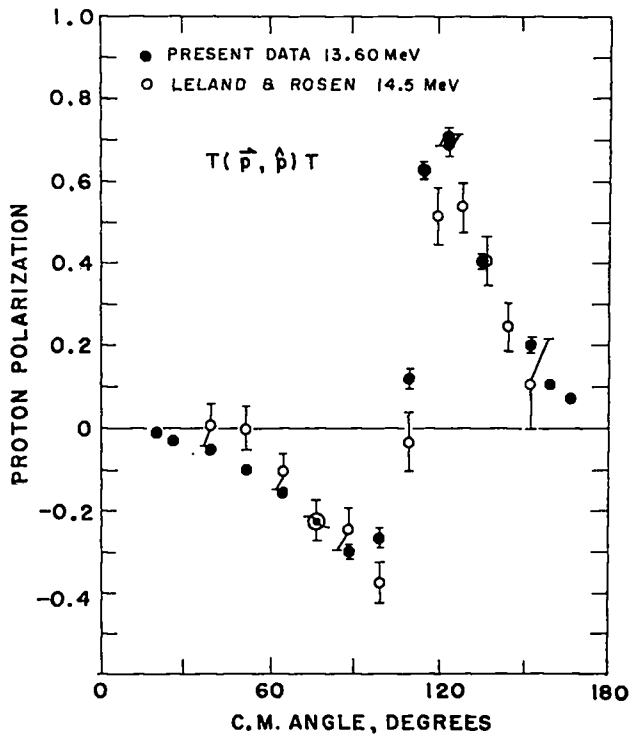

Figure 1. Asymmetries in $T(\vec{p},\vec{p})T$ scattering. The data of Leland and Rosen are from ref. 1.

POLARIZATION ANGULAR DISTRIBUTION FROM THE $T(d,\vec{n})^4He$ REACTION AT 7.0 AND 11.4 MeV*

W. B. Broste† and J. E. Simmons

Los Alamos Scientific Laboratory, University of California,
Los Alamos, New Mexico 87544

Angular distributions of the polarization of neutrons from the $T(d,n)^4He$ reaction have been measured for incident deuteron energies of 7.0 and 11.4 MeV. By accelerating tritons onto a deuterium target, it was possible to obtain data for $T(d,n)^4He$ neutron emission angles which could not be reached when deuterons were accelerated onto tritium.

Neutron polarizations were analyzed by scattering from liquid helium at laboratory angles between 115° and 125°. The measured asymmetries were corrected for the effects of multiple scattering in the helium and finite polarimeter geometry. Polarizations were derived using n-helium analyzing powers calculated from the phase shifts of Hoop and Barschall.[1] Analyzing angles for neutron energies above 20 MeV were chosen where the calculated analyzing powers showed the least discrepancy with recent n-helium polarization measurements.

Figures 1 and 2 show the present data: Solid circles represent polarizations obtained from the $T(d,n)^4He$ reaction, while the triangles are data obtained using the $D(t,n)^4He$ reactions at center-of-mass conditions equivalent to the $T(d,n)^4He$ at the lab angles for which the data are plotted. The open circles on the figures are the measurements of Brown and Haeberli[2] on the charge conjugate $^3He(d,\vec{p})^4He$ reaction at 8.0 and 12.0 MeV.[3] The two sets agree well, except for the magnitude of the polarization at $\theta = 30°_{lab}$, and small differences in shape between the 11.4 MeV $T(d,\vec{n})^4He$ and 12.0 MeV $^3He(d,\vec{p})^4He$ data beyond 90° lab. It should be noted that interpolation of the Brown and Haeberli data to 7.0 MeV yields a value for the 30° proton polarization which is consistent with the present value of neutron polarization within experimental errors. However, recent data[3] from this Laboratory on the $T(d,n)^4He$ polarization at 30° indicate that there are significant differences between the proton and neutron polarization from the two reactions for deuteron energies between 8 and 12 MeV.

Theoretical interpretations of the present results and other data on the $T(d,n)^4He$ reaction are being pursued within the framework of a phenomenological reaction matrix analysis. The effect of spin-orbit distortions in entrance and exit channels is also being studied.

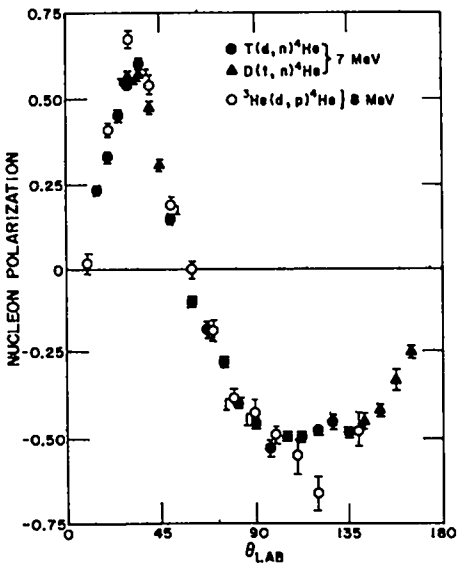

Figure 1

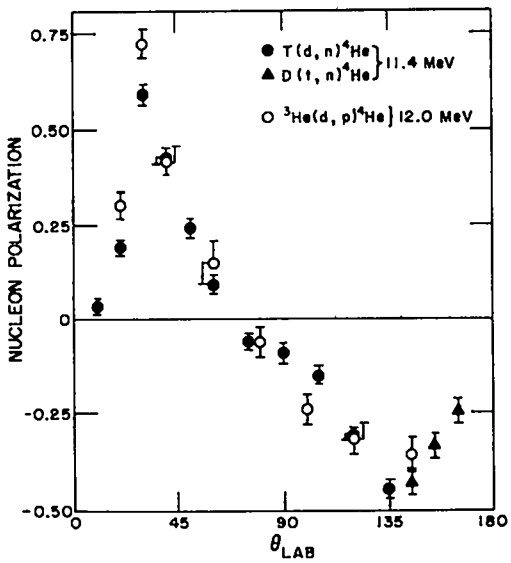

Figure 2

*Work supported by the U.S. Atomic Energy Commission.

†Associated Western Universities Fellow from University of Wyoming.

1) B. Hoop and H.H. Barschall, Nucl. Phys. 83 (1966) 65.

2) R.I. Brown and W. Haeberli, Phys. Rev. 130 (1963) 1163.

3) J.E. Simmons, G.S. Mutchler, W.B. Broste, to be published.

NEUTRON-HELIUM POLARIZATION AT 27.3 AND 30.3 MeV*

W. B. Broste† and J. E. Simmons

Los Alamos Scientific Laboratory, University of California
Los Alamos, New Mexico 87544

As part of an effort to obtain more accurate values for the polarization analyzing power of n-alpha scattering for neutron energies above 20 MeV, the n-alpha polarization angular distribution has been measured at this Laboratory for six neutron energies between 11.0 and 30.3 MeV. Data obtained at 11.0, 17.7, 23.7, and 25.7 MeV have been reported on at an earlier meeting.[1)]

The asymmetry in scattering polarized neutrons from helium was measured for neutron energies of 27.3 and 30.3 MeV for angles between 50° and 130° (lab.). Partially polarized neutrons were obtained from the $D(t,n)^4He$ reaction at an angle near $30°_{lab}$. Incident energies of E_t = 12.0 and 14.9 MeV provided neutron energies of E_n = 27.3 and 30.3 MeV, respectively. The value of the source polarization P_1 was determined for the 27.3-MeV data in a measurement on the $T(d,n)^4He$ reaction at the same center-of-mass conditions as were used in the $D(t,n)^4He$ source reaction. The resultant neutron energy is 13.2 MeV; therefore, P_1 may be determined fairly reliably from the measurement of the asymmetry in n-He scattering at 115° (lab). From this measurement, it was found that P_1 = .53 ± .015. P_1 for 30.3 MeV data was interpolated from $T(d,n)^4He$ data,[2)] and had a value P_1=.46 ± .05. The asymmetries were corrected for multiple scattering of neutrons in the helium, and the effects of finite geometry, then divided by P_1 to determine the n-He polarization function $P(\theta)$.

Figures 1 and 2 show the final polarization results for the two energies. Solid curves are the predictions of the Hoop-Barschall phase shift set[3)] at 27.3 and their smooth extrapolation to 30.3 MeV. Figure 1 also shows the data of Arifkhanov et al.[4)] at a neutron energy of 27.8 ± 0.9 MeV, where their asymmetry data have been converted to polarizations using a value for P_1 obtained in measurements of the $T(d,n)^4He$ 30° polarization at this Laboratory. Preliminary phase shift analyses have indicated that small changes in the Hoop-Barschall phases result in good fits to both cross section and polarization data at the two energies.

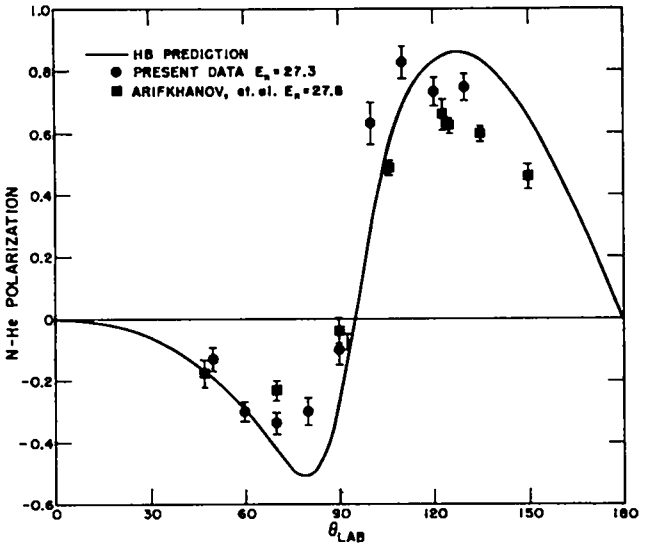

Figure 1

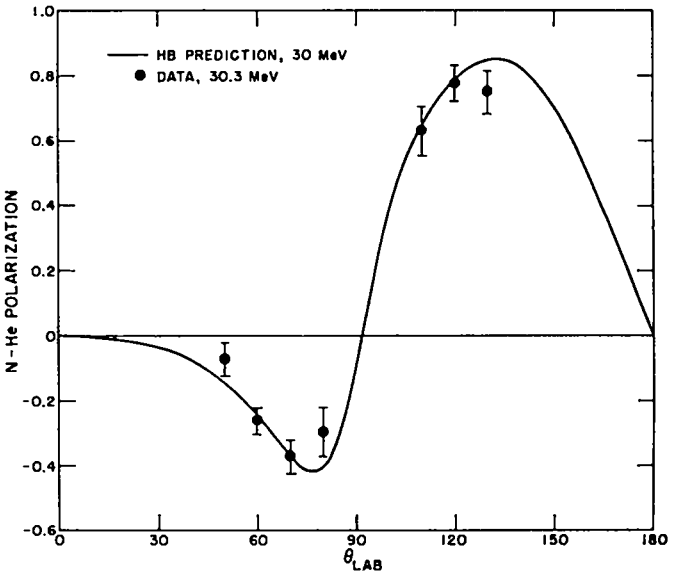

Figure 2

*Work performed under the auspices of the U.S. Atomic Energy Commission.

†Associated Western Universities Fellow from University of Wyoming.

1) W.B. Broste, J.E. Simmons, and G.S. Mutchler, Bull. Am. Phys. Soc. 14 (1969) 1230.

2) W.B. Broste and J.E. Simmons, "Polarization Angular Distribution from the T(d,n)^{4}He Reaction at 7.0 and 11.4 MeV," Proc. 3rd International Symposium on Polarization Phenomena in Nuclear Reactions (to be published).

3) B. Hoop and H.H. Barschall, Nucl. Phys. 83 (1966) 65.

4) U.R. Arifkhanov, N.A. Vlasov, V.V. Davydov, and L.N. Samoilov, Sov. J. Nucl. Phys. (Trans.) 2 (1966) 170.

Improvements in Performance of a Liquid Helium Scintillation Counter*

J. C. Martin, W. B. Broste† and J. E. Simmons

Los Alamos Scientific Laboratory, University of California
Los Alamos, New Mexico 87544

Since the liquid helium scintillation polarimeter of Simmons and Perkins[1], many improved LHe scintillators have been constructed[2,3,4,5,6,7,8]. For optimum energy resolution in a LHe scintillator one needs a uniform pulse-height response over the entire volume of the scintillator. This response depends on the uniformity of the wave shifter and the light collecting geometry. Recent publications have reported resolutions (FWHM) of between 11% and 30% for alpha-sources[2,3,5,7,8]; and between 9% and 13% for gated He-recoil distributions for elastic scattered neutrons[4,6]. Pulse-height uniformity measurements[3,7,8] with an alpha-source showed variations from >2% to ≈40%. Our recent work has shown that pulse-height uniformity can be significantly improved by using a thicker coating of wave shifter on the photomultiplier window of the scintillator cell relative to that on the wall.

In our present scintillation counter the vacuum ultraviolet helium scintillations are wave shifted by a vacuum evaporated deposit of p,p'-diphenylstilbene (DPS) on the reflector and window of the scintillation cell. The reflector is a ceramic shell of fired Al_2O_3. The window is 0.25 cm x 5.0 cm diam sapphire. The active volume of the cell is 150 cm^3 (4.7 moles LHe). The photomultiplier (RCA 7326), housed in the cryostat vacuum, views the scintillation cell through a hollow polished aluminum light cone, and is cooled to ≈120°K to minimize the radiant heat load on the LHe cell. Heretofore we employed DPS coatings of 100 $\mu g/cm^2$ on the reflector shell wall and 50 $\mu g/cm^2$ on the window. Under these circumstances our resolution was only about 25% FWHM for 15 MeV He recoils.

Recent measurements with a test cryostat and a movable α-source revealed a marked axial non-uniformity in the pulse-height response for the above DPS prescription. The light output variation along the cell seemed to indicate a light collection problem in the vicinity of the window. Consequently we increased the window DPS coating while holding the reflector coating constant. The result was an improvement in pulse-height uniformity with increasing DPS thickness on the window. For ≈200 $\mu g/cm^2$ on the window the light output variation was reduced to 7½% from an initial value of ≈40%.

In view of this information the polarimeter scintillation cell was recoated with ≈100 $\mu g/cm^2$ on the reflector and ≈200 $\mu g/cm^2$ on the window. Using 4 to 32 MeV neutrons from the $T(p,n)^3He$ and $T(d,n)^4He$ reactions at 0°, the response of the recoated cells was observed. A NE 102 (5.0 cm x 18.0 cm x 7.6 cm)-RCA 8575 detector for the recoil neutrons was used in coincidence with the LHe scintillation counter. The geometry of the experiment was: R_1 = 99.1 cm, θ_1 = 0°, $\Delta\theta_1$ = ±1.75°, R_2 = 42.2 cm, θ_2 = 137.7° and $\Delta\theta_2$ = ±3.45°. Both He-recoil singles and coincidence-gated He recoils were observed over the neutron energy range. Fig. 1 shows typical pulse distributions. The left panel shows the singles spectrum with the prominent n+He → d+t peak; the right panel shows the coincidence-gated He recoil spectrum. The gated He-recoil resolution (FWHM) ranged from 8%

* Work performed under the auspices of the U. S. Atomic Energy Commission.
† Associated Western University Fellow from University of Wyoming.

for E_{He} = 19 MeV to 22% for E_{He} = 3 MeV. The light output as a function of helium-recoil end-point energy exhibits the same nonlinear shape as reported by Piffaretti *et al*[4]. The resolution for the n-He (d+t) breakup peak varied from 10% for E_{d+t} = 14 MeV to 15% for E_{d+t} = 5 MeV.

By increasing the DPS thickness on the sapphire window to ≈200 μg/cm^2 we have improved the He-recoil resolution by a factor of three, without appreciably lowering the light output of the scintillator.

Fig. 1

Singles: d+t breakup peak
Res.(FWHM)=12%
E(d+t)=10.8 MeV

Coincidence Gated: gated He recoils
Res.(FWHM)=8%
Not corrected for kinematic spread.
E(He)=16.8 MeV

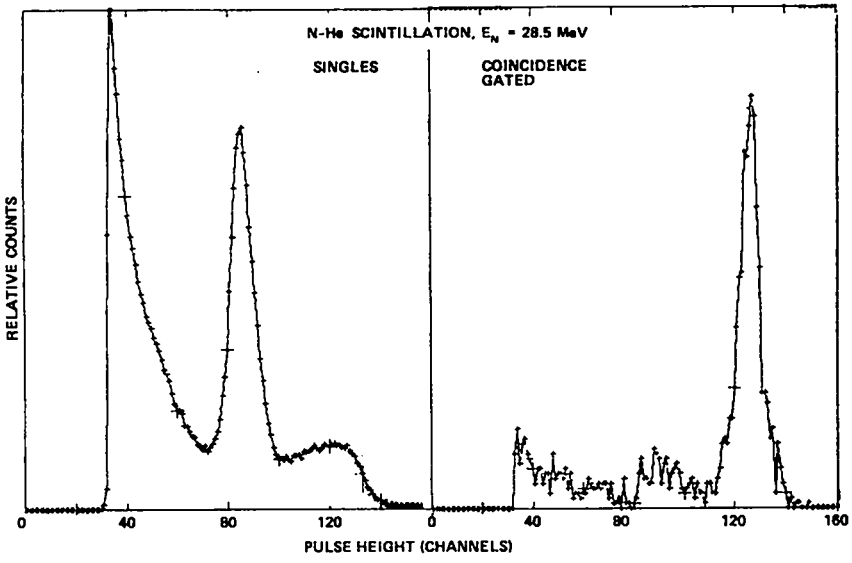

References

1) J. E. Simmons and R. B. Perkins, Rev. Sci. Inst. 32 (1961) 1173

2) T. G. Miller, Nucl. Inst. and Meth. 40 (1966) 93

3) J. R. Kane, R. T. Siegel and A. Suzuki, Rev. Sci. Inst. 34 (1963) 817

4) J. Piffaretti, J. Rossel and J. Weber, Proceedings of 2nd International Symposium on Polarization Phenomena of Nucleons, Karlsruhe 1965, Birkhäuser Verlag Basel, 1966

5) S. T. Lam *et al*, Nucl. Inst. and Meth. 62 (1968) 1

6) J. Birchall, M. J. Kenny, J. S. C. McKee and B. L. Reece, Nucl. Inst. and Meth. 65 (1968) 117

7) L. P. Robertson *et al*, Nucl. Inst. and Meth. A134 (1969) 545

8) D. C. Buckle *et al*, Nucl. Inst. and Meth. 77 (1970) 249

Asymmetries in Protons from the Reaction of Deuterons with a Polarized ^{3}He Target*

Bob E. Watt and W. T. Leland

Los Alamos Scientific Laboratory, University of California
Los Alamos, New Mexico 87544

We have investigated the asymmetry of the protons produced from $^3He(d,p)^4He$ reactions when using a polarized ^{3}He target. The general experimental setup and procedures were identical with those described in our paper on deuteron scattering[1], with the exception of the detector system. We used a pair of solid state detectors arranged as a telescope. By using appropriate absorbers, coincidence techniques and pulse height discrimination, we were able to reduce the background counting rates to a negligible amount.

Tables 1, 2, and 3 present our data along with that previously published by Baker et al.[2] (BRWP). To facilitate direct comparison, we have multiplied the data of BRWP by 1.2 to take into consideration the 20% difference in the target polarizations as calculated by the relation we used as compared to theirs. The listed errors are statistical only.

Table 1. Angular asymmetries for reaction protons at 6 MeV.

$\theta_{c.m.}$	Present $A_r(\theta)$	Ref. 2 $1.2\ A_{LR}(\theta)$
34.8°		-0.43±0.05
51.7		-0.70±0.07
59.4	-0.63 ±0.031	
63.3	-0.525±0.035	
68.3		-0.35±0.08
71.6	-0.44 ±0.04	
80.6	-0.38 ±0.04	
89.4		-0.08±0.06
90.6	-0.14 ±0.04	
102.0	+0.01 ±0.04	
104.5		+0.13±0.1
108.3	+0.16 ±0.03	
113.2	+0.32 ±0.04	
117.8	+0.24 ±0.03	
121.8	+0.33 ±0.04	
125.6	+0.37 ±0.03	
129.2	+0.35 ±0.04	
135.8	+0.43 ±0.06	
135.8	+0.34 ±0.04	

Table 2. Angular asymmetries for reaction protons at 8 MeV.

$\theta_{c.m.}$	Present $A_r(\theta)$	Ref. 2 $1.2\ A_{LR}(\theta)$
41°		-0.83±0.17
52.6		-0.85±0.19
60.3	-0.51±0.04	
69.4		-0.36±0.11
72.7	-0.33±0.04	
81.7	-0.17±0.04	
85.3		-0.1 ±0.11
91.9	+0.06±0.03	
101		+0.19±0.13
103.3	+0.29±0.04	
114.4	+0.50±0.04	
115.5		+0.42±0.17
122.9	+0.50±0.04	
130.2	+0.48±0.04	
136.7	+0.50±0.04	

Plattner and Keller[3] have pointed out the approximate agreement between their measurements of P_d and the data of BRWP. Figure 1 displays data of Plattner and Keller along with ours and that of BRWP multiplied by 1.2. We would agree that $P_d = A_{^3He}$ is a good approximation at higher energies and forward angles but do not agree that it holds at lower energies.

*Work performed under the auspices of the U. S. Atomic Energy Commission.

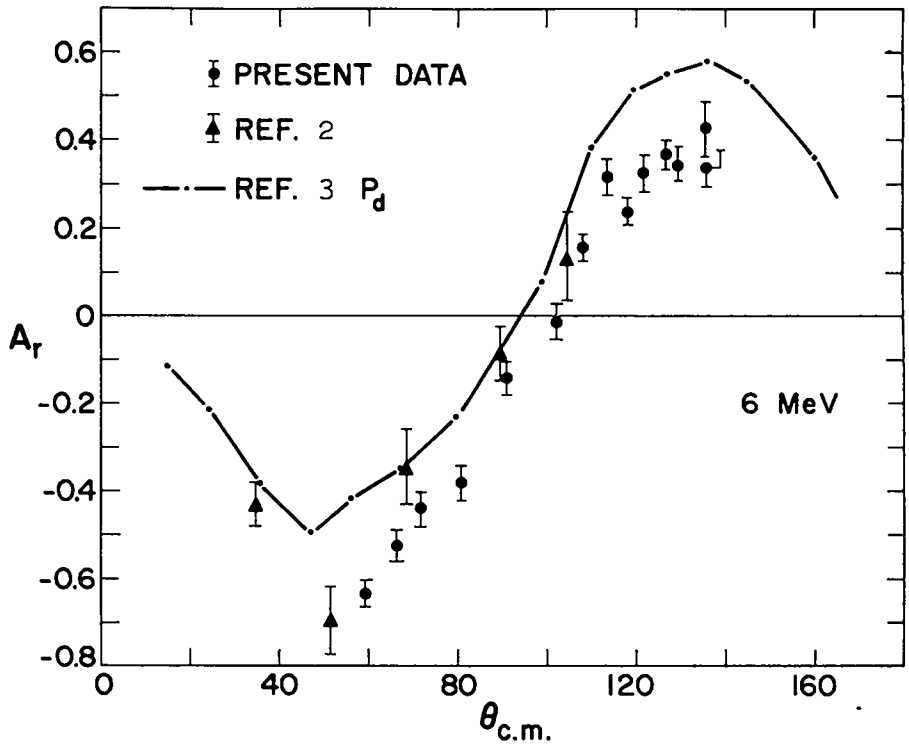

Fig. 1. Proton asymmetry from $^3He(d,p)^4He$ reaction with polarized ^3He.

Table 3. Angular asymmetries for reaction protons at 10 MeV.

$\theta_{c.m.}$	Present $A_r(\theta)$	Ref. 2 $1.2\ A_{LR}(\theta)$
35.8°		-0.76±0.08
53.3		-0.53±0.07
57.1	-0.39±0.1	
61.1	-0.39±0.1	
70.2		-0.17±0.06
86.3		-0.12±0.1
92.8	+0.07±0.08	
110.4	+0.03±0.1	
115.4	+0.35±0.04	
123.9	+0.32±0.04	
123.9	+0.41±0.05	
137.5	+0.24±0.2	
137.5	+0.45±0.04	

References

1. B. E. Watt and W. T. Leland, "Asymmetries in Deuteron Scattering from a Polarized ^3He Target," Proc. 3rd Internatl. Symp. Polarization Phenomena in Nuclear Reactions (to be published)

2. S. D. Baker, G. Roy, G. C. Phillips, and G. K. Walters, Phys. Rev. Letters 15 (1965) 115

3. G. R. Plattner and L. S. Keller, Phys. Letters 29B (1969) 301

A Proposed 0.4 K Polarized Proton Target Cryostat for LAMPF*

F. J. Edeskuty, C. F. Hwang, K. D. Williamson, Jr.

Los Alamos Scientific Laboratory, University of California
Los Alamos, New Mexico 87544

A polarized proton target cryostat design is described which is intended for 0.4 K operation in the LAMPF external beams for various scattering experiments. It has been shown by Hill et al.[1] that proton polarization of the order of 70% can be obtained in butyl-alcohol coped with porphyrexide at temperatures near 0.4 K. Previous experiments at CEA[2] and SLAC[3] indicated that an alcohol target is capable of tolerating 10^{10} minimum ionizing particles per second for periods of a few hours without losing a substantial part of its initial polarization. When annealed at 77 K at suitable time intervals, an alcohol target may last as long as 24-36 hours[4]. In consideration of the expected target life versus reaction yield, the optimized design beam intensity was chosen as 3×10^9 (300-800 MeV) protons per second (corresponding to $\sim 10^{10}$ minimum ionizing particles per second). Under these circumstances, even with the annealing process, it will be necessary to replace the target material periodically. The cryostat is designed to facilitate such target changes as required (daily). In order to avoid loss of ^{3}He while changing targets it is not desirable to have ^{3}He in direct contact with the target material. Therefore to transfer the heat from the target to the ^{3}He bath a ^{4}He heat-exchanger has been included in the design.

Hill et al.[1] estimated that 30 mW of refrigeration should suffice to cool a 10-gram target and the microwave cavity. This estimate is consistent with the experience of Masaike[5]. By anchoring the microwave at 1.0 K it is anticipated that the microwave loading to the ^{3}He system will be less than 5 mW. For protons of 300-800 MeV traversing a 2 gm/cm^2 alcohol target, the energy loss is between $0.8\text{-}1.2 \times 10^{-9}$ mW-sec per particle or 3-4 mW for design beam intensity. Combining these two loads a total refrigeration demand of about 10 mW at 0.4 K in the target material is anticipated.

A schematic diagram of the proposed target is shown in Fig. 1. The precooling of the ^{3}He gas as well as the 1 K and 77 K shields is provided by a modified Roubeau[6] cryostat, in which ^{4}He enters by a tube (13 on Fig. 1), is precooled by a heat exchanger (8 on Fig. 1), and evaporates at near 1 K (6 on Fig. 1). The pumped vapors provide the precooling in the heat exchanger (8 on Fig. 1). This Roubeau principle is repeated in the ^{3}He loop by means of inlet tube (14), condenser on (6) and evaporator (4) (all on Fig. 1) with an expected ^{3}He evaporator temperature of 0.3 K. Heat is transferred from the target to the ^{3}He evaporator by a closed superfluid ^{4}He heat exchanger. The ^{4}He is in direct contact with the polarized target material. The chief impedances in this heat exchanger are three Kapitza resistances and the relatively poor heat transport capability of the He II in this termprature range. A separate, preliminary experiment to study these impedances is in progress.

The features incorporated into the cryostat design to permit rapid sample changes are a completely removable target-refrigerator system and a quick disconnect joint between the target and the ^{4}He heat exchanger tube wall. The warm O-ring seal (12 on Fig. 1) permits removal of the entire inner structure of the cryostat and the ^{3}He handling system when one exterior flange (not shown in Fig. 1) is unbolted. After extraction of the double-Roubeau section from the vacuum

*Work performed under the auspices of the U. W. Atomic Energy Commission.

jacket the target cell can be replaced by removing the hemispherical cavity wall (5 on Fig. 1) and by opening the quick disconnect Indium O-ring joint (2 on Fig. 1).

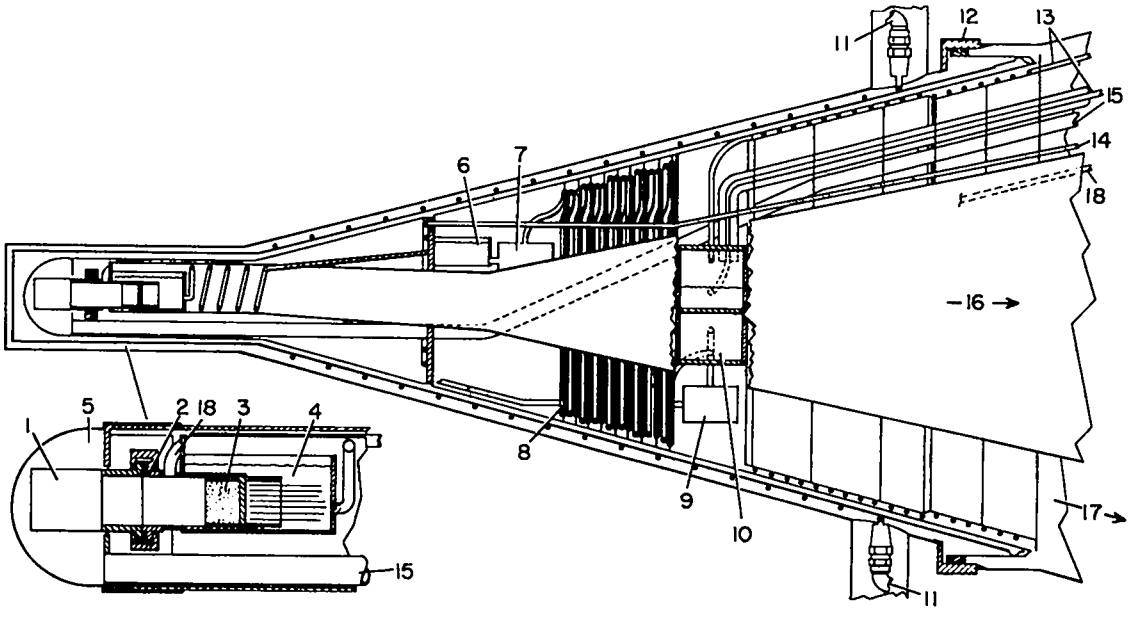

Fig. 1. Schematic Diagram of Cryostat: 1) target cell, 2) quick disconnect joint, 3) ^{4}He to ^{3}He heat exchanger, 4) ^{3}He evaporator, 5) microwave cavity, 6) ^{4}He evaporator, 7) ^{4}He expansion valve, 8) ^{4}He heat exchanger, 9) ^{4}He precooling valve, 10) ^{4}He separator, 11) N_2 supply inlet/outlet, 12) warm O-ring sliding joint, 13) ^{4}He fill and vent lines for separator, 14) ^{3}He fill line, 15) microwave guide, 16) ^{3}He pump-out, 17) ^{4}He pump-out, 18) ^{4}He fill line for low temperature heat exchanger.

The ^{3}He pumping system consists of three Edwards 9B4 diffusion booster pumps each with a pumping speed of 3800 ℓ/sec at an inlet pressure of $\sim 10^{-3}$ torr, backed by an Edwards 550 forepump. The ^{3}He stream can be continusouly purified by a cold trap between the forepump and cryostat inlet. With these pumps and the designed pumping line sizes, we anticipate the following temperature-power input relationships.

Power, mW	10	20	40	80
$T_{evaporator}$, K	0.30	0.32	0.34	0.37
T_{target}, K	0.40	0.42	0.44	0.47
M, $\frac{gm\text{-}moles}{hr}$	1.8	3.6	7.2	14.4

References

1. D. A. Hill, J. B. Ketterron, R. C. Miller, A. Moretti, R. C. Niemann, L. R. Windmiller, A. Yokosawa, C. F. Hwang, Phys. Rev. Letters 23 (1969) 460
2. J. R. Chen, J. Sanderson, J. A. Appel, C. J. Ladding, M. Goitein, K. Hanson, D. C. Imrie, T. Kirk, R. Madaras, R. V. Pound, L. Price, R. Wilson, and C. Zajde, Phys. Rev. Letters 21 (1968) 1279
3. T. Powell, M. Borghini, O. Chamberlain, R. Z. Fuzesy, C. C. Morehouse, S. Rock, G. Shapiro, H. Weisberg, R. L. A. Cottrell, J. Litt, L. W. Mo, and R. E. Taylor, Phys. Rev. Letters 24 (1970) 753
4. R. Z. Fuzesy, private communications
5. Akira Masaike, private communications
6. M. Borghini, P. Roubeau, and C. Ryter, Nucl. Inst. Meth. 49 (1967) 248

Analyzing Power of the $T(\vec{d},\alpha)n$ Reaction at Low Energies*

Gerald G. Ohlsen, J. L. McKibben, and G. P. Lawrence

Los Alamos Scientific Laboratory, University of California
Los Alamos, New Mexico 87544

For energies less than 100-200 keV, the $T(\vec{d},\alpha)n$ reaction is known to proceed almost totally through s-wave deuteron absorption. If one assumes s waves only, and further assumes that the polarization of the incident deuterons possesses an axis of symmetry, the cross sections may be written[1)]

$$I = I_o(1+\tfrac{1}{2}\langle P_{zz}\rangle P^o_{zz}) \ , \quad P^o_{zz} = -\tfrac{g}{2}(3\cos^2\theta_S - 1) \ , \qquad (1)$$

where $\langle P_{zz}\rangle$ is the tensor polarization of the deuterons and where θ_S is the center-of-mass direction of emission of the observed reaction product, both with respect to the quantization axis. g is the parameter which is to be measured; if the reaction proceeds completely through the $J = 3/2+$ intermediate state, $g = 1$. Note that the general analyzing tensor restriction $-2 < P^o_{zz} < 1$ requires that $-1 < g < 2$.

In the present paper, we report measurements of the $T(\vec{d},\alpha)n$ analyzing power at 51, 76, and 93 keV deuteron energies. Since a thick tritium-zirconium target was used, the quantities actually determined were energy averages of g of a certain form[1)]. The average values of g, which we shall call $\bar{g}$, are the quantities directly of interest for use of the reaction as a calibrated analyzer.

The experiment consisted of the determination of $\bar{g}p$, where p is the spin state purity of the beam, by a ratio method together with a determination of p by the quench ratio method. The beam quantization axis was parallel to the beam direction. Two detectors at 90° and two detectors at 165° were employed at azimuthal angles such that there was an unobstructed view of the solid tritium-zirconium target. The beam was collimated by 5 mm x 5 mm slits 30 cm upstream from the target.

Ratios between the yields for $m_I = 1$, $m_I = 0$, and $m_I = -1$ beams were used to determine $\bar{g}p$. (We refer to the states by the m_I value which characterizes the large magnetic field limit.) This requires an accurate knowledge of the relative tensor polarizations of the three states (see table 1). Since the field in the negative-ion formation region of the ion source was ∿60 G, i.e., strong with respect to the deuterium atom $2S_{1/2}$ hyperfine interaction, these ratios are well known and extremely insensitive to variation of the magnetic field. Experiments with the polarized beam accelerated to tandem energies have verified that the relative polarizations are as expected to an accuracy of ∿0.5% or better.

Table 1

State	Tensor Polarization
$m_I=1$	p
$m_I=0$	-1.966p
$m_I=-1$	0.952p

The quantity $\bar{g}p$ can be determined from the relative yields, Y, observed in a single detector with an $m_I = 1$ beam followed by an $m_I = 0$ beam, or by an $m_I = 0$ beam followed by an $m_I = -1$ beam:

$$\bar{g}p = \frac{4(Y_1 - Y_o)}{(-1.966Y_1 + Y_o)(3\cos^2\theta_S - 1)} \quad \text{or} \quad \bar{g}p = \frac{4(Y_o - Y_{-1})}{(0.952Y_o - 1.966Y_{-1})(3\cos^2\theta_S - 1)} \ . \qquad (2)$$

The value of $\bar{g}p$ obtained from each of the four detectors and from each of the types of ratios was consistent to within the ±0.007 to ±0.011 statistical error on each determination.

---

*Work performed under the auspices of the U. S. Atomic Energy Commission.

The factor p was measured by a quench ratio method. If we denote the yield and center-of-mass angle which corresponds to a 165° (90°) detector by Y_{165} and θ_{165} (Y_{90} and θ_{90}), it follows from eq. (1) that the sum Y, where

$$Y = Y_{90} - (\eta_{90}/\eta_{165})[(3\cos^2\theta_{90} - 1)/(3\cos^2\theta_{165} - 1)]Y_{165} \qquad (3)$$

is proportional to the number of deuterons incident on the target during the counting interval, irrespective of their polarization. The factor η_{165}/η_{90} is a relative detector efficiency factor (including kinematic factors); this was determined from the ratio

$$(\eta_{165}/\eta_{90}) = (Y_{165}/Y_{90})[(1 - \tfrac{1}{4}\bar{g}pK_\alpha(3\cos^2\theta_{90} - 1)]/[(1 - \tfrac{1}{4}\bar{g}pK_\alpha(3\cos^2\theta_{165} - 1))] \ , \qquad (4)$$

where K_α = 1, -1.966, or 0.952 for m_I = 1, 0, or -1 beams, respectively, and where the value of $\bar{g}p$ calculated from eq. (2) was used.

The data cycle consisted of five or more sets of six counting periods with the ion source conditions varied in the following sequence: m_I = 1 selection, quench, m_I = 0 selection, quench, m_I = -1 selection, and quench. Timed intervals were used (10 sec, 20 sec, or 40 sec) for each counting period. The source current varied by only a few percent during the acquisition of the data at a given energy, so the summing over 5 or more data sets is believed to assure that the amount of charge delivered in the various cases does not vary by more than a few tenths of a percent. The beam spin state purity was determined from ratios of the quantity Y with one of the spin states being selected by the spin filter and with the beam quenched, according to the formula

$$p = [Y(\text{filtered}) - Y(\text{quenched})]/Y(\text{filtered}) \ . \qquad (5)$$

Note that the data sequence employed measures the quench ratio and $\bar{g}p$ essentially simultaneously.

The final values for $\bar{g}p$, p, and $\bar{g}$ are given in table 2. Also given is $\bar{E}$, the mean energy estimated from yield versus energy data, and the corresponding c.m. angles for the detectors. Statistical errors only are shown on all quantities. We believe systematic effects could not be as large as 0.01. The results agree with preliminary results obtained in a similar experiment at this laboratory[2], and indicate a value of $\bar{g}$ somewhat larger than was previously believed[3]. Also, $\bar{g}$ appears to be independent of energy over the range studied.

Table 2

E_o (kev)	$\bar{E}$ (keV)	θ_{90} (90°lab)	θ_{165} (165°lab)	$\bar{g}p$	p	$\bar{g}$
51	40	93.8°	165.8°	0.868±0.006	0.905±0.001	0.959±0.006
76	58	94.1°	166.0°	0.856±0.003	0.901±0.001	0.950±0.003
93	67	94.4°	166.1°	0.856±0.004	0.902±0.001	0.949±0.004

References

1. G. G. Ohlsen, Phys. Rev. 165 (1967) 1268

2. G. G. Ohlsen, J. L. McKibben, and G. P. Lawrence, Bull. Am. Phys. Soc. 13 (1968) 1443

3. L. Brown, H. A. Christ, and H. Rudin, Nucl. Phys. 79 (1966) 459

Formalism for Spin-3/2 Beams*

P. W. Keaton, Jr.

Los Alamos Scientific Laboratory, University of California
Los Alamos, New Mexico 87544

Very recently, Holm et al.[1] produced polarized ^{6}Li nuclei using an atomic beam source. Consequently, the polarization of ^{7}Li, which has a nuclear spin of 3/2, would appear to be feasible in the near future. It is the purpose of this paper to discuss the formalism necessary to treat a beam of spin-3/2 particles.

The cross section for the interaction of a particle of spin j can be written

$$I(\theta) = I_o(\theta) \sum_{k,q} \langle T_{kq} \rangle T^*_{kq}(\theta) \ , \qquad (1)$$

where the spherical tensors[2], T_{kq}, have rank $k \leq 2j$ with the restriction $|q| \leq k$. The expectation values $\langle T_{kq} \rangle$ refer to the initial beam polarization and the $T_{kq}(\theta)$ are analyzing tensors for the reaction. The spherical tensors are orthogonal in the sense that $Tr[T^\dagger_{k'q'} T_{kq}] = (2j+1)\delta_{kk'}\delta_{qq'}$. Furthermore, using the operator property $T^\dagger_{kq} = (-1)^q T_{k-q}$, we see that eq. (1) is an invariant contraction of tensors. $I_o(\theta)$ in eq. (1) is the cross section for an unpolarized beam.

As a coordinate system for the interaction, we choose the z axis ($\hat{k}$) along the incident beam direction, $\vec{k}_{in}$, the y axis ($\hat{n}$) along $\vec{k}_{in} \times \vec{k}_{out}$ (where $\vec{k}_{out}$ is the outgoing particle direction), and the x axis ($\hat{p}$) along $\hat{n} \times \hat{k}$. Under parity inversion $\vec{k}_{in} \to -\vec{k}_{in}$, and $\vec{k}_{out} \to -\vec{k}_{out}$, which transforms $\hat{k} \to -\hat{k}$, $\hat{n} \to +\hat{n}$, and $\hat{p} \to -\hat{p}$. Therefore, conservation of parity requires that analyzing tensors be invariant under a 180° rotation of the above defined coordinate system about $\hat{n}$ (y axis). This operation places the restriction $T_{kq}(\theta) = (-1)^k T^*_{kq}(\theta)$. Substituting this relation into eq. (1) yields

$$I(\theta) = I_o(\theta)[1+2\mathrm{Im}\langle T_{11}\rangle \mathrm{Im}T_{11}(\theta)+\langle T_{20}\rangle T_{20}(\theta)+2\mathrm{Re}\langle T_{21}\rangle \mathrm{Re}T_{21}(\theta)+2\mathrm{Re}\langle T_{22}\rangle \mathrm{Re}T_{22}(\theta)$$
$$+2\mathrm{Im}\langle T_{31}\rangle \mathrm{Im}T_{31}(\theta)+2\mathrm{Im}\langle T_{32}\rangle \mathrm{Im}T_{32}(\theta)+2\mathrm{Im}\langle T_{33}\rangle \mathrm{Im}T_{33}(\theta)] \ , \qquad (2)$$

where all analyzing tensors odd in parity have been set equal to zero in eq. (2).

Due to the cylindrical symmetry of the ion source, the only nonvanishing polarization tensors produced are t_{10}, t_{20}, and t_{30}, in a coordinate system with the z axis along the axis of quantization. However, one can precess the spins to a desired orientation in the reaction coordinate system. We define β as the angle between $\hat{k}$ and the spin quantization axis $\vec{J}$. We define ϕ as the angle between $\hat{p}$ and $\vec{J} \times \hat{k}$. Using the fact that spherical tensors have the same rotation properties as spherical harmonics, we can show:

---

*Work performed under the auspices of the U. S. Atomic Energy Commission.

$\mathrm{Im}\langle T_{11}\rangle = -t_{10}(\sin\beta\cos\phi)/\sqrt{2}$ $\quad\quad$ $\langle T_{20}\rangle = t_{20}(3\cos^2\beta-1)/2$

$\mathrm{Re}\langle T_{21}\rangle = t_{20}(\sin\beta\cos\beta\sin\phi)\sqrt{3/2}$ $\quad\quad$ $\mathrm{Re}\langle T_{22}\rangle = -t_{20}(\sin^2\beta\cos2\phi)\sqrt{3/8}$

$\mathrm{Im}\langle T_{31}\rangle = -t_{30}(5\cos^2\beta-1)(\sin\beta\cos\phi)\sqrt{3}/4$ $\quad\quad$ $\mathrm{Im}\langle T_{32}\rangle = -t_{30}(\sin^2\beta\cos\beta\sin2\phi)\sqrt{30}/4$

$\mathrm{Im}\langle T_{33}\rangle = t_{30}(\sin^3\beta\cos3\phi)\sqrt{5}/4$.

The spherical tensors in terms of the components of angular momentum for spin-3/2 are

T_{00} = unit matrix(4×4), $T_{10} = J_z 2/\sqrt{5}$, $T_{1\pm1} = \mp(J_x \pm iJ_y)\sqrt{2/5}$,

$T_{20} = J_z^2 - 5/4$, $T_{2\pm1} = \mp[(J_zJ_x+J_xJ_z) \pm i(J_zJ_y+J_yJ_z)]/\sqrt{6}$,

$T_{2\pm2} = [(J_x^2-J_y^2) \pm i(J_xJ_y+J_yJ_x)]/\sqrt{6}$, $T_{30} = [J_z^3-(41/20)J_z](2\sqrt{5})/3$,

$T_{3\pm1} = \mp[(J_zJ_xJ_z-(7/20)J_x) \pm i(J_zJ_yJ_z-(7/20)J_y)]\sqrt{5/3}$,

$T_{3\pm2} = [(J_xJ_zJ_x-J_yJ_zJ_y) \pm i(J_xJ_zJ_y+J_yJ_zJ_x)]\sqrt{2/3}$,

$T_{3\pm3} = \mp[(J_x^3-3J_yJ_xJ_y-J_x) \mp i(J_y^3-3J_xJ_yJ_x-J_y)]/3$.

And finally, one might define "Cartesian tensors" for spin 3/2 as $S_k = \frac{2}{3}J_k$, $S_{k\ell} = \frac{1}{2}(J_kJ_\ell+J_\ell J_k) - \frac{5}{4}\delta_{k\ell}$, and $S_{k\ell m} = \frac{5}{9}[(J_kJ_\ell J_m+J_mJ_\ell J_k)-(\frac{7}{10}\delta_{km}+\frac{34}{10}\delta_{m\ell}\delta_{k\ell})]$, where k, ℓ, m = 1, 2, 3 (or x, y, z). However, these are overcomplete and $\vec{J}\cdot\vec{J} = j(j+1) = \frac{15}{4}$ leads to four constraints, namely, $S_{xx}+S_{yy}+S_{zz} = 0$ and $S_{xkx}+S_{yky}+S_{zkz} = 0$ for k = x,y,z. Furthermore, $S_{xyz} = S_{yzx} = S_{zxy}$.

It is convenient to use the Cartesian tensors to characterize a polarized beam with an axis of symmetry. Let the fractional population of the nuclear magnetic substate m be written N_{2m}, then the Cartesian tensors become $\langle S_z\rangle = \frac{1}{3}[3(N_3-N_{-3})+(N_1-N_{-1})]$, $\langle S_{zz}\rangle = [(N_3+N_{-3})-(N_1+N_{-1})]$ and $\langle S_{zzz}\rangle = \frac{1}{3}[(N_3-N_{-3})-3(N_1-N_{-1})]$, with the constraint $N_3+N_1+N_{-1}+N_{-3} = 1$. It can easily be seen that $\langle S_z\rangle$, $\langle S_{zz}\rangle$, and $\langle S_{zzz}\rangle$ are normalized such that they each can vary between the limits ±1.

The author wishes to express appreciation to S. Darden who brought ref. 1 to his attention and to D. A. Goldberg and G. G. Ohlsen for helpful discussions.

References

1. U. Holm, E. Steffens, H. Albrecht, H. Ebinghaus, and H. Neuert, Z. Phys. 233 (1970) 415

2. W. Lakin, Phys. Rev. 98 (1955) 139